Downstream gene expression of wild type p53 tumor suppressor gene versus mutated and null p53

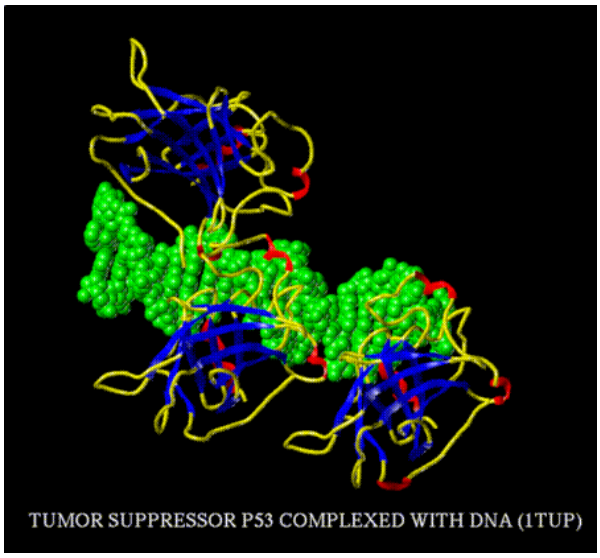

Master degree thesis in Molecular Biotechnology

By

M. Belal Al-Jabri

November 2006

Department of Molecular Biotechnology

Institute of Medical Biology

University of Tromsø

Norway

Table Of Contents

Acknowledgement

This work is the result of two years of work at the Department of Molecular Biotechnlogy, Institute of Medical biology, University of Tromsø - the northernmost university in the world -, Norway.

I would like to express my gratitude to all those who gave me the possibility to complete this study.

I respectfully acknowledge the supervision, assistance, guidance and support of my supervisor Prof. Raafat El-Gewely, without whom this work could not have been performed. I express my sincere gratitude to him for providing me with the opportunity to work within the field of p53.

I am also thankful and grateful to my co-supervisor Prof. Ugo Moens for his support and help, and also to our department's engineer Elisabeth Kjeldsen Buvang for providing technical help in the lab and for reading through this thesis.

I also express my thanks to Christian Karlsen for helping me in learning the 2D gel method, to Jack Brunn for performing the MS analysis, and to Umaer Nassir for the useful discussions and skills he has shared with me.

Many thanks to Karin Eilertsen the student consulant at the Institute of Medical Biology for her administrative help and consultancy.

And last but not least, I express my deep sense of gratitude to my parents and family and to my friends in both Norway and my homeland Syria for being very supportive and encouraging especially Khaled, Manar and my wife Maisoon for her unlimited support.

Tromsø, November 2006

M. Belal Al-Jabri

Abstract

P53 is a key tumor suppressor and transcription factor protecting us from cancer. The wild type p53 protein functions as a regulatory protein, triggering a variety of cellular responses to different signals. Activation of *p53* can lead to cell division arrest, DNA repair, or apoptosis. More than 60% of all human cancers contain *p53* mutations. *P53* is also reported in many studies to play a role in the control of other cellular important activities such as angiogenesis and glycolysis. In this study we aimed to to identify novel target genes of *p53* by investigating the difference in down-stream gene expression of wt *p53* in a the Saos-2 cell line which is devoid of *p53* expression, in comparison to mutated form of *p53* that has been reported to be associated with cancer and in relation to the lack of *p53* expression. The aim was also to study protein-protein interactions between *p53* and its protein partners in the different *p53* variants. Two different *p53* mutations (R249S and R273H), considered as hot mutations, were constructed by site-directed mutagenesis. The GeneSwitch system was used to make stable inducible *p53* cell lines. This expression is controlled by mifepristone (inducer). Total proteins were isolated from the different cell lines and separated on 2D gels. The total protein expression in Saos-2 cells containing wild type *p53*, R249S or R273H mutants, in addition to cells with no *p53* copy were compared. The expression patterns of the different samples were similar but not identical.

Our results showed a different expression patterns in some vital proteins. Our results suggest a role of *p53* in transcriptionally activating the β subunit of Prolyl 4-Hydroxylase which plays an important role in angiogenesis. Also our results show different patterns in expressing vimentin, which is the most abundant intermediate filament protein in various cell types, between the different cell lines. Also our results show a clear difference in the protein expression patterns of four proteins, which are essential in glycolysis (TIM, enolase 1, α-enolase and aldolase A.) suggesting a role of *p53* in the metabolism of tumors particularly in glycolysis. Recent studies have implicated some of these proteins in cancer if not to *p53* as well. Studies dealing with *P53* and its partner proteins from the total protein using anti V5 antibody were attempted, but was not pursued further due to the short time. The way of doing this was proteomics.

Abbreviations

2DE	Two Dimensional Gel Electrophoresis
2D-gel	Two Dimensional Gel separation
AA (aa)	Amino Acid
AD	Adenocarcinoma
Ant	Antibiotics
APS	Ammonium PerSulfate
ATCC	American Type Culture Collection
ATP	Adenosine Triphosphate
BLAST	Basic Local Alignment Search Tool
BSA	Bovine Serum Albumin
CA	Carbonic Anhydrase
CDK	Cyclin Dependent Kinase
CHAPS	[3-[(3-Cholamidopropyl)-dimethylammonio]-1-propanesulfonate]
DMEM	Dulbecco/Vogt Modified Eagle's Minimal Essential Medium
DMSO	Dimethyl Sulfoxide
DNA	Deoxyribonucleic Acid
dNTP	Deoxy Nucleotide Triphosphate
DTT	Dithiothreitol
E. coli	*Escherichia coli*
EV	Empty Vector
FBS	Fetal Bovine Serum
g	Gravity, relative centrifugation force
HCC	Hepatocellular Carcinoma
HCV	Hepatitis C Virus
IARC	International Agency for Research on Cancer
IP	Immunoprecipitation
IPG	Immobilized pH Gradient
Kb	Kilo Base
kDa	Kilo Dalton
LB	Luria-Bertani
MALDI	Matrix Assisted Laser Desorption Ionization mass spectrometry
MALDI TOF	MALDI time-of-flight mass spectrometry
MS	Mass Spectrometry
MW	Molecular Weight
NAD	Nicotinamide adenine dinucleotide
NCBI	National Center for Biotechnology Information
NSCLC	Non-Small Cell Lung Carcinoma
OD	Optical Density
P4-H	Prolyl 4-Hydroxylase
PBS	Phosphate Buffered Saline
PCR	Polymerase Chain Reaction
PDI	protein disulphide isomerise

p*I*	Isoelectric Point
R249S	Hot spot mutation in the *.p53* gene at aa position 249. Arg is changed to Ser.
R273H	Hot spot mutation in the *p53* gene at aa position 273. Arg is change to His.
RCC	Renal Cell Carcinoma
rpm	Round Per Minute
RT-PCR	Reverse Transcription Polymerase Chain Reaction
Saos-2	Human Osteosarcoma derived cell line, *p53*-null
SCC	Squamous Cell Carcinoma
SCO2	Cytochrome c Oxidase 2
SDM	Site Directed Mutagenesis
SDS	Sodium Dodecyl Sulfate
SDS-PAGE	Sodium Dodecyl Sulfate-Polyacrylamide Gel Electrophoresis
siRNA	Small (short) Interfering RNA
SSP	Standard Spot number
TEMED	N.N.N'.N'-Tetra-methylethylendiamine
Tris	(Hydroxymethyl)-aminomethane
Vh	Volt-hours
WB	Western Blot
WT (wt)	Wild Type

Introduction

P53 or TP53 is a key tumor suppressor transcription factor in the cell. The level of p53 protein is reported to be very low in normal cells; however, its level increases significantly in cells under stress (1). The wild type p53 protein functions as a regulatory protein, triggering a variety of cellular responses to different signals Activation of *p53* can lead to growth arrest, DNA repair, or apoptosis (2). P53 protein regulates cell responses to DNA damage to keep genomic stability by transactivation and trans-repression of its downstream target genes (3). More than 60% of all human cancers contain *p53* mutations (4). Mutations in *p53* are frequently found in human cancers owing to the loss of tumor suppressor activities (loss of function) as well as to the gain of tumorogenic activities (gain of function) (5). Both the *p53*-regulated genes and interacted proteins form a large network of cell system to regulate cell division, DNA repair and apoptosis. P53 function is often inactivated or suppressed in human cancers. Thus, functional restoration of this pathway is an attractive therapeutic strategy (6).

P53 structure:

DNA sequence:

The *p53* gene is located on chromosome 17 (17p13), Figure 1. *P53* gene is about 20 kb composed of 11 exons (2), Figure 2. There is a very large intron between exon 1 and exon 2. Exon 1 is untranslated region in the human *p53* (7).

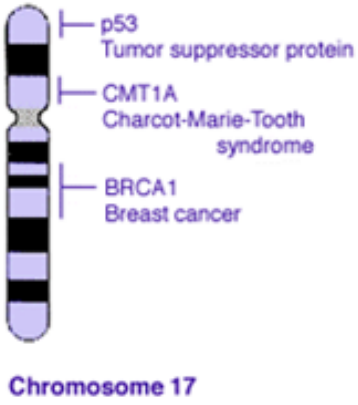

Figure 1: Chromosome 17. *P53* gene is located on the short arm of the chromosome

Figure 2: The *p53* gene consists of eleven exons. The pink region denotes the UTR (the untranslated region), the blue region denotes the coding region and the grey region denotes the internal exons within the introns. Figure is adapted after kind permission from *p53* knowledgebase: http://p53.bii.a-star.edu.sg/index.php (8)

P53 protein sequence (7):

The tumor suppressor protein p53 is a 393 amino acid transcriptional enhancer phosphoprotein that reversibly associates to form tetramers. The human p53 protein comprises of several domains, Figure 3:

1. The amino-terminus part (aa 1-44) contains the transactivation domain, which is responsible for activating downstream target genes.
2. A proline-rich domain (aa 58-101) mediates p53 response to DNA damage through apoptosis.
3. The DNA-binding domain (aa 102-292) is a core domain, which consists of a variety of structural motifs. 90% of *p53* mutations found in human cancers are located in this domain, preferable as a single aa mutation.
4. The oligomerization domain (aa 325-356) consists of a β-strand, which interacts with another p53 monomer to form a dimer, followed by an α-helix which mediates the dimerization of two p53 dimers to form a tetramer.
5. Three putative nuclear localization signals (NLS) have been identified in the C-terminus, through sequence similarity and mutagenesis. The most N-terminal NLS (NLSI), which consists of 3 consecutive Lysine residues to a basic core, is the most active and conserved domain.
6. Two putative nuclear export signals (NES) have been identified. The leucine-rich C-terminal NES, found within the oligomerization domain, is highly conserved and it has been suggested that oligomerization can result in masking of the NES, resulting in p53 nuclear retention.

Figure 3: Domains of human p53 protein. Figure is adapted after kind permission from *p53* knowledgebase: http://p53.bii.a-star.edu.sg/index.php (8).

P53 Functions:

The role of p53 in cell-cycle control:

The cell cycle is an ordered set of events, culminating in cell growth and division into two daughter cells. This process is composed of two basic phases: Mitosis and the Interphase, Figure 4. The Interphase consists of three phases which are G1, S and G2. During the cell cycle, chromosomal DNAs are replicated during S phase and equally delivered into two daughter cells during the M phase.

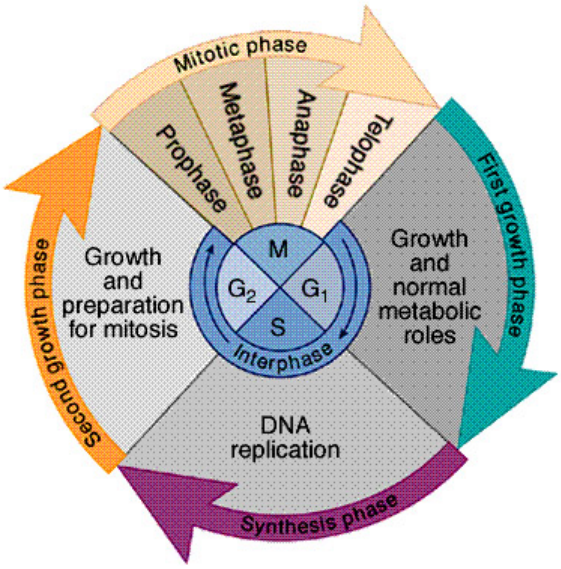

Figure 4: The Cell cycle. It is composed: Mitotic phase (M) and interphase. Interphase consists of three phases, which are G1, S and G2. Image is adapted from Biology Corner web site http://www.biologycorner.com .

Normally the cell cycle is under tight control through three major checkpoints, especially at the transition state from G1 phase to S phase and from G2 phase to M phase. P53 protein is stabilized in response to these checkpoints in the cell cycle which are activated by DNA damage, irradiation, hypoxia, viral infection, or oncogene activation resulting in diverse biological effects, such as cell cycle arrest, apoptosis, senescence, differentiation, and antiangiogenesis (9). The p53 protein is stabilized and activated by phosphorylation, dephosphorylation, acetylation, sumoylation and ribosylation at specific sites, yielding a potent sequence-specific DNA-binding transcription factor (9).

Activation of p53 as a transcription factor causes transactivation of downstream genes, leading to cell cycle arrest in G1, before DNA replication, and in G2, before mitosis. Also, genes involved in apoptosis are activated by p53 protein (2), Figure 5.

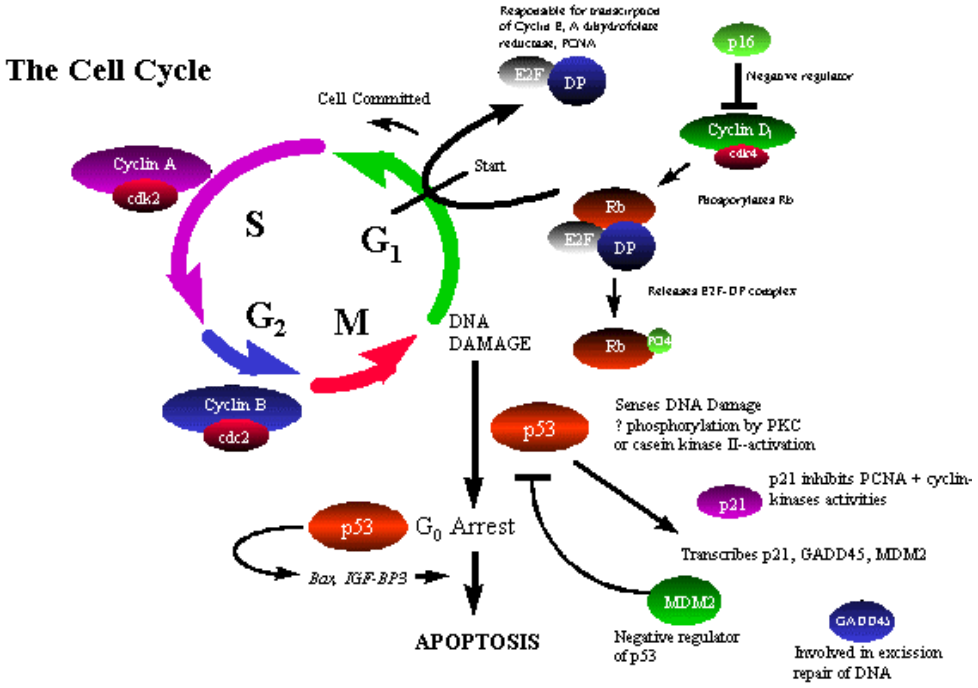

Figure 5: *P53* role in the cell cycle. *P53* is activated in response to activation of cell cycle checkpoints as a result of DNA damage or other oncogenic factors. Activation of *p53* downstream genes results in cell cycle arrest, senescence or apoptosis. Image is adapted from www.humpath.com.

G1 checkpoint:

Under normal growth conditions, progression through G1 is promoted by D-type and E-type cyclins and their associated cyclin-dependent kinases (cdk2, cdk4, and cdk6) (10). Arrest in the G1 phase of the cell cycle is critical for genomic integrity because it blocks entry into S phase and prevents replication of damaged DNA.

Upon DNA damage, *p53* is activated and induces $p21^{WAF1/CIP1}$, a cyclin-dependent kinase inhibitor [reviewed in (11)]. P21 sustains G1 arrest by inhibiting cdk2 and cdk4 activities. This inhibition prevents the phosphorylation of pRb, hence the release of E2F from the pRb-E2F complex. This blocks transcription of genes required for entry into S-phase by E2F, and as a result prevents entry into S-phase since the active released E2F is the transcription factor that transactivates the target genes important for the progression of cell cycle including cyclin E. (12;13).

G2/M checkpoint:

The G2/M checkpoint plays a role in genomic maintenance by preventing segregation of damaged chromosomes (10). In order to sustain a G2/M arrest, Cdc2-cyclinB activity must be inhibited. *p53* regulates many target genes that play critical roles during G2/M arrest [reviewed in (10)]. For example, *p53* regulates p21 which blocks G2/M progression by binding the Cdc2-cyclinB complex and preventing the activating phosphorylation of Cdc2 at Thr161 by CAK (14). *p53* also induces 14-3-3σ which blocks entry into mitosis [reviewed in (15)]. Moreover, other *p53* targets, such as GADD45, BTG2, REPRIMO, B99 (GTSE-1), hematopoietic zinc finger protein (HZF), and MCG10 have been implicated in the maintenance of the G2/M checkpoint [reviewed in (10)].

S checkpoint:

The intra-S phase checkpoint is activated when DNA damage occurs during S phase (10). Although it has yet to be confirmed, a newly identified *p53* isoform called Δp53 may participate in the intra-S checkpoint. This Δp53 may promote the intra-S arrest by inducing p21 and 14-3-3σ (10;16).

The role of p53 in DNA repair:

Various cellular insults including chemotherapeutic drugs, chemical carcinogens, gamma-irradiation, ultraviolet-irradiation (UV), reactive oxygen species (ROS), and endogenous stressors lead to DNA damage. Failure to repair damaged DNA results in cell death or oncogenic transformation, neither of which is a desired outcome for a biological system. Depending upon the type of DNA lesion, eukaryotic cells utilize multiple DNA repair pathways to mend damaged DNA including nucleotide excision repair (NER), mismatch repair (MMR), base excision repair (BER), translesion synthesis (TLS), homologous recombination (HR), and non-homologous end joining (NHEJ) pathways. Not surprisingly, studies show that *p53* promotes genomic integrity by regulating the DNA repair pathways. In addition, many *p53* target genes participate in the DNA repair process. Furthermore, *p53* directly modulates DNA repair through transcriptional-independent mechanisms (10).

The role of p53 in Apoptosis:

Under situations of extreme DNA damage, *p53*-dependent transcription is well known to stimulate apoptosis (10). *P53* regulates the transcription of genes in the apoptotic cascade. Two of such genes, Bax and Bcl-2, are important in the mitochondrial pathway of apoptosis (13). The Bax (pro-apoptotic gene) and Bcl-2 (anti-apoptotic gene) form homo- and heterodimers to control the mitochondrial permeability for the release of cytochrome c and AIF (apoptosis inducing factor). *P53* can transactivate Bax gene while transrepressing Bcl-2 gene, thus leads cell to apoptosis (13).

P53 promotes the extrinsic pathway through upregulation of the TRAIL receptors, death receptor-4 (DR4) and death receptor-5 (DR5, KILLER) [reviewed in (17)], as well as the FAS receptor (CD95) and the FAS/APO-1 ligand (18). *P53* activates the intrinsic apoptotic pathway through multiple mechanisms [reviewed in (19)].

The role of p53 in Senescence:

Senescence is well known as *p53*-dependent process and is characterized by an irreversible growth arrest of cells that remain metabolically active (20). Senescence can be triggered by DNA damage or oncogene activation. Cells entering senescence are

characterized in addition to permanent cell cycle arrest, by an altered transcriptional program, a large flattened morphology, and a failure to replicate their DNA. *p53* regulates both replicative senescence and premature senescence (10).

The role of p53 in Differentiation:

Differentiation may be another way in which *p53* eliminates damaged cells. Stem cells possess the ability to self-renew and are often resistant to cell cycle arrest and apoptosis, making them prime targets for tumorogenesis. Thus, *p53* may promote differentiation of stem cells into a less malignant cell type competent to undergo cell cycle arrest and apoptosis (10).

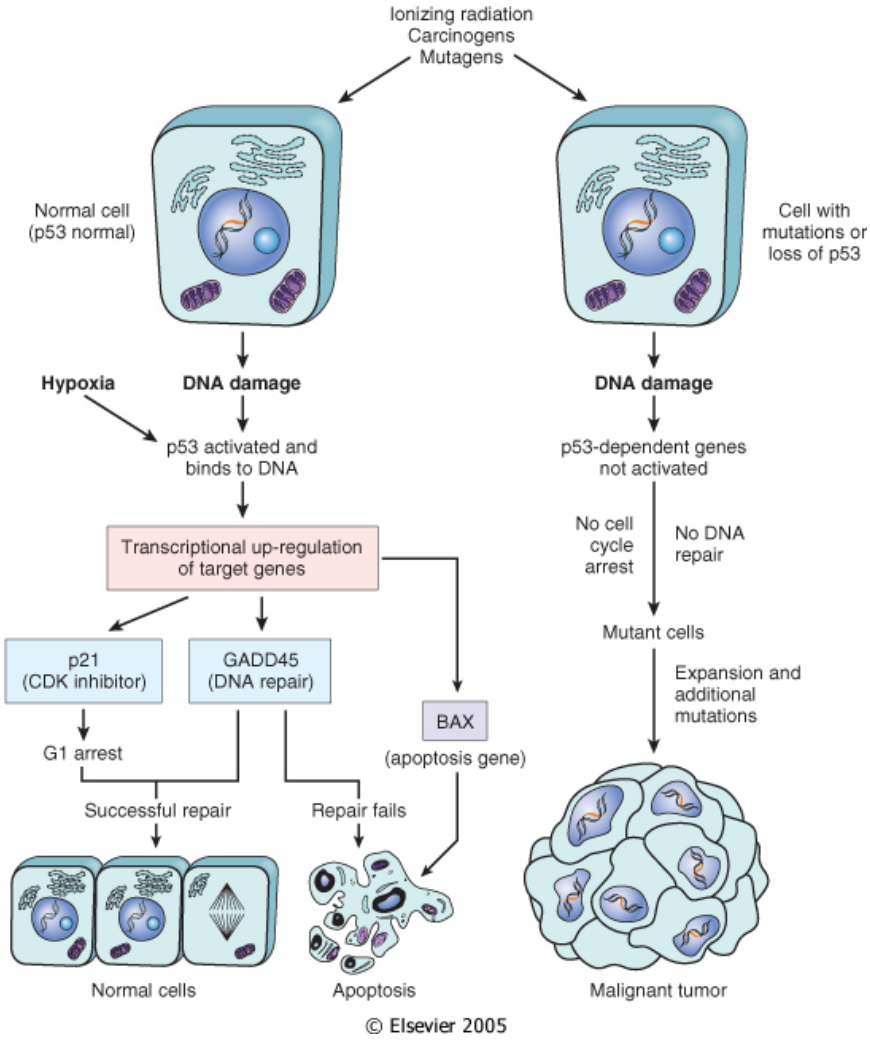

Figure 6: DNA damage and activation of *p53*. In normal cells, DNA damage activates *p53* which in turn binds to DNA and transcriptionally regulates target genes responsible for G1 arrest (p21 which is CDK inhibitor) and DNA repair (GADD45). If the repair succeeded, cells continue the cycle as normal cells. If not, *p53* activates apoptosis gene (BAX) and drives the cell to programmed cell death. This network is compromised in the absence or mutated *p53* resulting in tumors. This Elsevier image is adapted from http://www.humpath.com.

P53 mutations:

Because of the important role of *p53* in regulating normal cell growth, *p53* is frequently mutated in cancers. It has been reported that more than 60% of cancer cells contain mutated *p53* genes (4). Mutations can be either upstream of *p53* preventing DNA damage/oncogene overexpression signals from activating *p53*, or downstream of *p53* preventing *p53* target genes from executing their functions in cell cycle regulation [reviewed in (5)].

The International Agency for Research on Cancer (IARC) in Lyon, France has constructed an online TP53 mutation database. The current version of the database is R11, released in October 2006. The R11 release contained 23,544 somatic mutations, 376 germline mutations and functional data on more than 2300 mutant proteins http://www-p53.iarc.fr/Statistics.html. The statistics of IARC shows a dramatic increase of the *p53* mutations detected in relation to cancer, Figure 7.

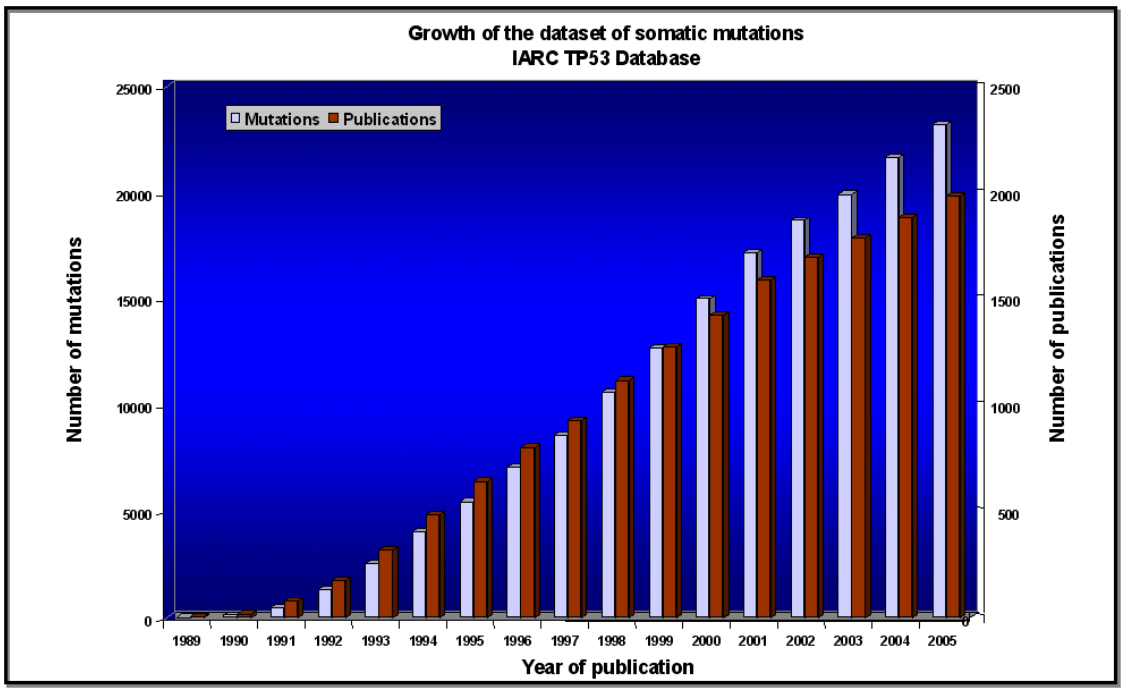

Figure 7: Growth of the dataset of somatic p53 mutations. (IARC TP53 database, R11 release, October 2006) (21).

73.7% of *p53* mutation in the IARC database are missense mutations caused by singular amino acid substitutions, although deletion and insertion can occur (5), which lead to either expression of a mutant protein (90% of cases) or absence of a protein (10% of cases) (21). Mutations of *p53* are distributed predominantly in the DNA binding domain, especially in the codons 175, 245, 248, 249, 273, and 282, which are often referred to as "hot spots" mutations, Figure 8.

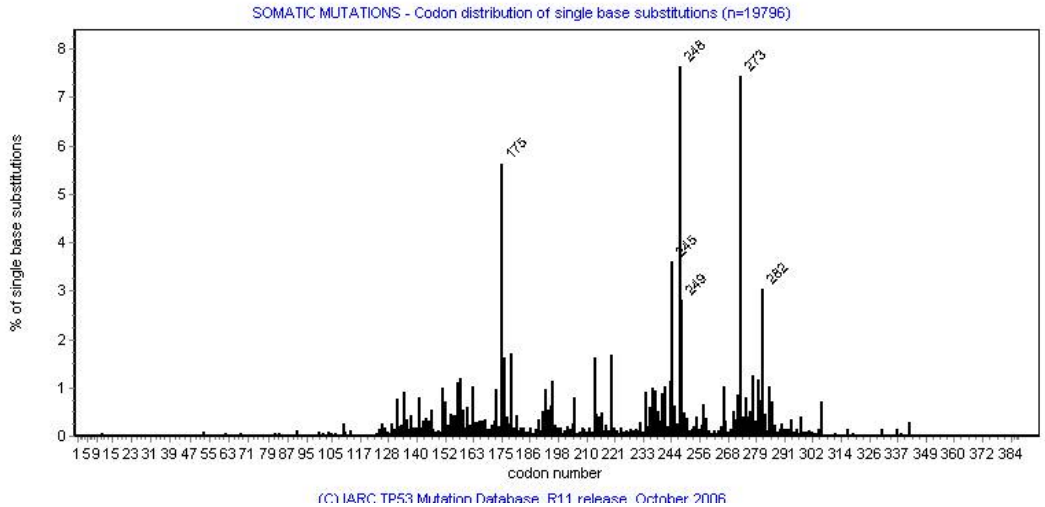

Figure 8: Codon distribution of somatic *p53* mutations. *p53* hot spots mutations have higher occurrence percentage as single base substitution. (IARC TP53 database, R11 release, October 2006) (21).

Mutations in *p53* were found in tumors in a wide variety of organs. Figure 9 shows tumor site distribution of mutations according to IARC.

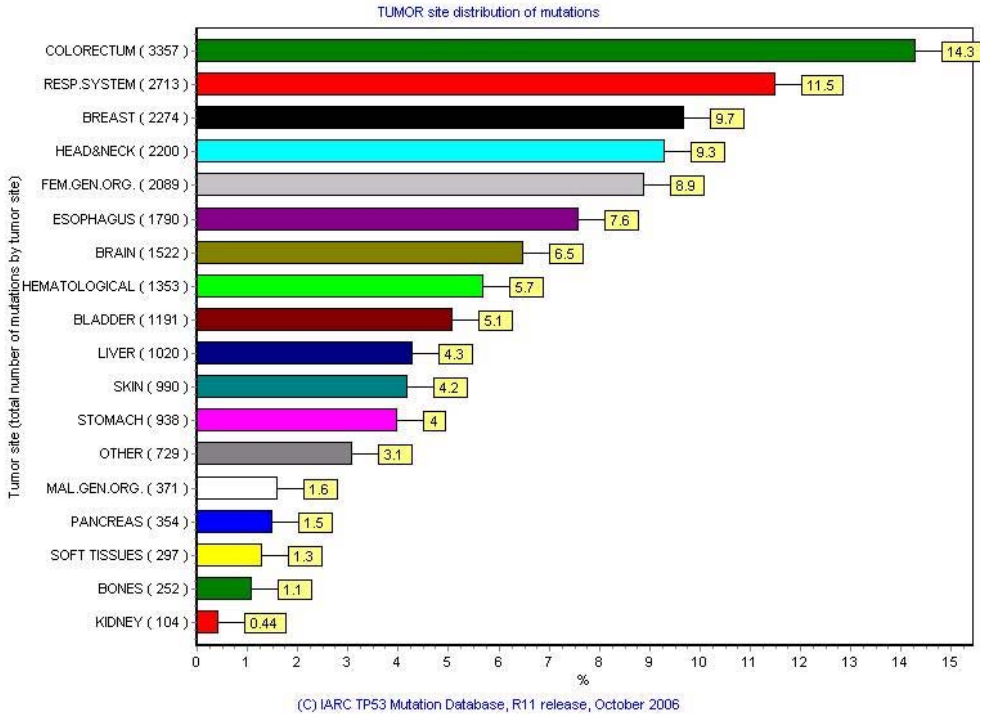

Figure 9: Tumor site distribution of mutations according to IARC, tumor site distribution of mutations according to IARC (21).

Mutations constructed in this study:

The two mutations constructed in this project were R249S and R273H, which are located within the "hot spot" region. Both mutations are positioned in the DNA binding domain. In the first mutation R249S, the wild type sequence AGG, which codes for the amino acid arginine (R), has been mutated into the sequence AGC that codes for the amino acid serine (S). In the second mutation R273H, the wild type sequence CGT, which codes for arginine (R) as well, was replaced by the mutant sequence CAT, which codes for histidin (H). R249S is associated mainly with hepatocellular carcinoma and to a lesser extent with Non Small Cell Lung Carcinoma (NSCLC) according to IARC. R273H is associated mainly with colo-rectal cancers and to less extent in breast cancer according to IARC. Table 1 summarizes the characteristics of the two mutations.

Table 1: The two mutations constructed in this study

Mutant	WT sequence	Mutant sequence	Prevalent Cancer Sites
R249S	AG**G**	AG**C**	Liver, Lung
R273H	C**G**T	C**A**T	Colo-rectal, Breast, Ovary, Brain

Figure 10 shows modulated images of p53 protein indicating the positions 249 (A: WT and B: mutant) and 273 (C: WT and D: mutant).

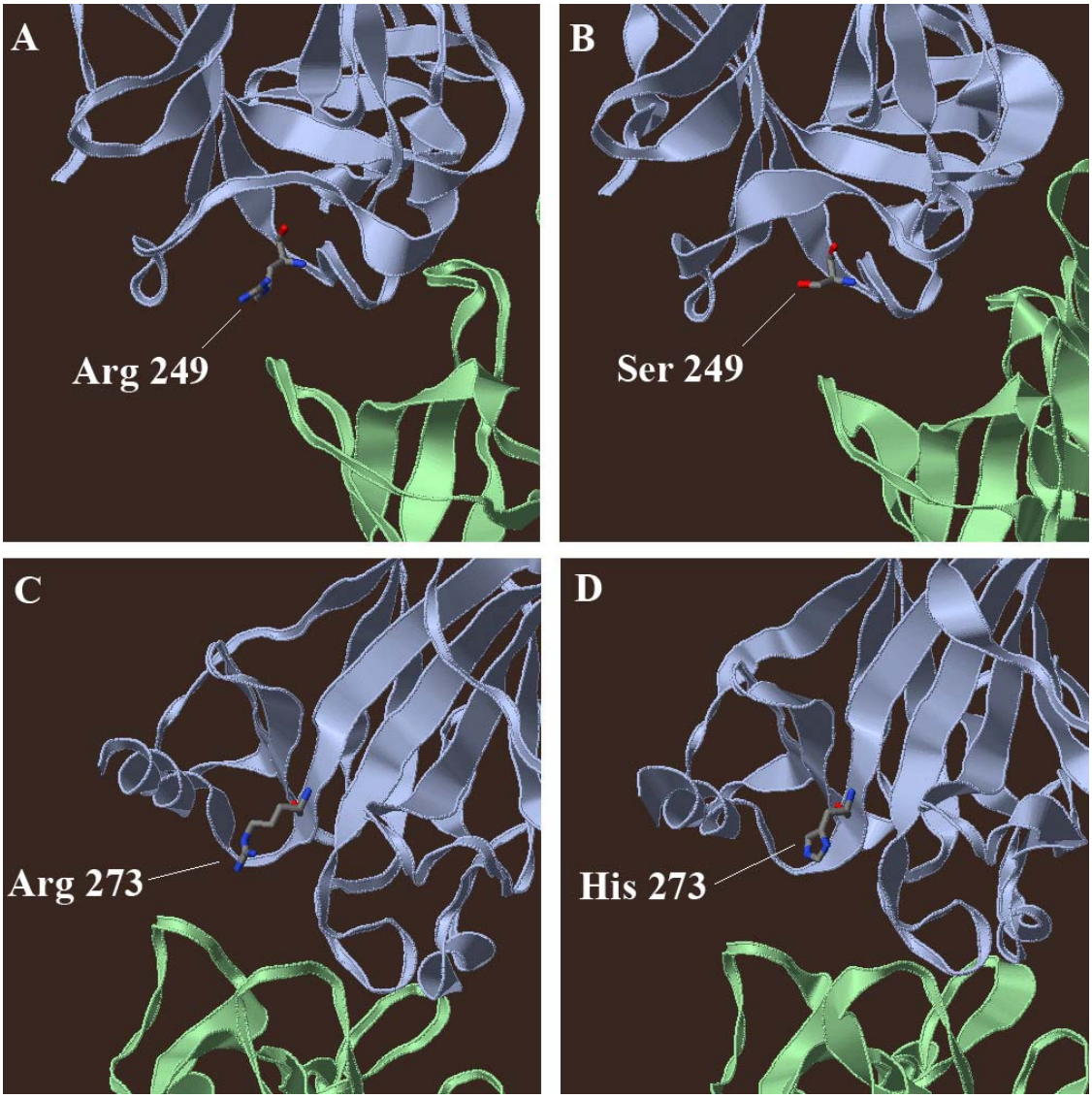

Figure 10: 3D modulated images of p53 protein indicating the position 249 (A: WT, B: R249S) and the position 273 (C: WT, D: R273H) Figures were generated using analysis tools in p53 knowlegebase website http://p53.bii.a-star.edu.sg/analysis/structmut/index.php (7).

P53 as a target for cancer therapy:

P53 has long been considered a prime target for cancer therapeutic modulation (22). Since many *p53* mutants with loss of transcriptional activity might still retain its ability to activate apoptosis through the transcription-independent pathway, there is considerable excitement that this newly identified mechanism will ultimately lead to a new generation of cancer therapeutics (23). Many chemotherapeutic agents cause DNA damage and activate the *p53* pathway to induce growth arrest and apoptosis (24). Functional restoration of this pathway is an attractive therapeutic strategy (23). *P53* is maintained at low levels in cells, largely through MDM2-mediated degradation. Thus, rescue of *p53* function by disrupting MDM2-p53 interaction is considered to be an efficient approach for anti-cancer therapy (25).

It was recently published in Biotech News International (October 2006) that researchers have shown that an approach to cancer treatment based on disrupting the activity of the p53 inhibitor Mdm2 is effective in preventing the development of tumors without causing premature aging (26).

In recent years, a number of therapeutic approaches aiming at modulation of the p53 pathway have been developed. Some of them are reviewed in (23).

Aim of study

The tumor suppressor activity of *p53* results from its ability to transcriptionally activate and repress a wide variety of target genes that in turn regulate among other things: cell cycle arrest, DNA repair, apoptosis, and suppression of angiogenesis (27). The *p53* tumor suppressor activity is also a result of *p53* involvement in cellular functions by protein-protein interactions (28). Functional diversity depends on the association with a large subset of partner proteins, which dictates the type of activity and corresponding selectivity (28).

P53 gene expression has been examined at the mRNA level, though many possibilities exist for intervention at the protein level, as the p53 protein is known to interact with many other cellular proteins in order to mediate its many important roles. In this study we analyzed changes in protein expression in Saos-2 cells in the absence of *p53* and in presence of mutated *p53* and compared them to the protein expression in Saos-2 cells containing wild type *p53*.

Our aims of this study were:

- To investigate the role of *p53* in downstream gene expression in relation to the lack of *p53* expression or the expression of mutated form of *p53* that was reported to be associated with cancer.
- To study protein-protein interactions between *p53* and other proteins in the different *p53* variants.
- By studying different mutants we try to identify the difference in the downstream gene expression between these mutants.
- By studying the protein expression of different mutants we try to see if there is any biomarker that can be linked to any mutant or only associated with wt which might help in diagnosis and prognosis related to *p53* status.

Materials and Methods

Materials

Table 2: Plasmids

Material	Source	Purpose	Comments
pGene/V5-His Plasmid	Invitrogen, Carlsbad, CA, USA	Cloning vector for *p53* gene cloning and expression in mammalian cells. The expressed protein will be in frame with V5 antigen	Inducible expression system
pSwitch Plasmid	Invitrogen	Control of gene expression of the inserted gene in pGene/V5-His	Inducible expression system

Table 3: Materials used for site-directed mutagenesis

Material	Source	Purpose
*Dpn*I restriction enzyme	Stratagene, La Jolla, CA, USA	Digestion of the methylated parental strand
Pfu Ultra DNA polymerase	Stratagene	
Template Pdest/HA-wtp53	Stratagene	
DNTP Mix	Stratagene	

Table 4: Sequences of primers used for site-directed mutagenesis of *p53* gene

Mutant	Coding sequence (wild type)	Coding sequence (mutant)	Forward and reverse primers sequence	No. of Bases
R249S	AGG	AGC	F: TGAACCGGAGCCCCATCCTC R:GAGGATGGGGCTCCGGTTCA	20
R273H	CGT	CAT	F:CTTTGAGGTGCATGTTTGTGCC R:GGCACAAACATGCACCTCAAAG	22

Table 5: Primers used for sequencing

Reagent	Source	Sequence	No. of Bases
pGene Forward Primer	Invitrogen	5′-CTGCTATTCTGCTCAACCT-3′	19
BGH Reverse Primer	Invitrogen	5′-TAGAAGGCACAGTCGAGG-3′	18

Table 6: Biological materials

Material	Source	Purpose	Description
E. coli XL1- blue cells Genotype: *rec*A1, *end*A1, *gyr*A96, *thi-1*, *hsd*R17(r_K^- ,m_K^+), *sup*E44, *rel*A1, λ^-, *lac*$^-$, [F' *pro*AB, *lac*I^qZΔ *M15*, Tn10(Tet^r)].	Stratagene	Competent cells to be transformed with the plasmid including the gene of target so the DNA amount will be multiplied.	Dam+ bacterial cells so can methylate the transformed DNA and protect it from being destroyed by the cell.
Saos2 cells	LGC Promochem – ATCC, USA.	To establish inducible mammalian cell lines with the *p53* gene	Human Osteosarcoma *p53*-null cell line
Anti-V5-Horse Horse Radish Peroxidase (HRP) antibody	Invitrogen	Immunoprecipitation	

Table 7: Materials used for cell culture

Material	Contents	Source	Purpose
FBS	Fetal Bovine Serum	Invitrogen	
DMSO	Dimethyl sulfoxide	Sigma-Aldrich (Missouri, USA)	Freezing cells
DMEM without serum or antibiotics	Dry powder Instamed® DMEM, 2,6 mM NaHCO3, 20 mM Hepes Acid and Hepes Na. pH: 7,2. Osm: 280	Prepared locally in the Institute of Medical Biology IMB, University of Tromsø Uitø	Media for cell culture, but used in Transfection mixture without serum
DMEM + Ant + 10% FBS	DME + 60 mg/L Penicillin-G (Sigma-Aldrich) + 100 mg/L Streptomycin (Sigma-Aldrich)	IMB, Uitø	Cell culture before transfection
DMEM + Selective antibiotics	DMEM + 20µg/L Zeocine + 20µg/L Hygromycine + 10% FBS	DMEM: IMB, Uitø Zeocine: Invitrogen Hygromycine: CALBIOCHEM®, a brand of EMD biosciences, La Jolla, CA, USA	Cell culture after transfection
DME+FBS 1:9		IMB, Uitø	Freezing cells
PBS	137 mM NaCl, 2,7 mM KCl, 4,3 mM Na2HPO4, 1,47 mM KH2PO4. pH: 7,2-7,3. Osm:320	IMB, Uitø	Washing and neutralizing Trypsin
Lysis buffer with Triton X-100	150 mM NaCl, 50 mM tris pH 8, 1% Triton X-100. Sterile filtered	Prepared locally in our lab	Lysis buffer for protein isolation
LB media	10 g/L Trypton, 5g/L Yeast Extract, 10 g/L NaCl, 1,1g/L Glucose, pH: 7,4	IMB, Uitø	Growing *E. coli*

Table 8: Materials used for western blotting

Reagent	Contents	Source
SDS PAGE sample application buffer	100 mM Tris-HCl pH 6,5, 4% SDS, 0,05% Bromophenol blue, 20% Glycerol, 200 mM DTT (added fresh), Milli Q-Water	Prepared locally in our lab.
Blue Plus 2 Prestained Standard		Invitrogen
Biotinylated SDS-PAGE standard kit, broad range AP.		Bio-Rad, Cat. No. 161-0322
NuPAGE 4-12% Bis Tris gel, 1,5 mm X 10 well		Invitrogen
NuPAGE Transfer buffer		Invitrogen
MES SDS-PAGE running buffer		Invitrogen
Transfer (blotting) buffer	25 mM Tris base pH: 8,3, 192 mM glycine, 20% v/v methanol (added fresh)	Prepared locally in our lab.
PBS-tween (PBST)	PBS buffer + 0,1% Tween 20	Prepared locally in our lab.
Blocking buffer	PBS-Tween + 5% (w/v) nonfat, dry milk	Prepared locally in our lab.
Western wash buffer	10 mM Tris-HCl pH 9,5, 10 mM NaCl, 1 mM MgCl2	Prepared locally in our lab.
Anti p53 antibody		Zymed, CA, USA
Goat anti mouse IgG (H+L)		Invitrogen
CDP star assay buffer pH 9.5		Applied Biosystems, USA
Immobilon ™-P membrane		Millipore cooperation, USA

Table 9: Kits

Kit	Source	Purpose
QuickChange®Multi Site Directed Mutagenesis kit	Stratagene	Site-directed mutagenesis
QIAGEN® plasmid purification kit	Qiagen, Hilden, Germany	Plasmid extracting and purification
GeneJammer® Transfection kit	Stratagene	Transfection
RC DC Protein Concentration Assay	Bio-Rad	Measuring protein concentrations

Table 10: Materials used for immunoprecipitation

Material	Source	Purpose
Anti-V5-HRP Antibody	Invitrogen	Binding to V5 epitope
Protein-G Sepharose™ 4 Fast Flow	Amersham Pharmacia Biotech, Ltd, Sweden	Forming Antibody-Protein complexes on the sepharose beads
Protease Inhibitor cocktail	Sigma-Aldrich, P8340	Inhibiting proteases

Table 11: Materials used in 2D gel

Material	Contents/Source
Rehydration solution (Sample application buffer)	8 M urea, 4% (w/v) CHAPS, 10% (v/v) glycerol, and 0.002% (w/v) bromphenol blue, (add at time of use) 0.2% (w/v) DTT (Amersham biosciences, Uppsala, Sweden) and 0.5% (v/v) Pharmalyte (pH 3-10) (Amersham)
SDS equilibration buffer I	6 M urea, 30% glycerol, 2% (w/v) SDS and 50 mM Tris-HCl, pH 8,8, (added at time of use) 1% DTT.
SDS equilibration buffer II	6 M urea, 30% glycerol, 2% (w/v) SDS and 50 mM Tris-HCL, pH 8,8, (add at time of use) 2.5% (w/v) iodoacetamide (GE Healthcare, UK) and a small amount of bromphenol blue
8% Acrylamide gel	(160 x 160 x 1.5 mm) 22.9 ml dH2O, 8.6 ml Acrylamide/Bis (40%) (Bio-Rad, Hercules, CA), 11 ml Resolving buffer (1,5 M Tris-HCl, pH 8,8), 425 µl 10% (w/v) SDS, 210 µl 10% APS: Ammonium Persulfate (Kastman Kodak company, Rochester, NY) and 21 µl TEMED (Amersham)
The running buffer	25 mM Tris, 192 mM Glycine, 0.1% (w/v) SDS, pH 8.3
Agarose	0.8% agarose (Invitrogen) in running buffer and a small amount of bromphenol blue
Polyacrylamide gel cast	Acrylamide/Bis (40%), Resolving buffer (1,5 M Tris-HCl, pH 8,8), SDS 10%
Staining	SimplyBlue™ SafeStain (Invitrogen) SYPRO Ruby (Bio-Rad, CA, USA)
Strips	7 and 13 cm IPG Immobiline® DryStrip, pH: 3-10 (GE Healthcare, Uppsala, Sweden).
PDQuest 8.0	2-D analysis software (Bio-Rad)
IPG® buffer	Amersham /GE Healthcare)
IPGphor™ (Pharmacia Biotech)	Equipment used for 1st dimension
PowerPac HC™ (Bio-Rad)	Equipment used for 2nd dimension

Table 12: Other materials used in this study

Material	Source	Purpose
BenchTop 1kb DNA ladder	Promega, Madison, WI, USA	MW Standard used for agarose gels
Big Dye 3.1	Amersham Biosciences	DNA Sequencing
Bovine Serum Albumin (BSA)	Bio-Rad	Protein concentration assay
Acetone	MERCK, Darmstadt, Germany	Organic solvent that can be used for concentrating diluted protein samples

Methods

The Gene switch™ system (Invitrogen®) (29)

The development of gene-technology has made it possible to produce large amounts of proteins by cloning the gene of interest in an expression vector. Expression vectors are often plasmids or viruses. The expression vector can be introduced in a suitable organism where the protein of interest can be expressed. The wild type and different variants (EV, R249S and R273H) of the protein can be expressed.

One of the major functions of *p53* is to induce cell apoptosis, it becomes unlikely to create a stably transfected cell line with a constitutive expression of *p53* (3). Therefore we have created four stable cell lines with inducible *p53* expression for wt, empty vector R273H and R249S.

The pGene/V5-His-wtp53 vector is capable of replicating in both bacteria and mammalian cells. Such a vector capable to replicate in two unrelated species is called a shuttle vector.

The GeneSwitch™ System for inducible mammalian expression is ideal for experiments that require the absolute lowest non-induced expression levels. The system is composed of two major components. The first component is the pGene/V5-His inducible expression vector, Figure 11A. Expression of our gene of interest (*p53*) is under the control of the hybrid promoter consisting of *Saccharomyces cerevisiae* GAL4 upstream activating sequences (UAS) (Giniger *et al.*, 1985; Wang *et al.*, 1994) linked to the TATA box sequence from the adenovirus major late E1b gene (Lillie and Green, 1989). Without additional factors, the GAL4-E1b promoter is transcriptionally silent.

The second component of the GeneSwitch system is the pSwitch regulatory vector, Figure 11B, which expresses a GAL4-DBD/hpR-LBD/p65-AD regulatory fusion protein.

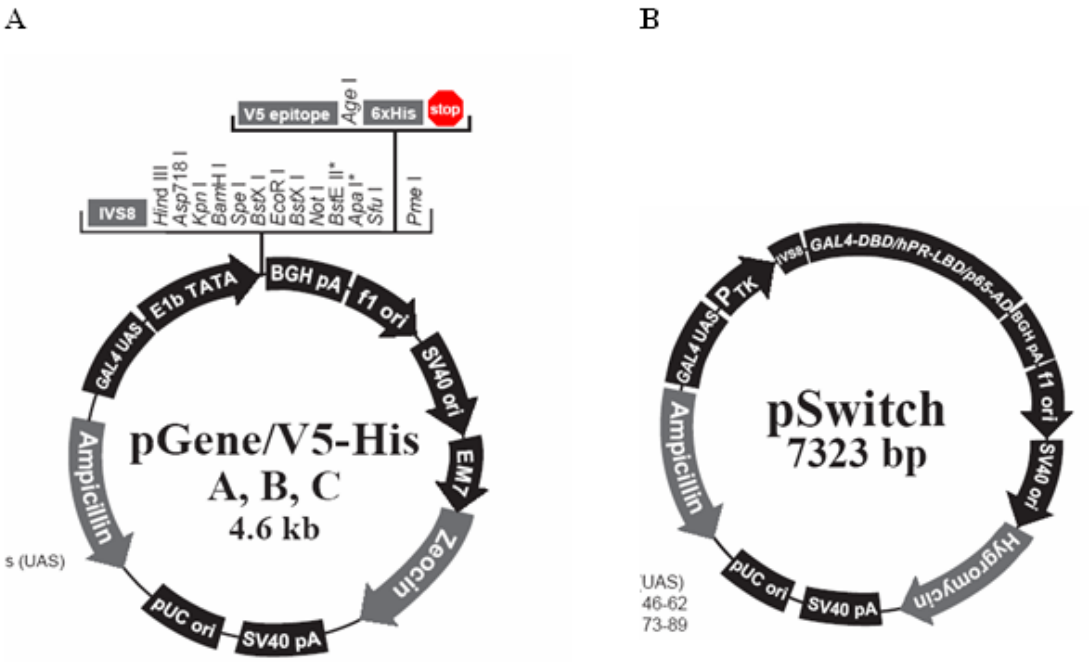

Figure 11: Plasmid vector maps of A) pGene/V5-His (B), prior to gene insertion, and b) pSwitch. The wild type *p53* gene was cloned into the pGene/V5-His vector. The mutations in *p53* were introduced by site-directed mutagenesis. pSwitch vector is used to allow control the gene expression of the cloned *p53* variant in pGene, Figures are adapted from Invitrogen (29).

The regulatory fusion protein functional domains are explained below:

- Gal4 DNA Binding Domain (Gal4-DBD) to bind the regulatory protein to the GAL4-E1b promoter
- Truncated human Progesterone Receptor Ligand Binding Domain (hPR-LBD) that undergoes a conformational change when it binds the progesterone antagonist, mifepristone
- Transcription activation domain from the NF-□B transcription factor p65 (p65AD) to activate transcription from the silent GAL4-E1b promoter (our gene of interest).

Low basal transcription of the regulatory fusion protein occurs in the cell. The synthetic steroid, mifepristone (Invitrogen), is used as an inducing agent to activate transcription of the gene of interest as well as transcription of the regulatory fusion protein.

This works as follows, in the absence of mifepristone, the conformation of the hPR-LBD region prevents the regulatory fusion protein from activating transcription from the GAL4-E1b promoter. When mifepristone is added and binds the hPR-LBD region, the regulatory fusion protein assumes a conformation that permits it to stimulate transcription from the GAL4-E1b promoter, Figures 12 and 13.

Accordingly this leads to activation of the gene of interest located on the vector pGene/V5-His. In addition, four Gal4 binding sites upstream of the minimal HSV TK promoter on pSwitch can bind the regulatory fusion protein. Therefore, adding mifepristone also up-regulates production of the regulatory protein, Figure 13. The increased levels of the GeneSwitch™ regulatory protein result in induction of the gene of interest from pGene/V5-His to levels that can approach those of viral promoters.

The following figures are adapted from Invitrogen manual for GeneSwitch System.

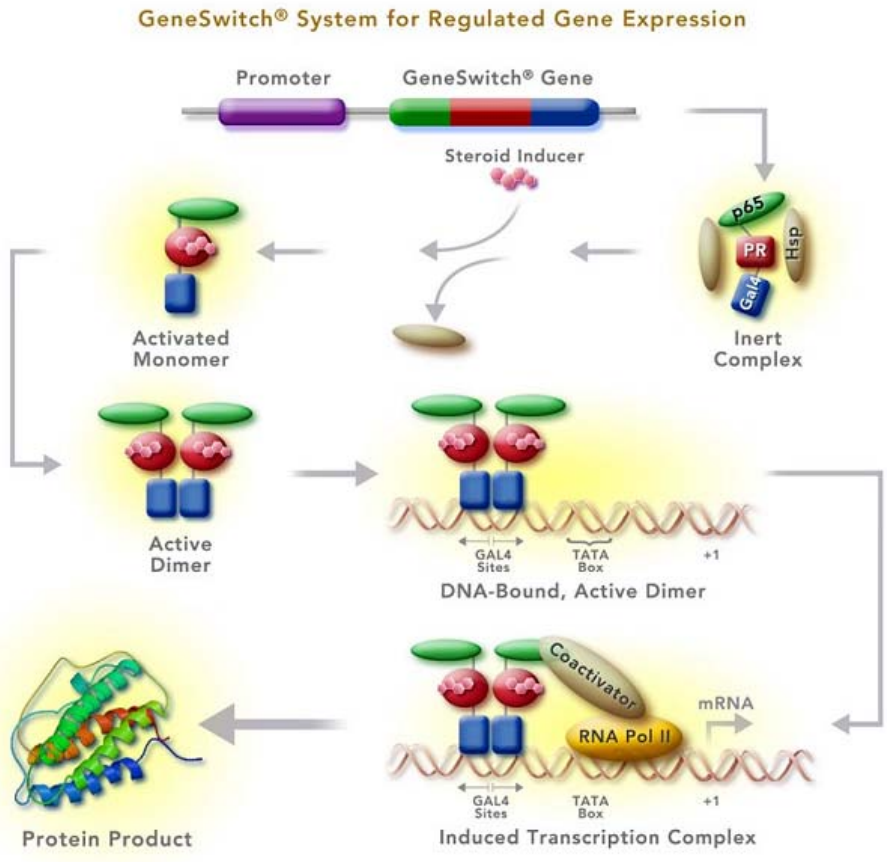

Figure 12: Regulating the expression of the gene of interest, the *p53* gene in this case (29).

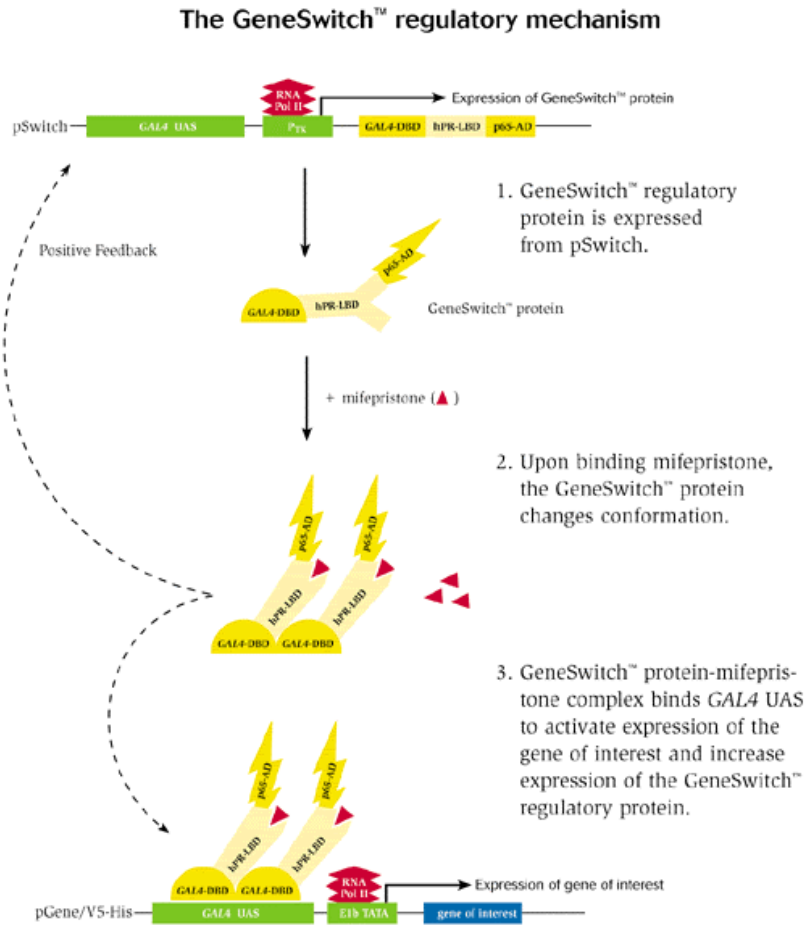

Figure 13 Regulating the expression of the gene of interest, the *p53* gene in this case (29).

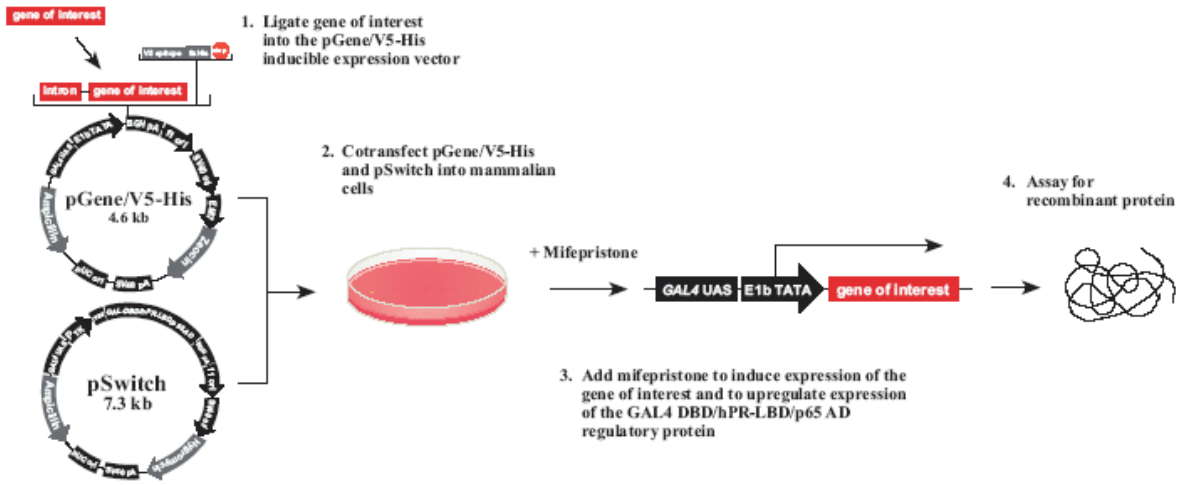

Figure 14: Illustrates the steps of expressing the gene of interest in GeneSwitch System (29).

Expression of p53 in pGene/V5-His-wtp53 vector:

The *p53* is expressed as a p53-V5-His-tag fusion protein in the pGene/V5_his-wtp53 vector. A fusion protein is a protein created through genetic engineering of two or more proteins/peptides. This is achieved by creating a fusion gene, which includes replacing the stop codon of *p53* gene and substituting it, in frame by tryptophan (W) then appending the DNA sequence of the V5 epitope in frame to the *p53* coding sequence. The normal *p53* stop codon (UGA) is changed to (UGG) which codes for Tryptophan (W) by site-directed mutagenesis such that the following peptides are fused in-frame. This reconstructed *p53* coding sequence can be expressed by the cell as a single fused protein. The size of this reconstructed *p53* gene insert is approximately 1.3kb giving rise to protein of 48 kDa.

Site-Directed Mutagenesis (SDM):

Site-directed mutagenesis, also known as site-specific mutagenesis is the method used to create specific mutations *in vitro*, in a given DNA sequence. Methods for site-directed mutagenesis can be classified into two groups: non-PCR (polymerase chain reaction) based and PCR based. Today, PCR based methods are most commonly used. Site directed mutagenesis could alter DNA sequences at a single site or at multiple sites. Alternatively, base pairs may be substituted, inserted or deleted (30).

PCR based mutagenesis:

The site-directed mutagenesis in this study was done by running a PCR (polymerase chain reaction) mutagenesis. The principles of a PCR mutagenesis are identical to the "basic" PCR principles; except that the primers used to introduce mutation(s) (mutagenic primers) are complementary in sequence and are in opposite direction (30).

Making mutations:

The specific method employed involves creating primers (forward and reverse) that are identical to the parental DNA with the exception for one specific base. The primers anneal to the parental single-stranded DNA template, and a high fidelity DNA polymerase (pfu) synthesizes the remainder of the plasmid. Site-specific mutations are most commonly designed in a synthetic oligonucleotide referred to as the mutagenic

oligonucleotide (or primer). For best results, mutations should be placed in the middle of the oligonucleotide sequence (30). An overview over PCR mutagenesis is outlined in Figure 15.

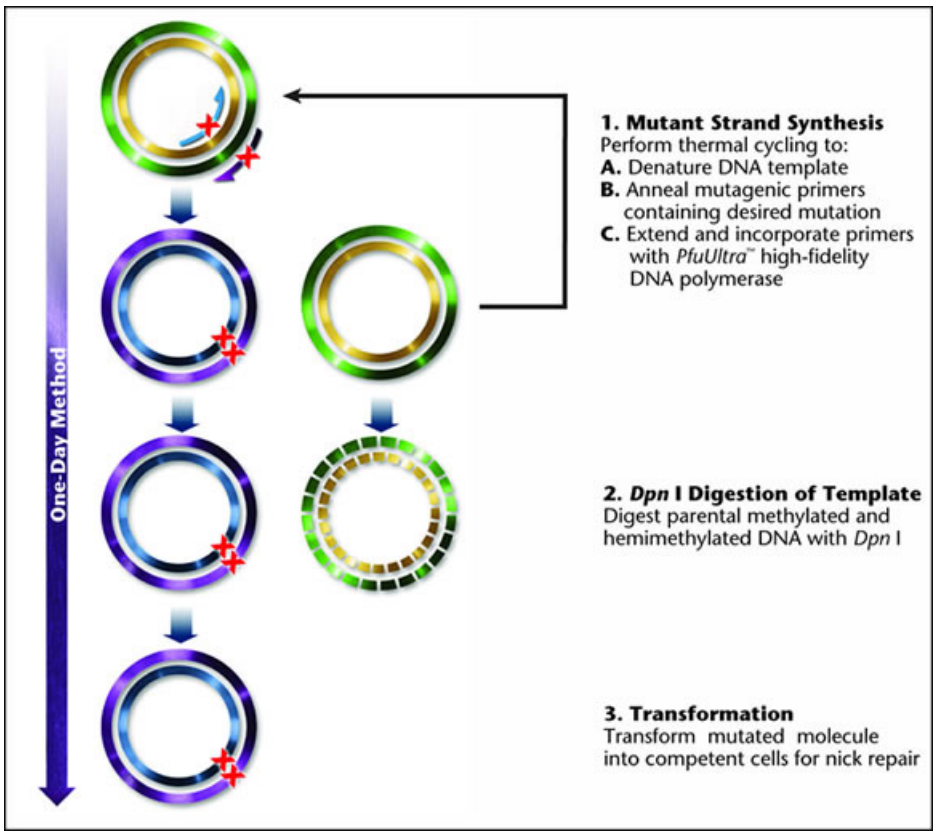

Figure 15: An overview of the PCR site-directed mutagenesis. Figure is adapted from Stratagene manual of site directed mutagenesis kit

The Quick Change® kit (Stratagene) was used in all generated mutations in *p53*. This method is a PCR based mutagenesis method employing two complementary primers in opposite directions, but containing the desired mutated sequence (30). Purified DNA of the entire cloned wt *p53* gene in pGene/V5-His6 was used as the DNA template. The primers used to generate the two mutations R249S and R273H are presented in Table 4.

*Dpn*I treatment:

After the PCR mutagenesis, the PCR mixture will contain a mix of newly synthesized plasmids with the desired mutation and parental DNA strands that do not contain the mutation (wt). To remove the undesired parental DNA containing the wt gene, the mixture was treated with *Dpn*I. *Dpn*I is an endonuclease that digests only methylated and

hemi-methylated DNA at the target sequence 5`-G$^{Me}$ATC-3`. Since the PCR is done in absence of methylated bases and methylating enzymes, the only DNA that would be digested is the methylated, non-mutated-parental DNA. This is because the parental DNA has been isolated from *Escherichia coli*, and almost all *E. coli* strains are dam+ methylated and therefore susceptible to *Dpn*I digestion. (QuickChange® Multi Site Directed Mutagenesis Kit).

Experimental steps of SDM:

QuikChange (Stratagene) protocol was followed in the site-directed mutagenesis. The PCR mixture for site-directed mutagenesis of the different mutations was composed of 1X reaction buffer, 50ng DNA template pGene/V5-His6 50pmol of each forward and reverse primer, Table 4, 10mM of each dNTP, and distilled water to a total volume of 50µL. 2.5U of Pfu Ultra DNA polymerase (Stratagene) was added subsequently. The PCR cycle was as follows: 1 cycle at 95°C for 3 minutes**,** 16 cycles at 95°C for 30 seconds, 70^{o}C for 13 minutes and hold at 4°C.

Following the PCR, 10µL of the product was mixed with 5µL loading buffer and loaded into a well in 0.8% agarose electrophoresis gel. BenchTop 1kb DNA ladder (Promega, Madison, WI, USA) was used as a molecular weight standard. The gel was run at 120V for 1 hour.

10U of *Dpn*I (Stratagene) was added to each PCR mixture and mixed gently and were then incubated at 37°C for 1 hour.

Competent cells and transformation:

Competent cells are bacteria that can accept extra-chromosomal DNA or plasmids. Transformation is defined as the uptake of DNA. This means that the pGene/V5-His-p53 vector is "transferred" into *E. coli* cells. The aims of transformation are to:

- Seal the staggered nicks in the vector, introduced by the site directed mutagenesis.
- Amplify the vector of interest.

A bacterium does not normally take up much free DNA from the environment; competent bacteria cells are therefore used in transformation. Competent cells are cells treated with

(among other things) a high salt concentration solution. The pores in the cells will open, and DNA may enter more easily in these cells. Also, when performing the transformation the cells are heat shocked, and this increases the transformation efficiency.

Transformation:

The pGene/V5-His-p53 containing wt or the engineered mutants were transformed into competent *E. coli* cells using the XL1 blue strain (Stratagene). The plasmid DNA was purified using QIAGEN Plasmid Purification kit: mini and midi protocols, (QIAGEN, Hilden, Germany).

pGene/V5-His empty vector DNA was used as control and referred to as Empty Vector EV. Wild type *p53* and mutants were cloned into pGene plasmid and sequenced before the start of this study (El-Gewely unpublished data). The engineered *p53* mutant R273H was also cloned in this vector. (El-Gewely and Stromberg unpublished data).

Experimental steps of transformation:

Growing E.coli for plasmid preparation:

25 ml of LB media containing 10mM $MgSO_4$ and 100 μg/ml ampicillin was added into each of five sterile flasks. Using a sterile hot needle, colonies were picked from the plates marked with different plasmids and inoculated accordingly in the five flasks:

- pGene/V5 His-Empty Vector
- pGene/V5 His-R249S
- pGene/V5 His-R273H
- pGene/V5 His-wtp53
- pSwitch

The flasks then were incubated in a shaker at 37° C overnight. The cultures were transferred to tubes and centrifuged at 6000 x g for 15 minutes (6000 rpm in Sorvall GSA rotor). The tubes containing the cell pellets were placed on ice and a 4 ml resuspension buffer (provided with the kit as P1) was added to each tube. Then 4 ml lysis buffer (P2) were very gently mixed and incubated for 5 minutes at room temperature. The same was repeated with neutralizing buffer (P3).

After 15 minutes of incubation on ice, tubes were centrifuged at ≥ 20.000 x g for 30 minutes (13000 rpm in a Sovarall SS-34 rotor). The supernatants were then applied on

equilibrated QIAGEN-Tip 100 and allowed to enter the resin by gravity flow. After washing with the washing buffer (4ml), all the QIAGEN-Tip 100 were moved to new tubes and DNA was eluted by adding 5ml QF buffer provided with the kit. In order to precipitate the DNA, isopropanol (0.7 Volume) was added to the eluted DNA, mixed and centrifuged immediately at ≥15000 x g for 30 minutes. The supernatant was carefully decanted and the DNA was washed with 70% ethanol, dried then re-suspended in TE buffer then frozen at –20°C until used.

DNA Sequencing:

DNA sequencing was made according to the Sanger *et al.*, 1977 method using chain-terminating nucleotide analogs (31)

Experimental steps of DNA sequencing:

Two sequencing reactions were run to sequence both strands of DNA using forward and reverse primers.

pGene forward primer, Table 5.

BGH reverse primer, Table 5.

The reaction mixture was as follows:

300 ng ds DNA template,

2.5X BigDye 3.1,

3.2 pmol pGene forward or reverse primer,

5X sequencing reaction buffer

Sterile distilled water to a total volume of 10μL.

The reaction cycling was as follows:

1 cycle at 96°C for 5 minutes,

30 cycles at 96°C for 10 seconds,

30 cycles at 50°C for 5 seconds,

30 cycles at 60°C for 4 minutes,

hold at 4°C.

Tubes were centrifuged in a microcentrifuge. The capillary system part of DNA sequencing was done locally in the Department of Medical Genetics, Tromsø University,

using 3130X Genetic Analyzer, Applied Biosystems/HITACHI). Sequence analysis was done using "BLAST 2 SEQUENCES" in NCBI BLAST engine for local alignment. http://www.ncbi.nlm.nih.gov/blast/bl2seq/wblast2.cgi

Mammalian Cell Culture:

Saos-2 cells used in this study:

A human osteosarcoma Saos-2 cell line (ATCC, USA) was used as the transfection recipient of the *p53* variants. Saos-2 cell line is *p53*-null cell line

Establishing permanent cell lines with inducible p53 variants:

The cell cultures were cultivated in incubators 37°C with the presence of O_2, 5 % CO_2 and humidity.

Transfection:

Transfection is the delivery of foreign molecules such as DNA into eukaryotic cells. Two principally transfection approaches can be used, transient or stable transfection. Transient transfection is when the DNA is introduced to the nucleus of the cell, but does not integrate into the chromosomes. Expression of transiently transfected gene can typically be analyzed within 24-96 hours after introduction of the DNA. But a stable transfection, as was performed in this study, is when the transfected DNA is either integrated into the chromosomal DNA or maintained as an episome. Using the selective drugs resulted in selection of the cells containing the desired vectors and eliminating the cells that does not contain the desire plasmid constructions.

Transfection was performed using GeneJammer® Transfection kit (Stratagene®, CA, USA).

Experimental steps of transfection:

The same amounts of plasmid DNA (2µg DNA) were transfected into equal numbers of cells from the same batch. 2.5 x 10^5 exponentially growing cells were inoculated in each well of 6 wells culture plate and grown in appropriate volume of DMEM + Serum + Antibiotics for 24 hours prior to transfection. The DNA amounts were detected according to Stratagene GeneJammer® Transfection kit as outlined in Table 13.

Table 13: DNA amounts used for transfection

	p Switch	**Wild Type p53-** pV5- His plasmid	**R249S-** pV5- His plasmid	**R273H-*** pV5- His plasmid	**Empty pV5- His plasmid**
DNA Concentration	0.18 μg/μL	0.35 μg/μL	0.15 μg/μL	0.25 μg/μL	0.30 μg/μL
Mass at 4:1 ratio	0.4 μ g	1.6 μg	1.6 μg	1.6 μg	1.6 μg
Corresponding Volume	2.2. μL	4.6 μL	10.6 μL	5 μL	5.3 μL
Tubes 1 & 2	2.2. μL	0	0	0	5.3 μL
Tubes 3 & 4	2.2. μL	4.6 μL	0	0	0
Tubes 5 & 6	2.2. μL	0	10.6 μL	5 μL*	0

Transfected human osteosarcoma Saos-2 cells, grown in DMEM with 10% fetal bovine serum (FBS) (Invitrogen), were then selected using both 20 μg/L** Hygromycine (Invitrogen), selection agent for the pSwitch regulatory plasmid, and 20 μg/L** Zeocin (Invitrogen), selection agent for the pGene/V5-His-p53. The cells were then transfered to flasks where stable colonies formed in two weeks in average. When the flasks were approximately 70% confluent, 1 x 10^{-8} M of the mifepristone was added to induce *p53* expression and the cells were incubated for 24 hours.

*The transfection of the mutation R273H was done in a separate experiment under the same conditions.

** The concentrations of zeocine and hygromicine have been optimized in an earlier experiment based on minimal toxic concentration. (Dana Kate Mersich and Raafat El-Gewely, unpublished data).

Isolating Total Proteins from the stably engineered cell lines after induction of gene expression:

When isolating total proteins, the proteins can be in either denatured or non-denatured state. To be able to "fish out" the *p53* protein and its partners by immunoprecipitation, it is essential that the proteins keep their native conformational structure. Therefore, non-denaturating, non-reducing method was used in order to keep the proteins in their native status. This method uses lysis buffer containing Triton X-100 to which protease inhibitor cocktail was added.

Experimental steps of protein isolating:

The monolayer cultures were washed with PBS at room temperature and the flasks were incubated on ice for 1 hour after adding the Triton X-100 lysis buffer. Then the cells were scraped off using rubber policeman. The cell membrane and cell organelles were removed after centrifuging the whole contents for 10 minutes at 16000 x g at 4°C.

The protein concentrations were measured using protein concentration assay (RC DC BioRad) by making standard curves based on known concentrations of Bovine Serum Albumin (BSA). Absorbance was read using spectrophotometer (Medinor produkter, MediSpec III) at 750 nm and the unknown concentrations were calculated from the equation of the standard curve.

Western Blot:

It was important that the stable cell lines made express *p53* in an inducible manner. So in order to verify that the cell lines express *p53* when induced with mifepristone, and only when induced with it, a western blotting was performed.

Experimental steps of western blot:

Electrophoresis:

Total proteins were extracted from Saos-2 cells with different *p53* variants, both induced and non-induced *p53*. 15 µg extract and 10 µl SDS-PAGE sample application buffer containing freshly added 200 mM DTT was mixed. Biotinylated standard was diluted in sample buffer 1:20. The samples were heated (85-95°C) for 10 minutes using a heat block and were then cooled and centrifuged at max speed for a few seconds. The samples were applied on the gel and the gel was run for 50 minutes at 200 V.

Immunoblotting:

Immobilon™-P nitrocellulose membrane (Millipore cooperation, USA) was washed for 3 seconds in methanol and for 10 seconds in dH_2O and incubated for at least 5 minutes in the blotting buffer. The gel and the Immobiline-P membrane were assembled in Mini Trans-Blot and blotting was run at 400 mA, 100 V for 1 hour.

Immunodetection:

Nitrocellulose membrane was washed at room temperature with gentle agitation in 25 ml PBS and in 25 ml blocking buffer for 10 minutes and 1 hour, respectively. The membrane was then incubated in Anti p53 antibody (Zymed, CA, USA) overnight at +4°C. The membrane was washed 3X for 5 minutes with 25 ml PBST with gentle agitation. Goat anti mouse IgG (Invitrogen) secondary antibody was added after having been diluted according to the manufacturer's recommendation into blocking buffer. The membrane was then incubated with gentle agitation for 1 hour. The membrane was then washed again 3X for 5 minutes in 25 ml PBST and 2X for 5 minutes in western wash buffer.

Alkaline Phosphatase detection reaction:

Detection of secondary antibody: alkaline phosphate (using CDP-Star).

6 ml CDP star assay buffer and 12 µl CDP star were added to the membrane and shaked manually. The membrane was wrapped in plastic foil and sealed properly so it does not dry. Then the sealed membrane was wrapped in aluminum film and kept in darkness at room temperature for 30 minutes. A western blotting image was then taken by exposing the membrane in Lumi-Imager F1.

Immunoprecipitation:

In order to isolate protein partners of p53 and study the protein-protein interaction, immunoprecipitation using antibodies against V5 epitope was performed.

IP followed by SDS-PAGE immunoblotting, 2D gel etc., is routinely used in a variety of applications to determine the molecular weights of protein antigens, to study protein-protein interactions, to determine specific enzymatic activity, to monitor protein post-translational modifications and to determine the presence and quantity of proteins. The IP technique also enables the detection of rare proteins which otherwise would be difficult to detect since they can be concentrated up to 10,000-fold by Immunoprecipitation (32).

In the IP method, the protein(s) from the cell or tissue homogenate is precipitated in an appropriate lysis buffer by means of an immune complex which includes the antigen protein (here: p53 and its partners), primary antibody (V5 antibody) and Protein G- (or A-, or L)-agarose conjugate, Figure 16, (32).

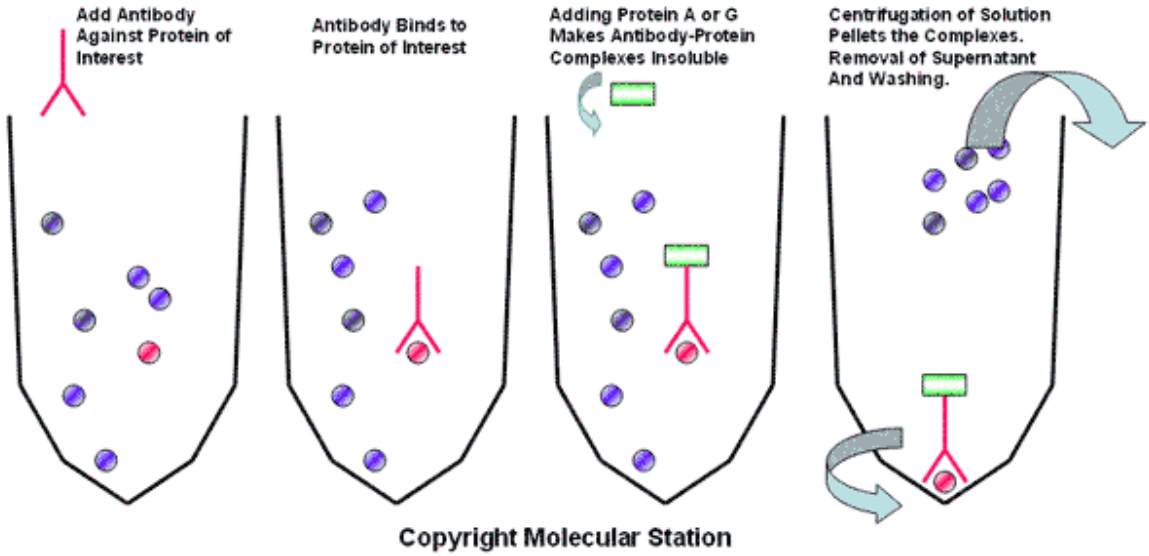

Figure 16: Schematic representation of the principle of Immunoprecipitation. An antibody is added to a mixture of proteins and binds specifically to its antigen. Antibody-antigen complex is absorbed from solution through the addition of an immobilized antibody binding protein such as Protein A-Sepharose beads (or protein G) (third panel). Upon centrifugation, the antibody-antigen complex is brought down in the pellet (fourth panel). Figure is adapted from Molecular Station website http://www.molecularstation.com (33).

Experimental steps of immunoprecipitation:

50µl of -G Sepharose™ resin slurry in lysis buffer (containing 2,5µl/ml protease inhibitor cocktail) was added per 1 ml of supernatant to pre-clear cell-lysates. The mixture was incubated at 4°C with continuous rocking for 1 hour and then centrifuged at the same temperature.

1.5 µg (typically, 1.5 µl) of Anti-V5-HRP Antibodies and 50 µl of the Protein-G Sepharose™ resin slurry were added to the supernatant and rocked overnight at 4°C. The mixture was centrifuged for 1 minute at 10000g at 4°C and the resin slurry was washed 5X in pre-chilled lysis buffer containing 2,5µL/ml protease-inhibitor. The beads were then resuspended in sample application buffer and then centrifuged again under the same conditions (10000 g at 4°C for 1 minute). The supernatant was stored at -80°C.

Two Dimensional Gel Electrophoresis:

Proteomics:

Proteomics, the large-scale analysis of proteins is contributing greatly to our understanding of gene function in the post-genomic era. Proteomics is used for identifying and quantifying expressed proteins in cells, organisms or fluids. It is also a mean for localizing proteins in the cell and detecting protein modifications and interactions (34).

High-resolution two dimensional polyacrylamide gel electrophoresis (2D-PAGE or 2D-gels) is a powerful technique for analyzing protein composition of a cell, tissue and fluids, as well as for studying changes in global patterns of gene expression elicited by a wide array of effectors. The method has become increasingly important after the development of identifying the individual spots on the gel by mass spectrometry analysis (35).

The 2D-gels separate polypeptides on the basis of their ioselectric points (p*I*) in the first dimension and the molecular weights in the second dimension. Adding ampholytes to an acrylamide strip generates the IEF (isoelectric focusing) gradient. The ampholytes are a mixture of amphoteric species with a range of pH values. This IEF separates protein based on their ioselectric point (p*I*) and is accomplished by the pH gradient established in the acrylamide. Proteins migrate through the pH gradient until they reach the pH at which their net charge is zero whereupon the protein stops and focuses at that point. The second dimension separates the proteins on the basis of molecular weight in an SDS gel. This is accomplished by laying the strips (from 1 dimension) on top of a slab-type SDS-polyacrylamide gel. Prior to this, the strips were equilibrated in equilibration buffers, Table 11. Most of the proteins will dissociate into their polypeptide subunits and will be coated with SDS. This protein-SDS complex (mass ratio 1:14) consists of the hydrocarbon chains of the detergent in a rigid association with the polypeptide chain leaving negatively charged sulfate ions of the detergent (SDS) exposed to the aqueous medium. The native charge of the polypeptide is overcome and the complex migrates as an anion. The rate of the migration correlates with the molecular weight of the protein (36) .

Experimental steps of 2-DE:
Sample preparation:

Concentrating the samples:

When the total protein concentration was low, the following method was used to concentrate the samples:

Five volumes of acetone was added to each diluted sample and incubated at room temperature for 30 minutes. The samples were then centrifuged for 15 minutes at 6400 x g (corresponds 6000 rpm in BS4402/A HERAEUS SEPATECH) at 4°C. The supernatant was removed and the samples were rehydrated using 125 µl or 250 µl sample application buffer, Table 11.

1 µl IPG buffer and 1,3 µl of 1,5 M DTT were added to each 125 µl of sample application buffer. The samples were then loaded on the strips ceramic holders and the strips were placed upon them. Liquid paraffin was used to cover the strips. First and second dimensions of electrophoresis were run according to Tables 14 and 15, respectively.

We have increased the concentration of total protein gradually until we could get some better results. The amount of total protein run on a gel was 450 µg. This amount was decided after several pilot experiments. In immunoprecipited proteins experiments, we used 2 mg total protein for immunoprecipitation. Of the immunoprecipitation final product, we tried various volumes to run on a gel and after pilot experiments we found that 45 µl was the minimal volume that could show some faint spots when the gel is stained with SYPRO Ruby.

The first-dimension: Isoelectric focusing (IEF):

IPGphor (Pharmacia Biotech) was used for 1st dimension Electrophoresis.

Table 14: Shows the conditions of first dimension separating, S1 is rehydration step

	S1	**S2**	**S3**	**S4**	**S5**	**S6**	**S7**	**Total**
7 cm	30 V	300 V	1000 V	2500 V	5000 V	5000 V	-	20000
strips	10:00 hrs	1:00 hr	1:00 hr	1:00 hr	1:00 hr	3:00 hrs	-	vhr
13 cm	30 V	300 V	600 V	1000 V	4000 V	8000 V	8000 V	40000
strips	10:00 hrs	1:00 hr	1:00 hr	0:30 hr	2:00 hrs	2:00 hr	4:00 hr	vhr

When the first dimension is complete, the strips were equilibrated equilibration in buffers 1 and 2, for 15 minutes, Table 11.

The second dimension: SDS-PAGE electrophoresis:

PowerPac HC™ (Bio-Rad) was used for 2nd dimension.

The gels were made and formed in our labs, Table 11. The strips were placed on the tops of the gels. One or two strips per gel for 13 or 7 cm strips, respectively. The tops of the gels were sealed by 1 ml 5% Agarose and the gels were run under the conditions shown in Table 15.

Table 15: Shows the conditions of second dimension separating

	Volt	**Amp**	**Watt**	**Hours**
7 cm strips	250	0,16	150	2-2,5
13 cm strips	250	0,32	150	3-4

Protein spot detection:

Protein spots can be resolved on 2D gels visualized using a variety of methods, including Coomassie brilliant blue staining and SYPRO Ruby. In this experiment we mainly used Coomassie brilliant blue staining. SimplyBlue® Safe Stain from Invitrogen. Sometimes we used SYPRO Ruby (Bio-Rad) staining for immunoprecipitated proteins in an attempt to show the spots resulting from low protein concentration. SYPRO Ruby is known to be 30 times more sensitive than Coomassie blue. Staining was done according to the instruction of the manufacturer.

Gel Analysis:

Protein profiles for the empty vector, wild type and mutant *p53* were scanned and quantified to search for differences in expression, such as change in the level of protein expression or appearing/disappearing of peptides/proteins. The current 2D PAGE techniques make it possible to visualize maximum about 4000-5000 proteins. This number is only a fraction of the number presented in any eukaryotic cell. Some proteins are also not detected, since they are not resolved by the pH gradient, because they are too basic or too acidic. Solubilization problems may prevent them for entering the first

dimension, because they precipitate and streak the run or because of limitations in the sensitivity of current detection methods.

PDQuest software from Bio-Rad was used to analyze the protein spots and compare the spots in different gels for the different *p53* alleles. Spots were studied and 12 differentially expressed spots were selected, excised from the gels and sent to further analysis by mass spectrophotometry.

Mass Spectrometry:

Matrix-assisted lasers desorption/ionization time-of-flight mass spectrometer (MALDI TOF MS) was performed.

Mass spectrometry (MS) is an extremely useful tool in many fields of chemistry and biochemistry. The particular nature of MS that was employed in this experiment involves the trypsinization of the sample protein into many smaller fragments, then a comparison of the mass spectrometry spectra of these fragments with those known peptides in NCBI database http://www.ncbi.nlm.nih.gov/.

MS employed *in situ* trypsinization of the isolated protein spots in gel into smaller peptide-fragments.

GC 8000^{Top}, CEINSTRUMENTS, ThermoQuest, Italy MS was used in the Faculty of Pharmacy, University of Tromsø. Generated data were investigated further using NCBI database.

Results

Site-Directed Mutagenesis (SDM):

Site-directed mutagenesis of *p53* WT to generate *P53*-R249S mutation:

Agarose gel Electrophoresis (0.8%) was run for PCR product in order to check that PCR mutagenesis has generated DNA product and to verify that the product is of the expected size before DNA sequence analysis. The PCR based SDM products revealed a band of the expected size of the linear pGene/V5-His-p53 vector DNA, Figure 17.

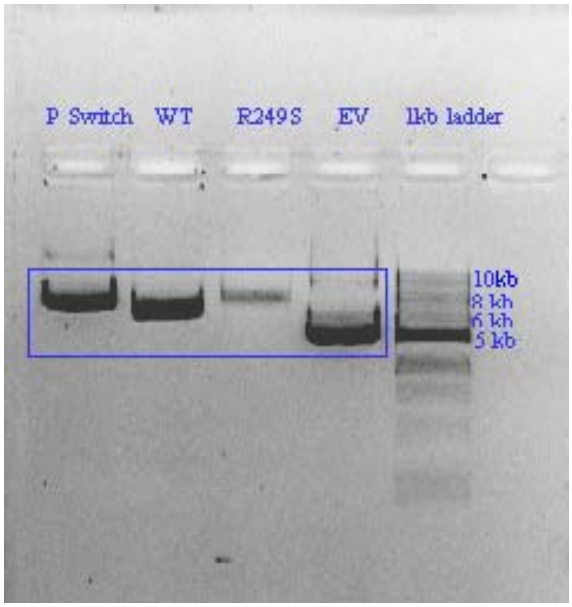

Figure 17: Agarose gel of R249S SDM PCR products, WT plasmid preparation product, pSwitch and pGene (EV). The gel shows bands of the expected size of the pGene/V5-His-p53 vectors, P Switch and empty pGene/V5-His vector

DNA Sequence of pGene/V5-His-p53 (mutants) vectors:

In order to confirm that the targeted mutations were successfully introduced, the *p53* gene cloned in pGene/V5-His vector was sequenced using Sanger chain terminating sequencing method and using Big Dye protocol. The results of the DNA sequence analysis confirmed the presence of the introduced mutation in *p53* coding sequence. Only

one mutation (R249S) will be presented here as an example of how the mutations for the other *p53* mutant (R273H) presented in this work was made.

The sequences analysis obtained were aligned and blasted against WT *p53* using BLAST 2 SEQUENCES in NCBI blast engine:

http://www.ncbi.nlm.nih.gov/blast/bl2seq/wblast2.cgi. This engine offers the possibility to compare two sequences. The alignment revealed the targeted mismatching at the correct place, Figure 18. Full sequence analysis of R249S is presented in appendix 3.

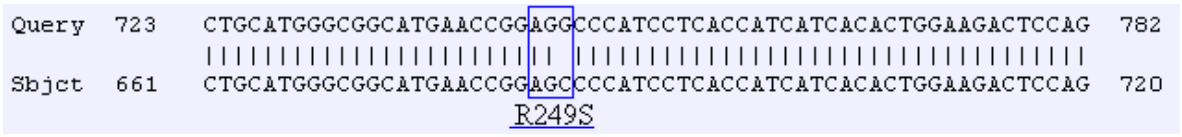

Figure 18: Alignment of the R249S sequence (forward primer) (Subject) with the WT *p53* sequence (Query). (BLAST 2 SEQUENCES RESULTS VERSION BLASTN 2.2.14)

Western blot:

Saos-2 cells were chozen to establish the cell lines because these cells are *p53* null. Permanent cell lines were established expressing wild type *p53*, mutant *p53* or non-*p53* (EV). This expression is controlled through a mifepristone induction system. The selection agents are Zeocine and Hygromycine at concentration of 20 µg/ml of both drugs. Total protein extracts, both induced with mifepristone and non-induced, were checked for the presence of *p53*. Western blotting and Coomassie staining of SDS-PAGE gel were done. Using monoclonal Anti p53 antibody, several bands were observed. The p53-V5 fusion protein has theoretical molecular weight of 48 kDa. The additional bands could be as a result of cross reactivity. As expected and as shown in figure 19 A and B, samples of total proteins isolated from induced p53 showed bands in the three *p53* alleles: WT, R249S and R273H (Lanes 3, 5 and 6, respectively). No bands could be detected in the non-induced WT (Lane 7) and neither induced nor non-induced EV (Lanes 4 and 8, respectively). Two bands appear in the non-induced R249S (Lane 9) and non-induced R273H (Lane 10) indicating some leakage in the *p53* expression in our system. However, the Western experiment needs to be optimized by changing the type of antibody as well as the concentration and also the concentration of total protein used.

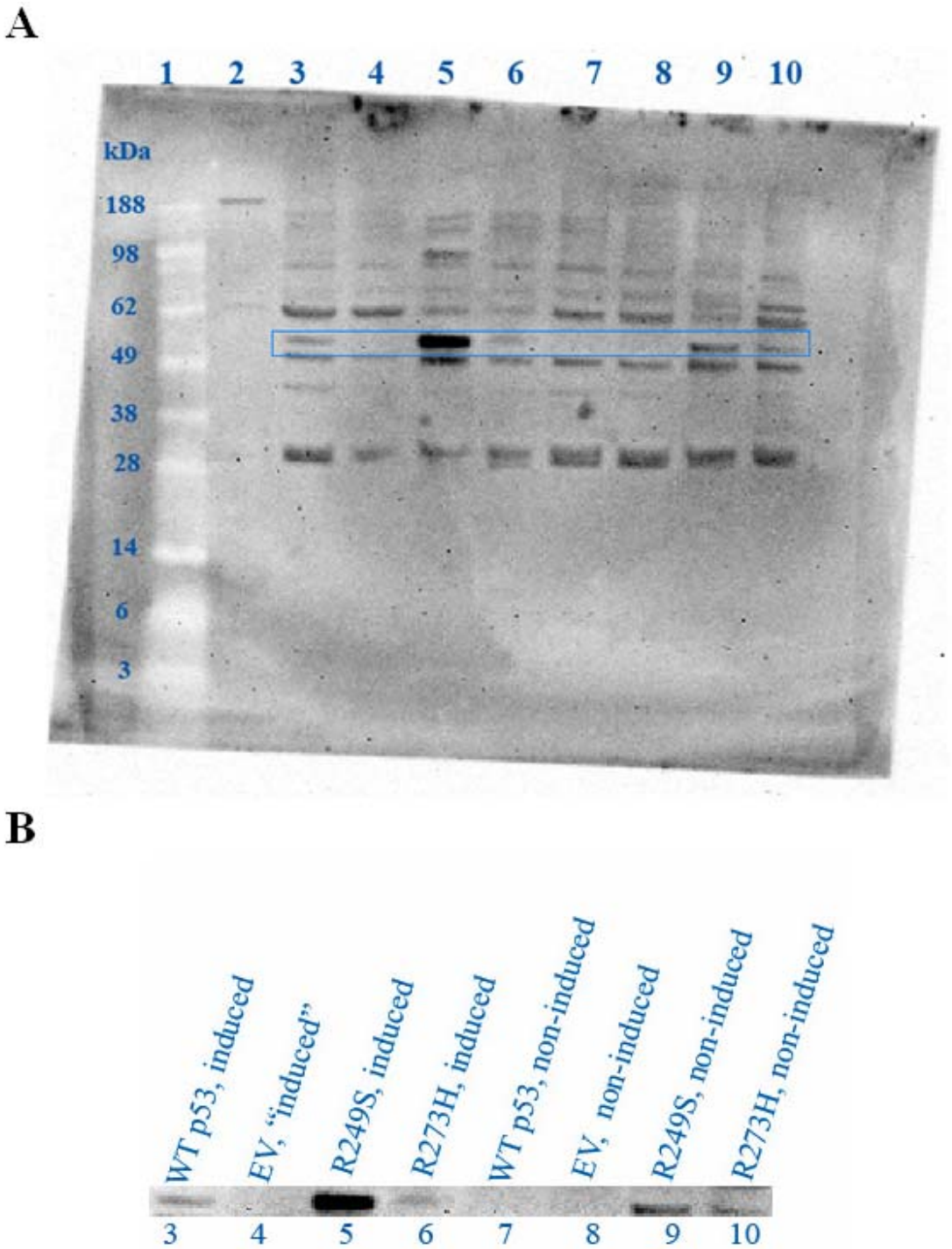

Figure 19: Western blot analysis of *p53* expression in Saos-2 cells. A: Full image. B: Samples of total proteins isolated from induced *p53* showed bands in the three *p53* alleles: WT, R249S and R273H (Lanes 3,5 and 6, respectively). No bands could be detected in the non-induced WT (Lane 7) and neither induced nor non-induced EV (Lanes 4 and 8, respectively). Two bands appear in the non-induced R249S (Lane 9) and non-induced R273H (Lane 10) indicating some leakage in the *p53* expression in our system. Lane 1 Blue Plus 2 Prestained standard. Lane 2 Biotinylated standard did not work.

2D- Gel Electrophoresis

Total proteins expressed under the conditions described earlier, were isolated from the constructed stable cell lines that are based on Saos-2 cells, but contain different alleles of *p53* gene (WT: Wild Type, EV: Empty Vector, and Mutation R249S or R273H). These engineered cell lines were grown in the presence of Hygromycine and Zeocine. Hygromycine is selection agent for the pSwitch regulatory plasmid and Zeocin is selection agent for the pGene/V5-His-p53. The expression of the different *p53* alleles was induced by Mifepristone 1 x 10-8 M for 24 hours.

Aliquots of 450 μg of total protein were used for each gel. This amount was decided after several pilot experiments. As for the immunoprecipitated protein, the gels presented here were run using 45 μL of the immunoprecipitation proteins resulting from 2 mg total protein prior to the IP.

Immunoprecipitated p53- V5 fusion protein:

P53 and its partner proteins were isolated from the total protein using anti V5 antibody.

Figure 20 shows 2D gel resulted from running 45 μL immunoprecipitated R249S and R273H mutant p53-V5. Two 7 cm IPG strips were applied on the same gel, which was stained with Coomassie Blue. No spots were detected.

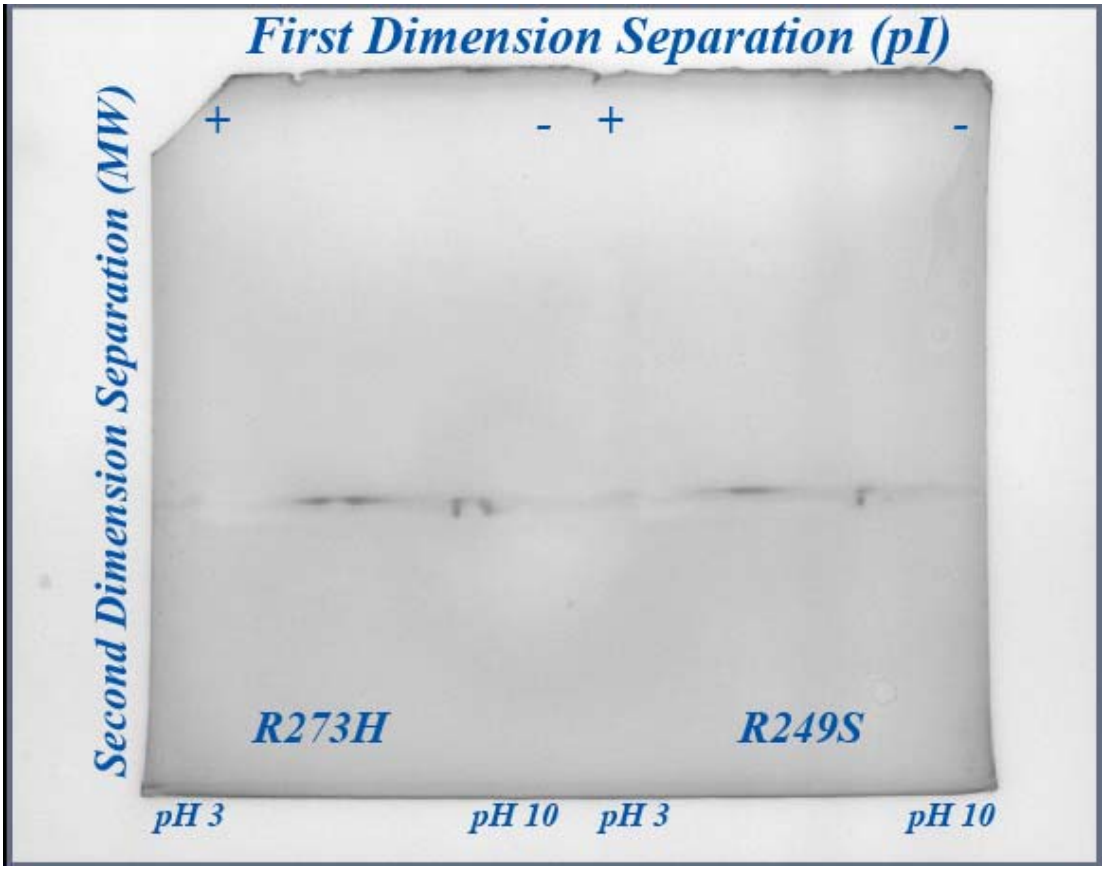

Figure 20: Immunoprecipitated *p53*-V5 fusion protein as precipitated by anti V5 antibody and run on 2D gel and stained with Coomassie Blue. The gel showed no spots.

Figures 21 and 22 show 2D gel results using the 45 µl of the IP protein isolated from 2 mg total protein. Gels were stained with SYPRO Ruby, which is known to be 30 times more sensitive than Coomassie Blue. Some faint spots could be detected. However, the results are still unreliable since it has not been repeated and the spots were not as differential as expected. This could reflect problems with the IP procedures optimization or the type of antibody used.

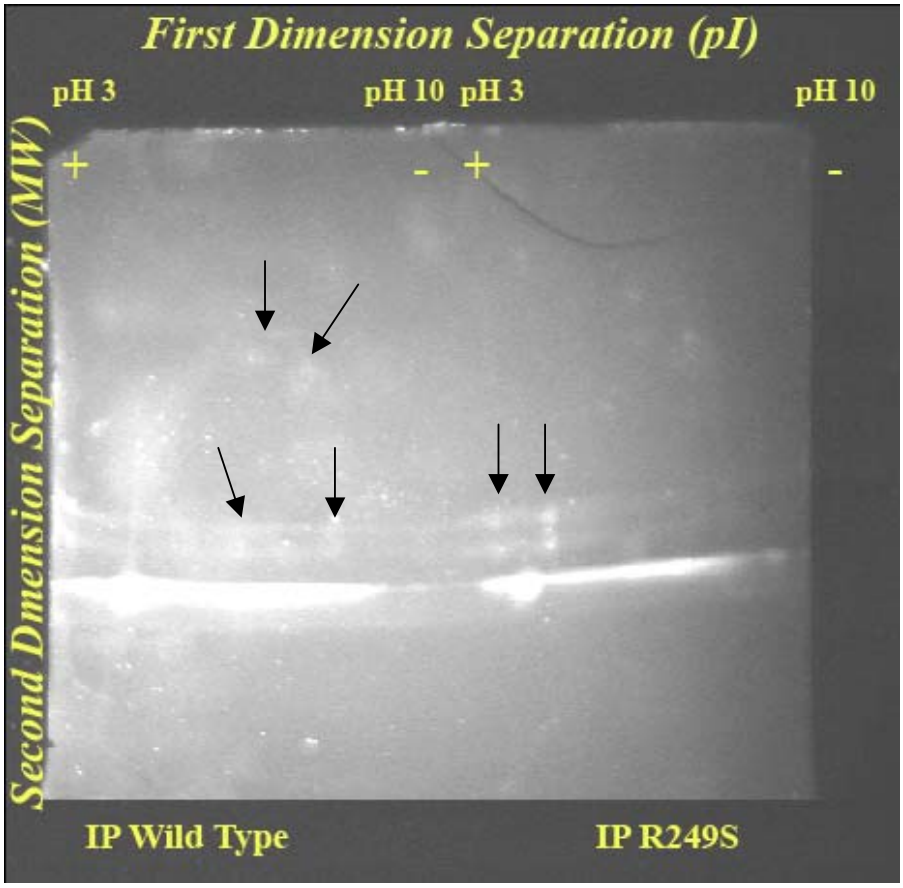

Figure 21: 2D gel of immunoprecipitated *p53*-V5 protein (WT and R249S) with anti V5 antibody and stained with SYPRO Ruby. Arrows indicate few faint spots. Spots are poorly separated and the quality of the 2D gel makes it not possible to conclude any differences in the expression patterns between the two *p53* variants shown here.

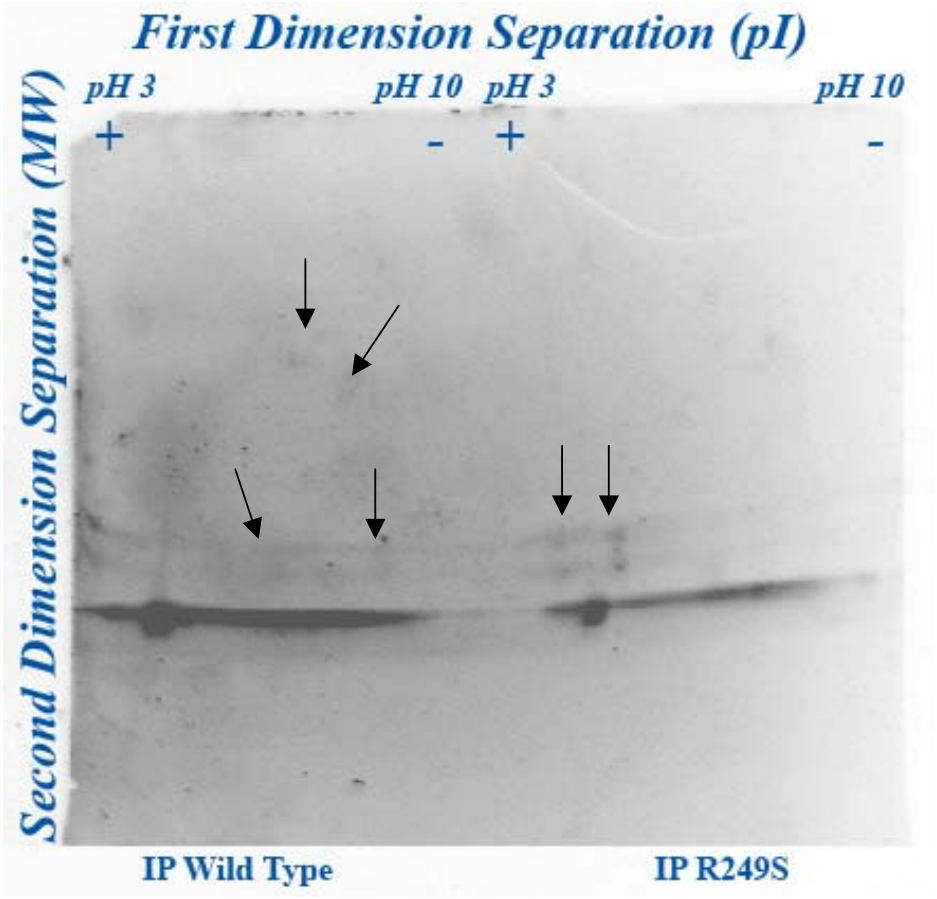

Figure 22: The same 2D gel of immunoprecipitated p53-V5 protein (WT and R249S) with anti V5 antibody and stained with SYPRO Ruby, inverted colors. Arrows indicate the same spots marked in Figure 21.

Limited attempts to increase the intensity of the spots by increasing the amount of protein samples loaded on the gels and the amount of the protein used for immunoprecipitation, were not successful. Due to these IP results and limited time available for this study, we concentrated on the total protein analysis by 2D gel electrophoresis rather than immunoprecipitated protein from the different *p53* variants as compared to the empty vector and the WT.

Total proteins:

Total protein sample of 450 µg from each corresponding cell line were loaded on 13 cm strips holders. The 2D gel electrophoresis was run according to the criteria mentioned in Materials and Methods section. The Coomassie Blue staining of 2D gel separations of the different *p53* types extracts indicated some differences in the resolved proteins spots. The expression patterns of the different samples were similar but not identical.

In this experiment two gels for each *p53* variant were run at the same time and conditions. Figure 23: A, B, C, and D shows one raw 2D-Gel for each *p53* allele.

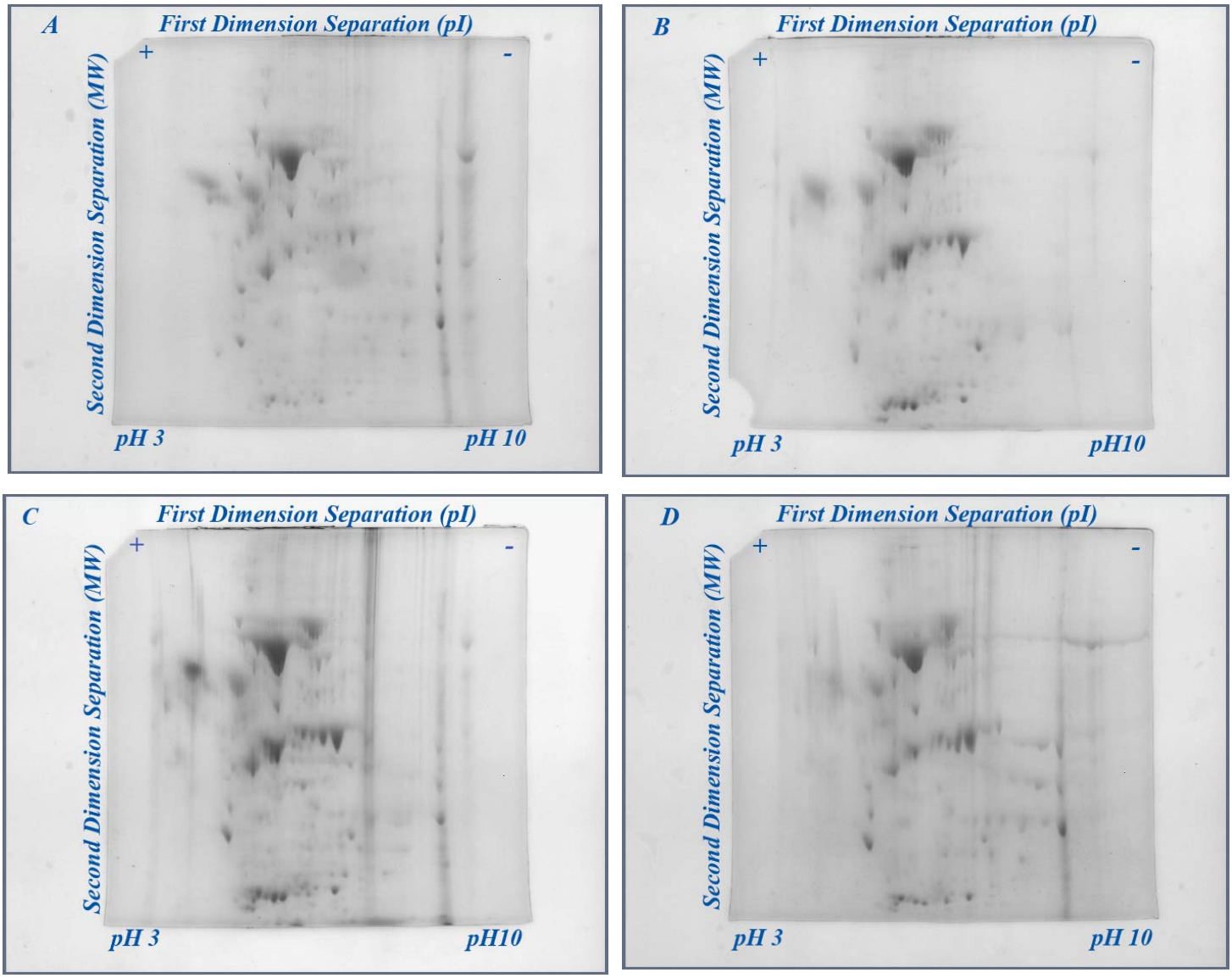

Figure 23: Raw 2D gels of total proteins isolated from Saos-2 cells expressing different *p53* variants. A: Wild Type, B: Empty Vector, C: R249S mutant, D: R273H mutant

The gels were analyzed and the spots were annotated using PDQuest software (Bio-Rad). Twelve protein spots were selected to be isolated and sent to MS analysis because they represented differentially expressed proteins. Figure 24 shows the locations of all the spots on the master gel and the corresponding locations on the appropriate gels. Table 16, presents the expression status of the selected spots in the different *p53* variants.

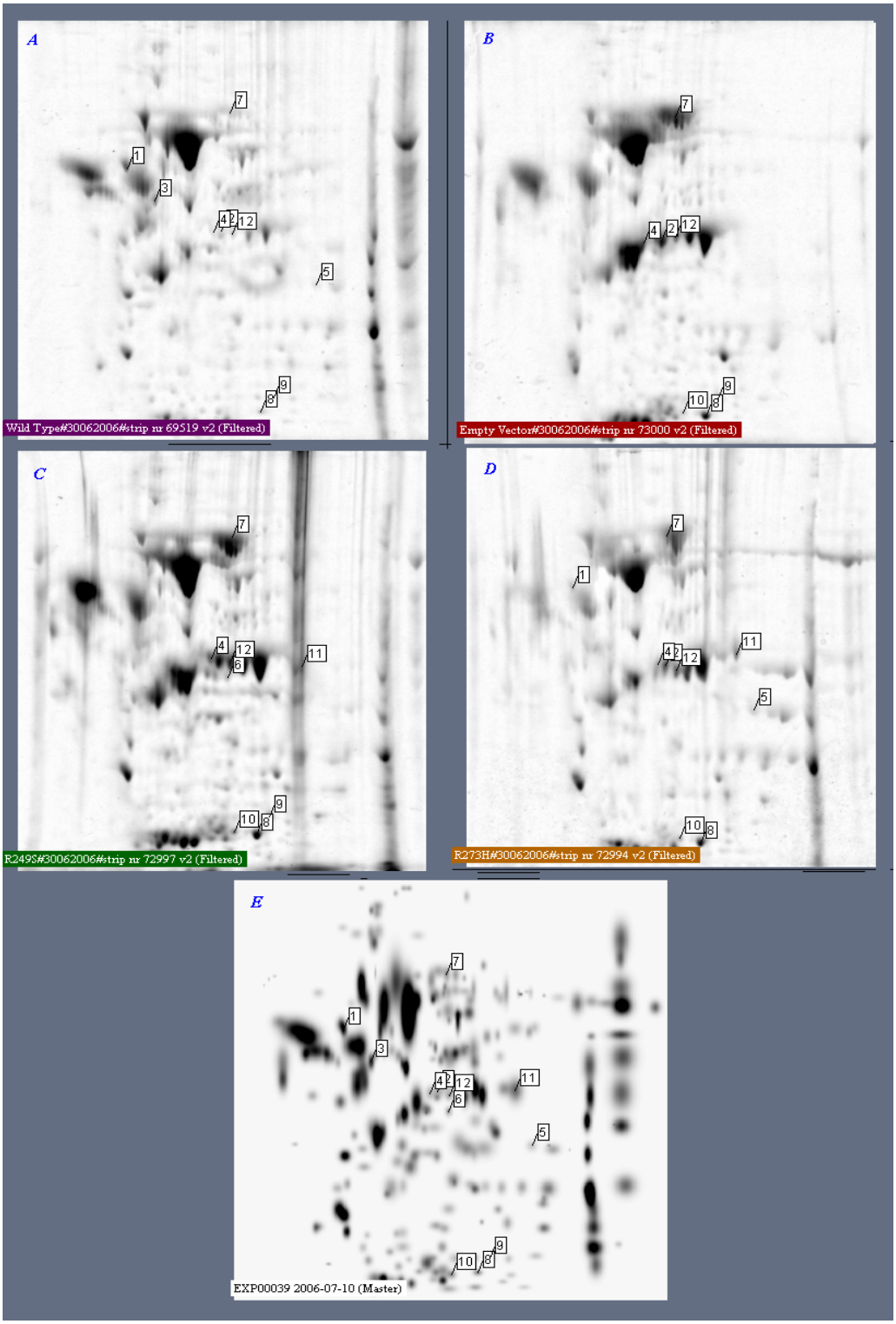

Figure 24: The 2D gel electrophoresis results for total protein from Saos-2 expressing different *p53* variants. A: Wild Type, B: Empty Vector, C: R249S mutant, D: R273H mutant. Numbers indicate the selected differentially expressed spots. Master gel (E) is shown in Gaussian form while all other gels are in filtered forms.

Table 16: The selected differentially expressed spots and the expression status of them

Spot no.	SSP no.	Cut from	Expression in the different types			
			Found in	Missed	Under expressed	Over expressed
1	1702	WT	WT, R273H	EV, R249S	R273H	WT
2	5502	R273H	WT, R273H, EV	R249S	WT	R273H, EV,
3	2503	WT	WT	EV, R249S, R273H		WT
4	4502	R249S	All types, but at variable relative concentrations		WT	EV, R249S, R273H
5	8301	R273H	WT, R273H	EV, R249S	WT	R273H
6	6403	R249S	WT, R249S	EV, R273H	WT	R249S
7	5805	EV	All types, but at variable relative concentrations		WT	EV, R249S, R273H
8	7001	R273H	All types, but at variable relative concentrations		WT	EV, R249S, R273H
9	7102	R249S	WT, EV, R249S	R273H		WT,EV, R249S
10	6001	R249S	EV, R249S, R273H	WT		EV, R249S, R273H
11	7504	R273H	R273H, R249S	WT, EV		R273H, R249S
12	6401	R273H	All types, but at variable relative concentrations		WT	EV, R249S, R273H

MS results of the selected Protein spots:

The MS results could specify 8 previously known and annotated proteins, while it failed to identify the spots numbers 2,4,6 and 7 therefore these spots are addressed further in this study, but these spots will be subjected again for MS analysis. Table 17 summarizes the MS results of the spot/protein identification.

Table17: Mass spectrometry results of the studied spots

Spot nr	GI Identifier	*p53* status of the gel	Identified Protein
1	gi|190384	WT	Prolyl 4-hydroxylase beta-subunit [Homo sapiens]
2	-	R273H	No significant hits
3	gi|37852	WT	Vimentin [Homo sapiens]
4	-	R249S	No significant hits
5	gi|28595	R273H	Aldolase A protein [Homo sapiens]
6	-	R249S	No significant hits
7	-	EV	No significant hits
8	gi|17389815	R273H	Triosephosphate isomerase 1 (TIM) [Homo sapiens]
9	gi|179780	R249S	Carbonic Anhydrase II [Homo sapiens]
10	gi|54855	R249S	Triosephosphate isomerase [Mus musculus]
11	gi|13325287	R273H	Enolase 1 [Homo sapiens]
12	gi|693933	R273H	2-phosphopyruvate-hydratase alpha-enolase; carbonate dehydratase [Homo sapiens]

The 2D gel results represent two gels of the total isolated protein from cells expressing each of the *p53* variant. Although we have delivered twelve spots for MS analysis, only eight spots gave protein identification. Therefore in this thesis, only the spots with identified proteins are discussed further. The spots with poor MS identification are spots

2, 4, 6 and 7, Table 17. Analysis of the identified spots from Mass Spectrometry including amino acid sequence and coding sequence is shown in Appendix no. 4.

In the MS analysis, only the first hit which constituting the most significant probability are analyzed further in details while the next three hits, if any, are only listed and can be searched in NCBI protein database.

Spot No. 1:

This protein spot is overexpressed in WT, but is not expressed in EV, R249S. It is only underexpressed in R273H. This protein spot was cut from the WT gel.

The MS Result for this protein spot identified it as **prolyl 4-hydroxylase beta-subunit** [Homo sapiens]. This enzyme has a central role in the biosynthesis of collagens.

Figure 25 shows the different expressions of the corresponding spot in the different gels.

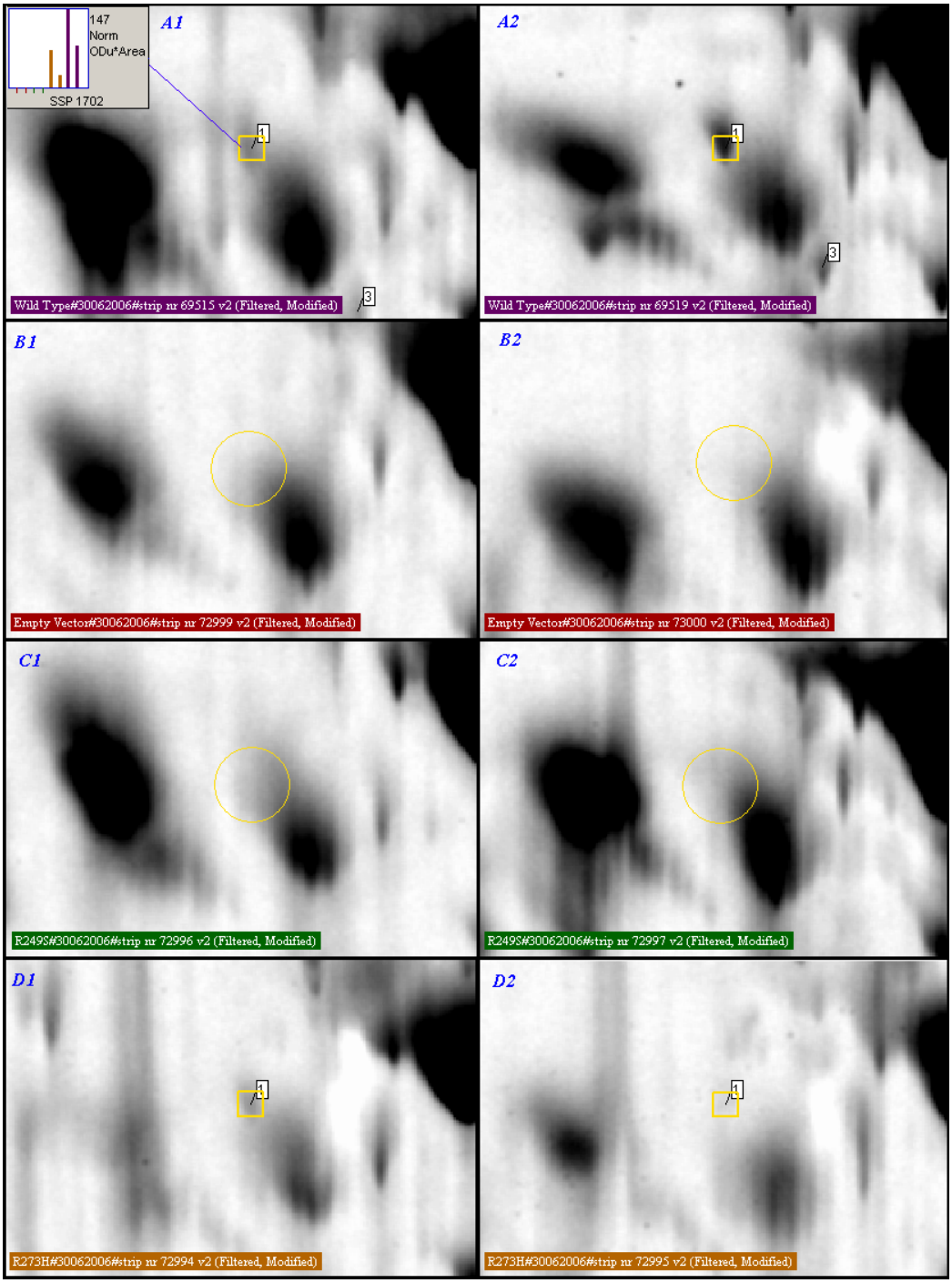

Figure 25: Shows spot no.1 in the different *p53* variants' gels. A1 and A2: WT, B1 and B2: EV, C1 and C2: R249S, D1 and D2: R273H. Squares indicate that the spot is observed while the circles indicate that the spot is not expressed. Spot 1 is overexpressed in WT (A2 and to a less extent in A1), under-expressed in R273H (D1 and more under-expressed in D2) and not expressed in other types. Every column in the graph in the upper left corner of the gel A1 represents the spot in one of the gels. The colour of the column matches the colour of the gel name. The heights of the columns reflect the quantity of the protein and missed columns reflect non-expressed spots in the corresponding gels.

Spot No. 3:

This spot is overexpressed in WT, from which it was cut, while it is not expressed in EV, R249S, and R273H. The MS Result for this protein spot identified it as **vimentin** [Homo sapiens]. Vimentin is the major structural component of intermediate filaments in cells of mesenchymal origin, e.g. fibroblasts and endothelial cells (37). Figure 26, shows the different expressions of this protein spot in the different gels.

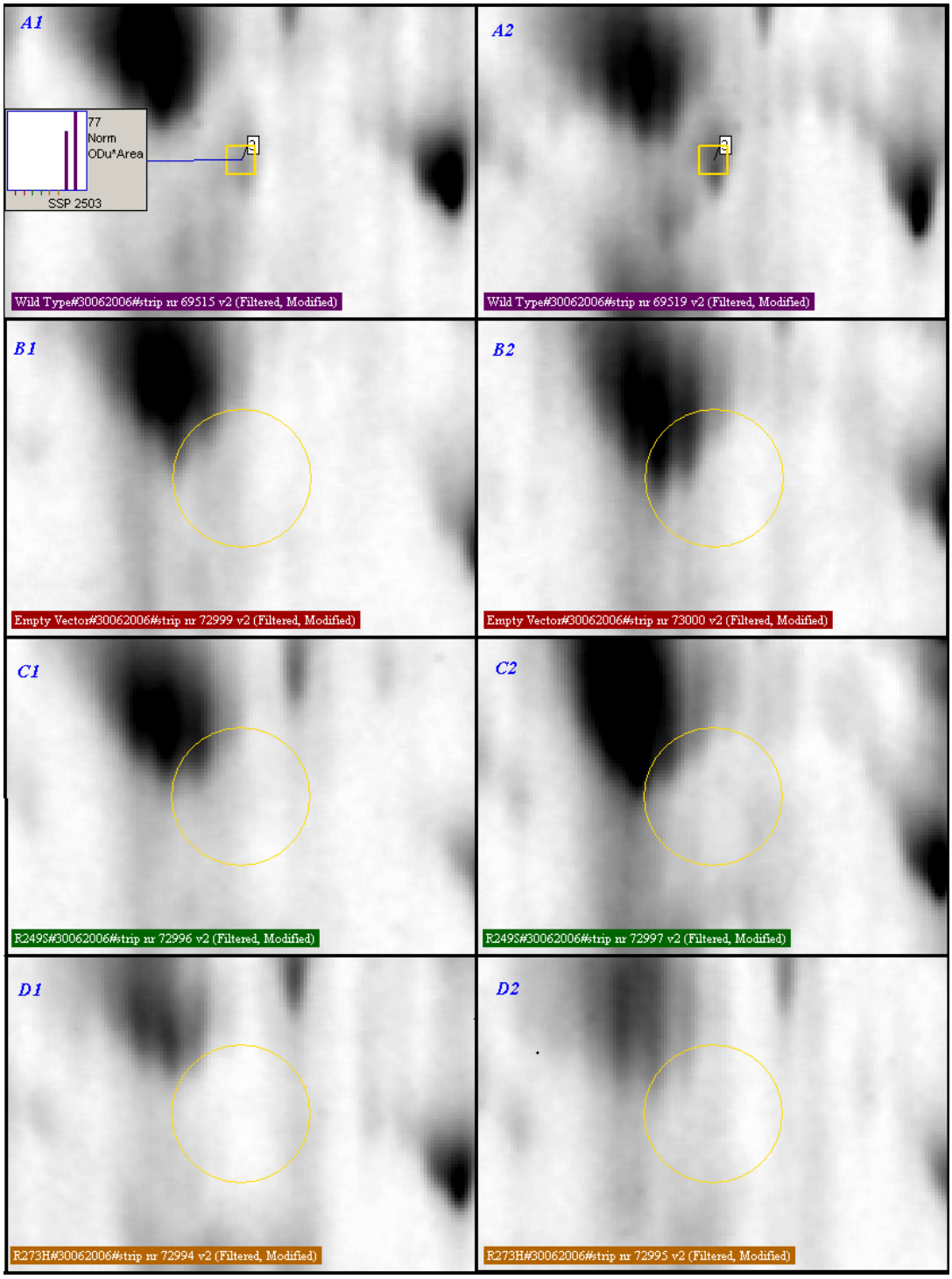

Figure 26: Shows spot no.3 in the different *p53* variants' gels. A1 and A2: WT, B1 and B2: EV, C1 and C2: R249S, D1 and D2: R273H. Squares indicate that the spot is observed (WT: A1 and A2) while circles indicate that the spot is not expressed (the rest of the gels). Every column in the graph shown in gel A1 represents the spot in one of the gels. The color of the column matches the color of the gel name. The heights of the columns reflect the quantity of the protein and missed columns reflect non-expressed spots in the corresponding gels.

Spot no. 5:

This spot is expressed in WT and R273H, from which it was cut, while it is not expressed in EV and R249S. The MS Result for this protein spot identified it as **Aldolase A protein** [Homo sapiens]. **Aldolase** plays an important role in glucose metabolism. Figure 27 shows the different expressions of this protein spot in the different gels.

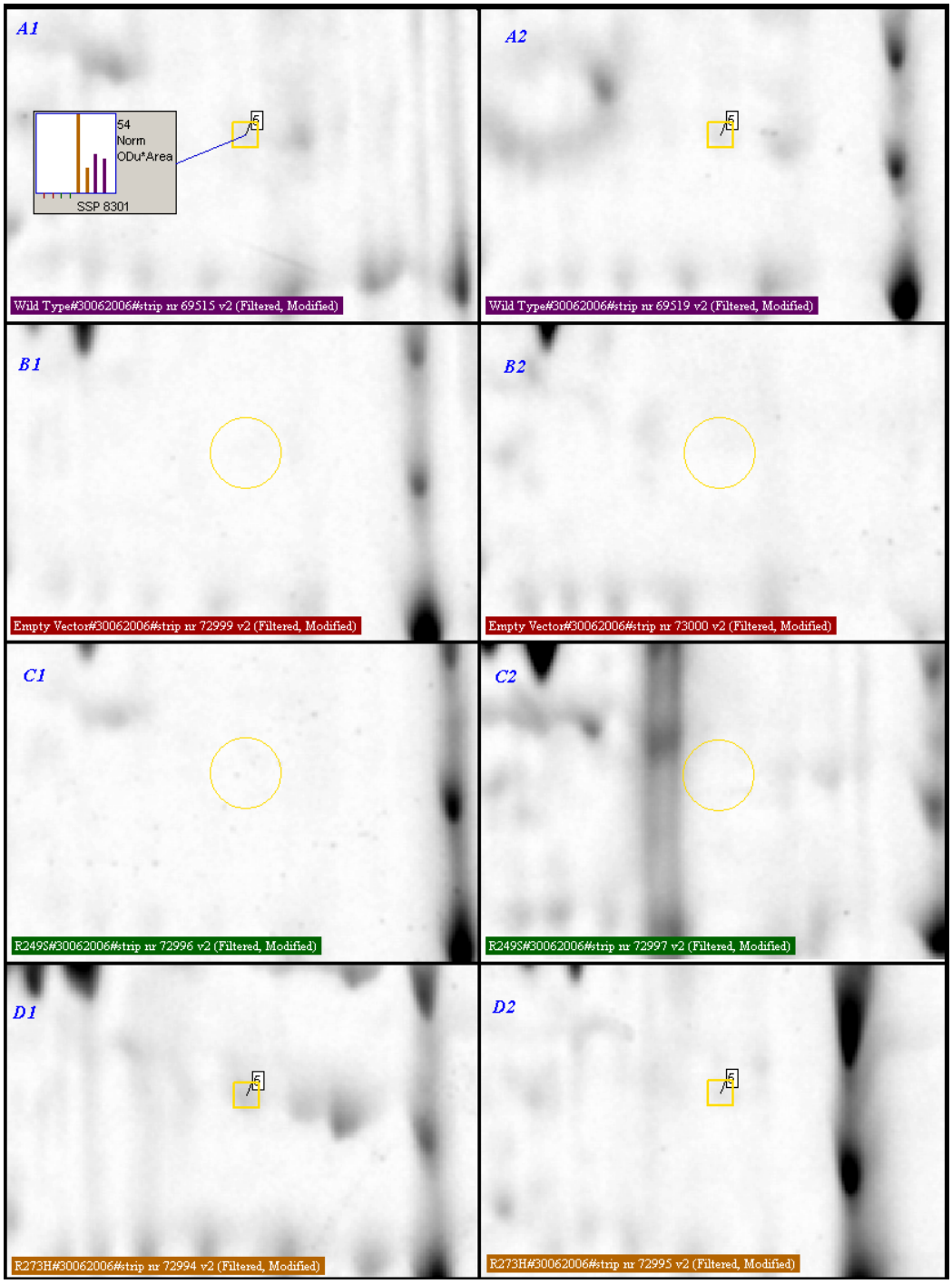

Figure 27: Shows spot no. 5 in the different *p53* variants' gels. A1 and A2: WT, B1 and B2: EV, C1 and C2: R249S, D1 and D2: R273H. Squares indicate that the spot is observed (WT: A1 and A2, R273H: D1 and D2) while circles indicate that the spot is not expressed (EV: B1 and B2, R249S: C1 and C2). Every column in the graph shown in gel A1 represents the spot in one of the gels. The color of the column matches the color of the gel name. The heights of the columns reflect the quantity of the protein and missed columns reflect non-expressed spots in the corresponding gels.

Spot no. 8:

This spot is overexpressed in EV, R249S and R273H from which it was cut, while it is underexpressed in WT. The MS Result for this protein spot identified it as **Triosephosphate isomerase 1 [Homo sapiens].** Triosephosphate isomerase (TIM) is involved in glycolysis, gluconeogenesis and triglyceride synthesis (38). Figure 28 shows the different expressions of this protein spot in the different gels.

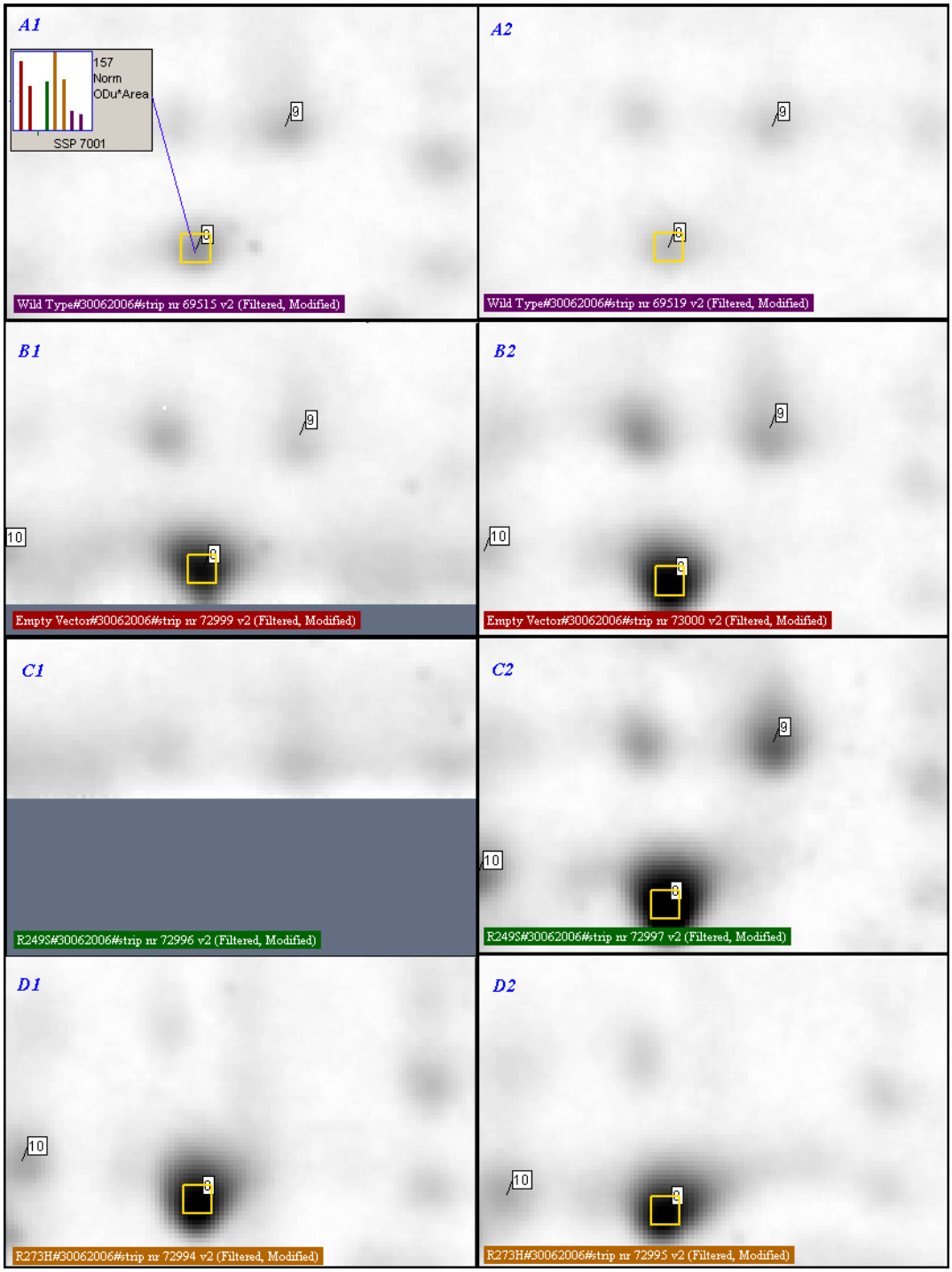

Figure 28: Shows spot no. 8 in the different *p53* variants' gels. A1 and A2: WT, B1 and B2: EV, C1 and C2: R249S, D1 and D2: R273H. Squares indicate that the spot is observed in all gels. The lower part of the gel C1 does not show all the expected spots as the gel C2 of the same type does. Every column in the graph shown in gel A1 represents the spot in one of the gels. The color of the column matches the color of the gel name. The heights of the columns reflect the quantity of the protein in the corresponding gels. The first two columns from right represent the spot in gels A1 and A2 and show that it is considerably underexpresses in wild type.

Spot no. 9:

This spot is overexpressed in WT, EV and R249S from which it was cut while it is missed in R273H. The MS Result for this protein spot identified it as **Carbonic anhydrase II [Homo sapiens].** This enzyme catalyzes the reversible hydration of carbon dioxide and participates in various biological processes. Figure 29 shows the different expressions of this protein spot in the different gels.

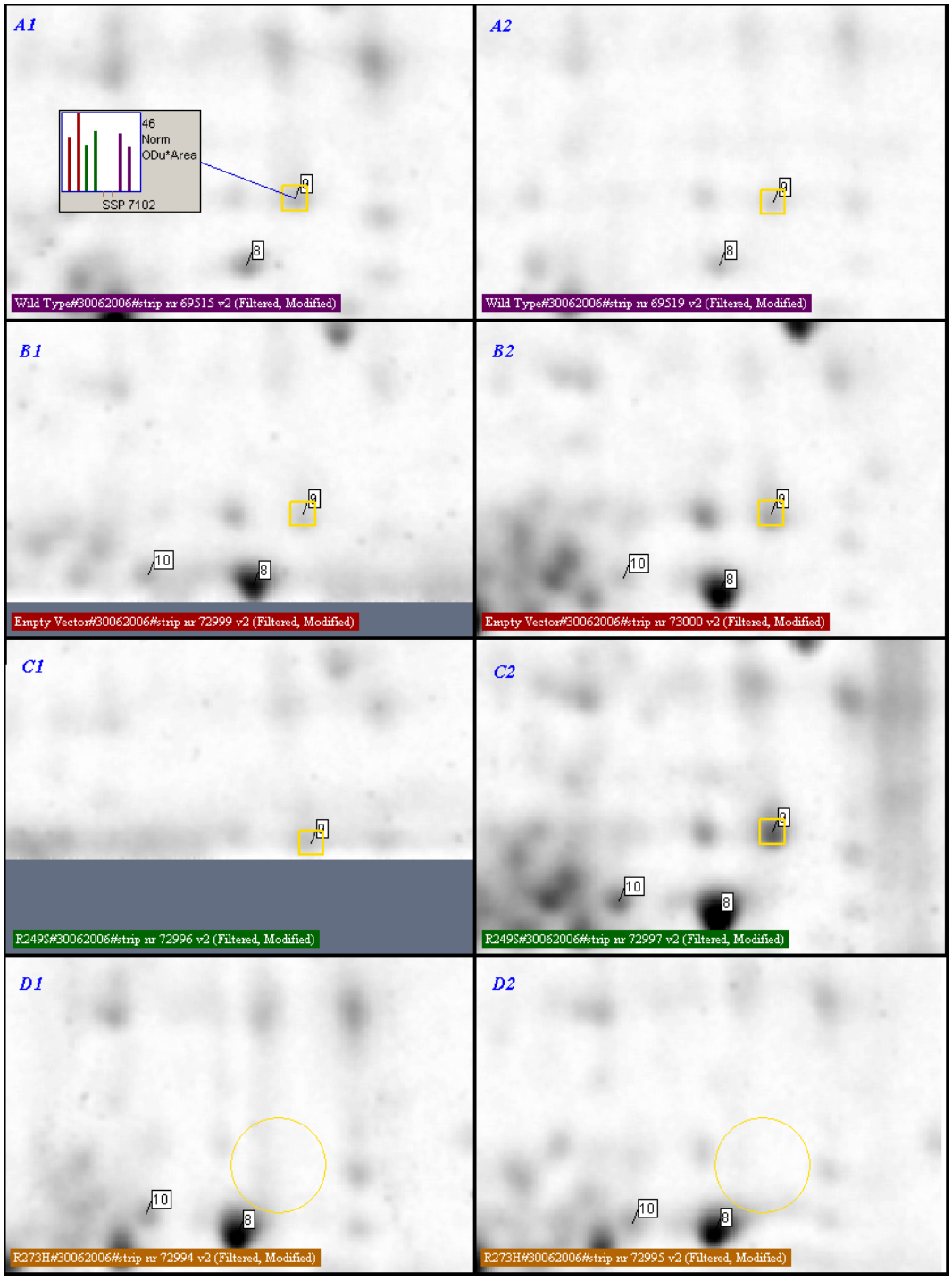

Figure 29: Shows spot no.9 in the different *p53* variants' gels. A1 and A2: WT, B1 and B2: EV, C1 and C2: R249S, D1 and D2: R273H. Squares indicate that the spot is observed while circles indicate that the spot is not expressed. The lower part of the gel C1 does not show all the expected spots as the gel C2 of the same type does. Every column in the graph shown in gel A1 represents the spot in one of the gels. The color of the column matches the color of the gel name. The heights of the column reflect the quantity of the protein and missed columns reflect non-expressed spots in the corresponding gels.

Spot no. 10:

This spot is overexpressed in EV, R273H and R249S from which it was cut, while it is not expressed in WT.

The MS Result for this protein spot identified it as **triosephosphate isomerase** [Mus musculus]. Figure 30 shows the different expressions of the corresponding spots in the different gels.

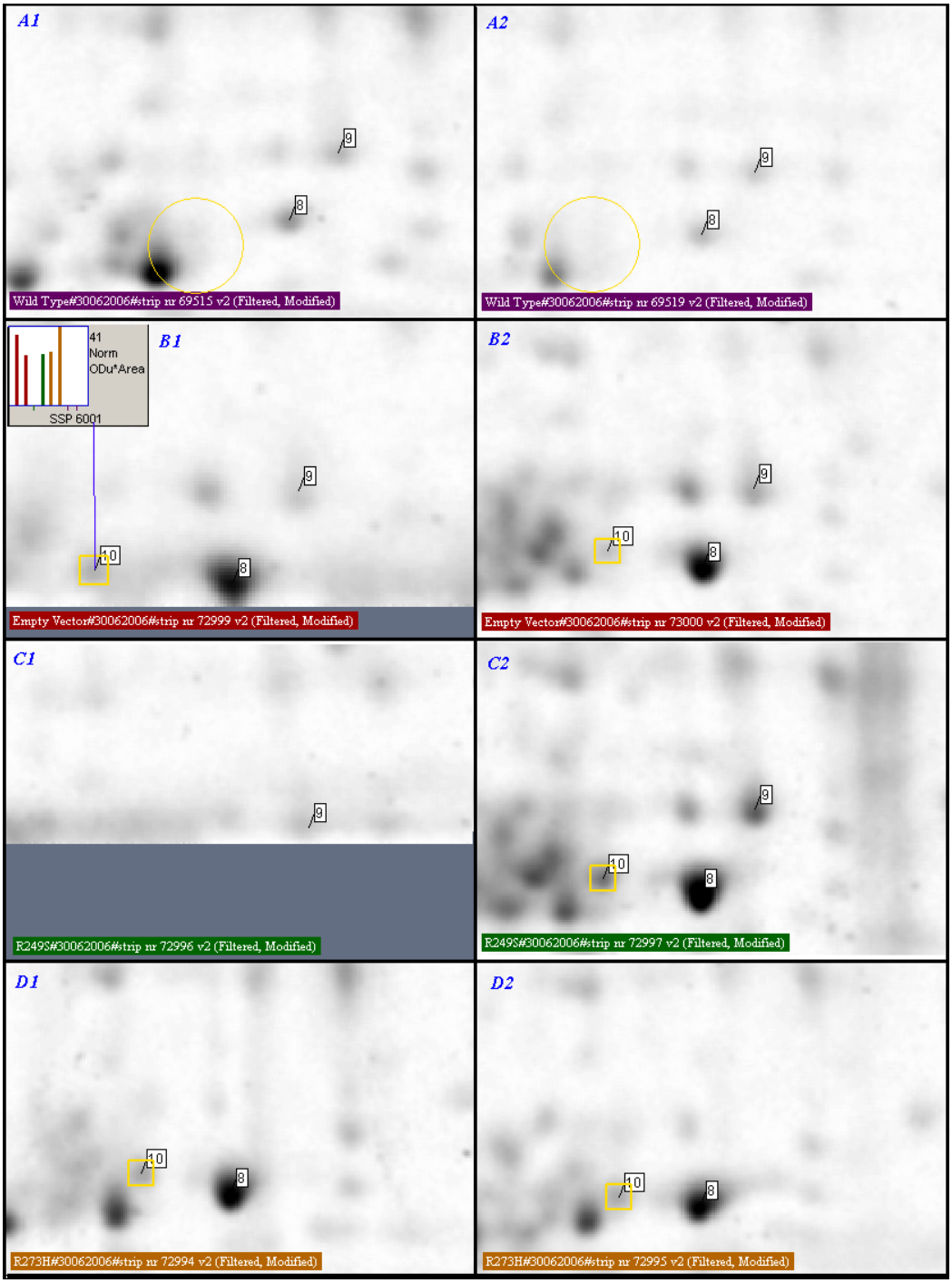

Figur 30: Shows spot no.10 in the different *p53* variants' gels. A1 and A2: WT, B1 and B2: EV, C1 and C2: R249S, D1 and D2: R273H. Squares indicate that the spot is observed while circles indicate that the spot is not expressed. The lower part of the gel C1does not show all the expected spots as the gel C2 of the same type does. Every column in the graph shown in gel B1 represents the spot in one of the gels. The color of the column matches the color of the gel name. The heights of the columns reflect the quantity of the protein and missed columns reflect non-expressed spots in the corresponding gels

Spot no. 11:

This spot is expressed only in R273H from which it was cut while it is not expressed in WT, EV and R249S. The MS Result for this protein spot identified it as **Enolase 1** [Homo sapiens]. This enzyme is involved in glycolysis. Figure 31 shows the different expressions of this protein spot in the different gels.

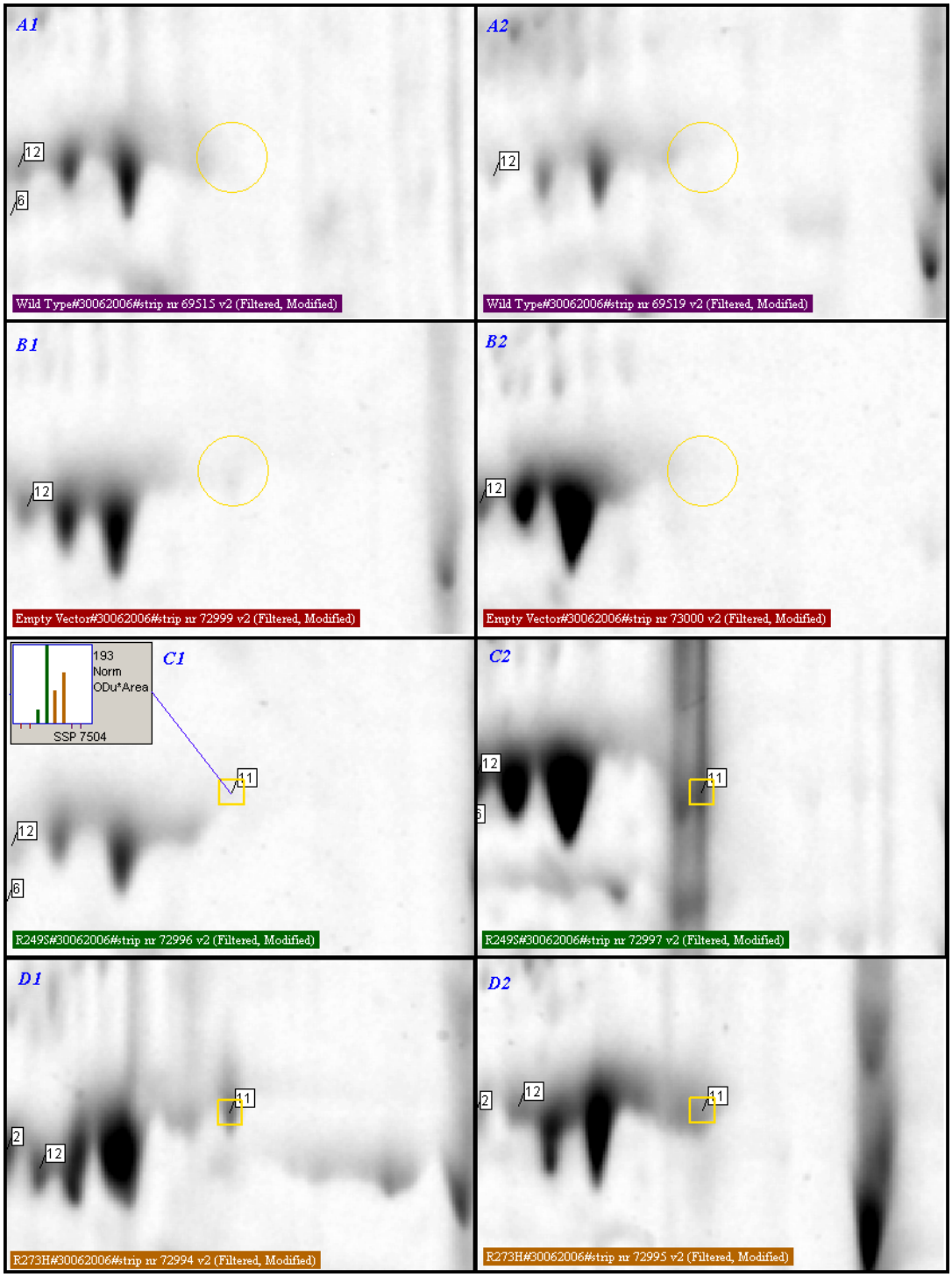

Figure 31: Shows spot no.11 in the different *p53* variants' gels. A1 and A2: WT, B1 and B2: EV, C1 and C2: R249S, D1 and D2: R273H. Squares indicate that the spot is observed while circles indicate that the spot is not expressed. Every column in the graph in gel C1 represents the spot in one of the gels. The color of the column matches the color of the gel name. The heights of the columns reflect the quantity of the protein and missed columns reflect non-expressed spots in the corresponding gels.

Spot No. 12:

This spot is overexpressed in EV, R249S and R273H from which it was cut, while it is underexpressed in WT.

The MS Result for this protein spot identified it as **2-phosphopyruvate-hydratase; alpha-enolase; carbonate dehydratase** [Homo sapiens]. This enzyme is involved in glycolysis. Figure 32 shows the different expressions of this protein spot in the different gels.

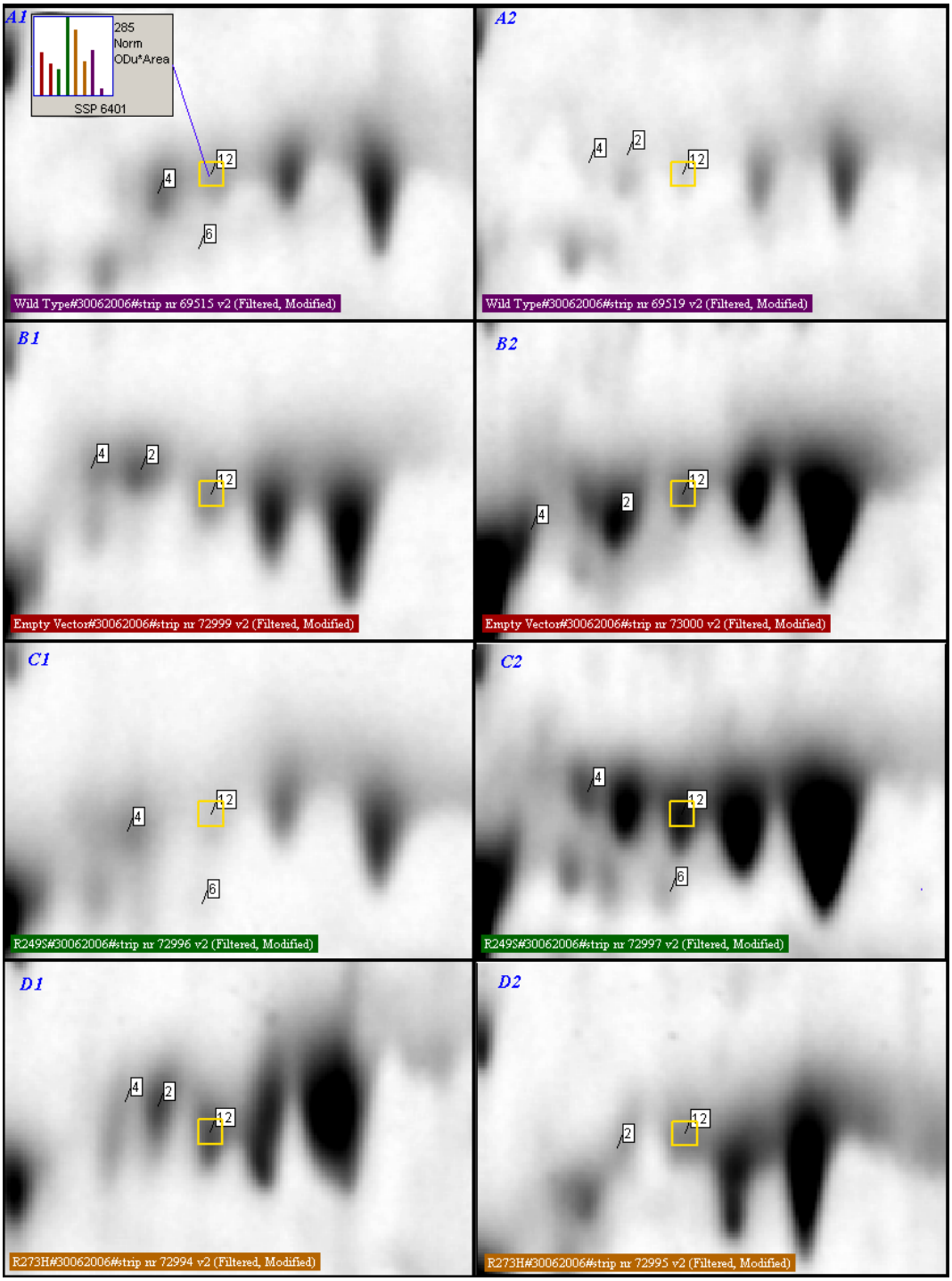

Figure 32: Shows spot no.12 in the different *p53* variants' gels. A1 and A2: WT, B1 and B2: EV, C1 and C2: R249S, D1 and D2: R273H. Squares indicate that the spot is observed in all gels. Every column in the graph shown in gel A1 represents the spot in one of the gels. The color of the column matches the color of the gel name. The heights of the columns reflect the quantity of the protein in the corresponding gels. This spot is underexpressed in WT compared to EV and mutants. Gel C1 does not show the spot as strong as it appears in the gel C2 of the same type.

Discussion

Abnormalities of the *p53* tumor suppressor gene are among the most frequent molecular events in human and animal Neoplasia (39). Mutations in *p53* have been observed in over 60% of all human cancers (4).The current version (October 2006) of IARC database (R11) contains 23,544 *p53* somatic mutations (40). It is now accepted that the inactivation of this gene, as a result of mutation, is a key step in neoplastic transformation and progression (41). The tumor suppressor activity of *p53* results from its ability to transcriptionally activate and repress a wide variety of target genes whose products in turn regulate among other things: cell cycle arrest, DNA repair, apoptosis, and suppression of angiogenesis (27). The *p53* tumor suppressor activity is also a result of *p53* involvement in cellular functions by protein-protein interactions (28). Functional diversity depends on the association with a large subset of partner proteins, which dictates the type of activity and corresponding selectivity (28).

In this study we have analyzed changes in protein expression in Saos-2 cells in the absence of *p53* and in presence of a cancer causing *p53* mutations. The total protein expression patterns in Saos-2 cells containing wild type *p53*, R249S or R273H in addition to cells with no *p53* copy were compared. These two mutations, R249S and R273H, are in the DNA binding domain of *p53* and are involved mainly in liver cancer and colon cancer, respectively. Differential gene expression of normal and cancer causing *p53* mutations will help in establishing biomarkers that can be used in diagnosis, prognosis and therapy of relevant cancers.

Mutagenesis:

Agarose gel electrophoresis of site-directed mutagenesis PCR products indicated product of the expected size suggesting that the PCR was successful as was later confirmed by DNA sequence analysis, Figure 17. The PSwitch plasmid is 7.3 kb while the pGene/V5-His vector (EV) is 4.6 kb. Cloning WT or mutant *p53* into the pGene/V5-His vector results in molecule of 5.7 kb size.

Establishing a stable inducible p53 cell lines:

One of the major functions of *p53* is to induce cell apoptosis, it becomes unlikely to create a stably transfected cell line with a constitutive expression of *p53* (3). Therefore we have created four stable cell lines with inducible *p53* expression for WT, EV, R273H and R249S. Additional advantages to engineered cell lines with inducible *p53* expression are the relative homogeneity among cells in comparison to biopsies from patients with different ages and sex. Moreover, all engineered cells would express *p53*, albeit with different levels, while tumors often contain other cells that would interfere with gene expression profiling experiments.

Xu and El-Gewely, 2002 and Xu, 2003 using cells with transient gene expression gave good results that were validated, but the transfection had to be repeated for every experiment since *p53* expression was constitutive. Also we wanted to eliminate any contribution of cells that do not contain a *p53* gene copy in a transient gene expression experiments since transfection is never any close to 100%. Therefore permanent transfection was made and permanent inducible cell line was established. The inducible *p53* cell line Saos-2/p53, wild Type or mutant, was derived by cloning human *p53* cDNA into the expression vector pGene/V5-His (Invitrogen) to generate the plasmid pGene/V5-His-p53. pGene/V5-His-p53 was then co-transfected with the plasmid pSwitch (Invitrogen), which allows control of gene expression. This means that the gene will be expressed in a tightly and inducible manner. We added mifepristone for only 24 hours before isolating total protein in order to minimize the loss of cells by apoptosis.

The bands on the western blotting gel shown in Figure 19 A and B represent p53 fusion protein which has theoretical molecular weight of 48 kDa. However, and probably due to post translational modification, the protein looks to have higher MW on the WB gel.

Total proteins with induced *p53* variants exhibited bands in lanes 3 (WT), 5 (R249S) and 6 (R273H), but not in lane 4 (EV). This confirms that *p53* is expressed in these three cell lines with pGene/V5-His-p53, but not expressed in the cell line with pGene only (empty vector). Similarly, no p53- band can be seen in lanes 7 and 8 that contain total proteins from non-induced WT *p53* and EV, respectively. The Saos-2/wt *p53*, Saos-2/R249S and Saos-2/R273H inducible cell lines expressed *p53* when induced with the inducer mifepristone. Theoretically, *p53* should not be expressed until the mifepristone is added.

However, the system seems to have some leakage in *p53* expression and the bands appeared in both Saos-2/R249S and Saos-2/R273H cell lines indicate a *p53* expression without mifepristone induction indicating either leakage in the system or cross reactivity. An interpretation of this leakage might be a spontaneous stimulation of unknown reason of one of the promoters either on pSwitch or pGene/V5-His plasmids.

Although the results of our western blotting were encouraging, the validation of our established cell lines needs to be optimized by changing the type of the antibody as well as the concentration of total proteins used. This could not be performed because of the limited time available to complete this study.

Study of p53 partners:

It was aimed to isolate protein partners with affinity purifications using antibodies against V5 epitope that was previously cloned in-frame with *p53* gene. For unclear reasons, the 2D gels of immunoprecipitated *p53* and its partner proteins were not successful. Because the immunoprecipitation did not work, the p53 partner protein study could not be done. This part of the study needs also to be optimized by changing one or more of the experiment elements. Using more protein for immunoprecipitation, loading more proteins in the 2D gels, using another antibody for the IP, or even trying another total protein isolation and immunoprecipitation protocols might lead to better results.

The focus of the thesis is to study the difference in protein expression profile in Saos-2 cells expressing WT *p53* or mutated *p53* and in the absence of *p53*.

The 2D gels of total proteins showed similar, but not identical protein expression patterns. The twelve spots were chosen according to their different expressions in the different *p53* variants, Table 16. Other differentially expressed proteins can be found in our gels which will be analyzed later.

P53 and angiogenesis:

Spot no. 1: Prolyl 4-Hydroxylase beta-subunit [Homo sapiens]:

The collagen prolyl 4-hydroxylases (P4-Hs), enzymes residing within the endoplasmic reticulum, have a central role in the biosynthesis of collagens. In addition, cytoplasmic P4-Hs play a critical role in the regulation of the hypoxia-inducible transcription factor HIF alpha (42).

Prolyl 4-hydroxylase consists of two distinct polypeptides, the catalytically more important alpha-subunit and the beta-subunit, which is identical to the multifunctional enzyme protein disulphide isomerase (PDI). The enzyme appears to be assembled *in vivo* into an alpha 2 beta 2 tetramer from newly synthesized alpha-subunits associating with an endogenous pool of beta-subunits (43).

Our results show that Prolyl 4-Hydroxylase β subunit is overexpressed in WT *p53*, not expressed in EV, R249S and underexpressed in R273H. This suggests that the β subunit might be transcriptionally activated by *p53* just like α subunit (as mentioned below (44)) Thus, *p53* might be one of the factors that control the expression of both subunits of prolyl 4-hydroxylase with the inhibition of angiogenesis as one result.

It is important to consider the possible roles of PDI in the P4-H complex. However, at least one role for the β-subunit/PDI has been clearly demonstrated, namely that the C-terminal -KDEL sequence of the β-subunit/PDI is required for retention of the P4-H complex within the ER lumen (45). The second role of β-subunit/PDI could be to provide a structural framework for binding and preserving native α-subunits in a catalytically active, non-aggregated conformation. In addition, there is some evidence to suggest that non-active site sequences of the β-subunit/PDI are involved with the α-subunit in forming parts of the P4-H catalytic sites (46). As PDI is generally accepted as being the *in vivo* catalyst of disulphide bond formation in proteins destined for export from the ER (47). It is also possible that a further function of β-subunit/PDI may be to catalyze the formation of intramolecular disulphide bonds in the α-subunit of P4-H (43).

It has been reported that the P4-H play a role in inhibition of angiogenesis, and therefore makes it an important component in tumors suppression regulation. This because tumors do not grow larger than a few millimeters in size unless vascularized by the host (48). (In 1998, Holmgren *et al.* (1998) showed that *p53* acts as a tumor suppressor gene

independent of its anti-proliferative effects and by inhibiting angiogenesis, *p53* can indirectly induce apoptosis *in vivo*, but not *in vitro*. Thus, *p53*-gene therapy which alters a tumors angiogenic potential, can revert tumors to a dormant phenotype (49).

It has been recently reported that *p53*-mediates inhibition of angiogenesis through up-regulation of a collagen prolyl hydroxylase (44).

Recent evidence suggests that antiangiogenic therapy is sensitive to *p53* status in tumors, implicating a role for *p53* in the regulation of angiogenesis (44). Teodoro GJ *et al.* (2006) showed that *p53* transcriptionally activates the α(II) collagen prolyl-4-hydroxylase (P4-H) [α(II)PH] gene, resulting in the extracellular release of antiangiogenic fragments of collagen type 4 and 18 (44). The antiangiogenic fragments of several human collagens, including collagen 4 and 18, can inhibit endothelial cell proliferation either by inducing growth arrest or apoptosis (50). Although it is well established that C terminal collagen fragments have an antiangiogenic activity (51), their physiological role and connection to cellular growth pathways have not been elucidated (44). α(II)PH induction by *p53* results in increased synthesis and secretion of full-length collagens, which are then proteolytically processed in the extracellular matrix to produce antiangiogenic peptides (44). Although this extracellular proteolytic processing occurs, at least to some extent, constitutively in the absence of *p53*, *p53* expression greatly enhances the processing of full-length collagen 18 to endostatin. On the basis of these observations, Teodoro *et al.* (44) proposed that *p53* activates a transcriptional program that increases synthesis and processing of collagen-derived antiangiogenic peptides.

In an earlier study by Tsukamoto *et al.* (1999), PLC/PRF/5 hepatoma cells secreted an inhibitor of the proliferation of vascular endothelial cells, which was enhanced by *p53*-gene transfer. Results of this study suggested that the production of this *p53*-inducible angiogenesis inhibitor is responsible, at least partly, for the regulation of angiogenesis in human hepatomas (52).

α subunit is well studied while the full function of β subunit is still not completely known. Yet, as mentioned above, β subunit is important for α subunit and the whole P4-H complex to complete its catalytical activity.

P53 and intermediate filaments:

Spot no. 3: Vimentin [Homo sapiens]:

Vimentin is the major structural component of intermediate filaments in cells of mesenchymal origin, e.g. fibroblasts and endothelial cells (37). The intermediate filament framework is one of the three cytoskeletal systems in mammalian cells. Its well-spread filamentous structure from the nucleus to the plasma membrane is believed to provide protection against various mechanical stresses (53). The dynamic property in the intermediate filament system plays a fundamental role in mediating changes in cell shape, cell division and migration, signaling molecule distribution, and smooth muscle force development. Vimentin is the most abundant intermediate filament protein in various cell types (54-56).

In our study the vimentin was expressed in WT but not expressed in any of the cells expressing *p53* mutants or in the EV. According to the MS results, the sequence coverage was 11%, which, is relatively low and makes the MS analysis in more need for validation. With this restriction in mind, our results are not in accordance with the results reported in the literature and mentioned below although it still suggests that *p53* may play a role in regulating vimentin expression.

Eckes B. *et al.* (1998) reported that stiffness of vimentin-deficient fibroblasts was reduced by 40% in comparison to wild-type cells. Vimentin-deficient cells also displayed reduced mechanical stability, motility and directional migration towards different chemo-attractive stimuli. Absence of a vimentin filament network does not impair basic cellular functions needed for growth in culture, but cells are mechanically less stable, and therefore they are impaired in all functions depending upon mechanical stability (57).

In a study by Hu L. *et al.* (2004) overexpression of vimentin was significantly associated with hepatocellualar carcinoma (HCC) metastasis which strongly suggests that the overexpression of vimentin may play an important role in the metastasis of HCC (58). The poor prognosis of HCC has been associated with the recurrence and the intrahepatic metastasis (59). Another study reported that co-expression of vimentin and cytokeratin (CK) in breast cancer showed a more aggressive phenotype associated with poor prognosis as compared with keratin-high/vimentin-negative or keratin-low/vimentin-positive tumors. (60).

In a recent study, Kudo *et al.* (2006) established a spindle cell squamous carcinoma SCSC cell line from a primary tumor expressing cytokeratin and vimentin, indicating carcinosarcoma-like characters. The established SCSC cell line was spindle-shaped and showed identical immunohistochemical characters to those of primary tumor cells. Similar to the primary tumor, the cell line showed *p53* overexpression and had *p53* mutation at another codon 132: AAG (lys)-->AAT (asp) (61). This suggests that *p53* may play a role in the regulation of vimentin expression.

P53 and glycolysis:

Spots no. 5: Aldolase A, no.8: Triosephosphate isomerase 1 (TIM) [Homo sapiens], no.11: Enolase 1 [Homo sapiens] and no.12: alpha-enolase:

The proteins identified in these spots are all involved in glucose metabolism and particularly in glycolysis, therefore they will be discussed together.

Aldolase plays an important role in glucose metabolism (38). It catalyzes the aldol reaction where the substrate fructose 1,6-bisphosphate is broken down into glyceraldehyde 3-phosphate (G3P) and dihydroxyacetone phosphate (DHAP) (62). Aldolase becomes elevated in serum with malignant tumors, and isozyme A is predominant in serum (63).

Triosephosphate isomerase (TIM) is a homodimeric enzyme catalyzing the interconversion of D-glyceraldehyde-3-phosphate and dihydroxyacetone phosphate, and is involved in glycolysis, gluconeogenesis and triglyceride synthesis (38).

Alpha-enolase (α-enolase) is involved in glycolysis and catalyzes the conversion of 2-phosphoglycerate to phosphoenolpyruvate, which in turn is dephosphorylated into pyruvate to yield ATP (38).

In fact enolase 1 (spot 11) and α-enolase (spot 12) seem to be isoforms or isozymes. Though they are referred to be synonyms of the same protein in some web sites together with other names as well like carbonate dehydratase and 2-phosphopyruvate-hydratase. (iHOP: Information Hyperlinked Over Protein http://www.ihop-net.org/UniPub/iHOP/gs/87985.html and http://getentry.ddbj.nig.ac.jp/) in spite of having

two different GI identifying numbers on NCBI protein database where the Enolase 1 is named as : Enolase 1 (alpha).

But by comparing the amino acid sequences and the coding sequences obtained from NCBI protein database of the proteins identified in spots 11 (enolase 1) and 12 (alpha-enolase), we found that they are different only in one nucleotide and as a result in one amino acid which is the amino acid number 252 where phenylalanine is found in enolase 1 instead of serine in α-enolase. Since the two proteins have the same theoretical p*I* value (7.01), it is expected to find them on the same vertical line on the 2DE. However, the two spots from which the samples were collected were clearly differentiated on the first dimension separation, Figure 24. They have similar molecular weights 47.1689 kDa (enolase 1) and 47.1088 kDa (alpha-enolase), which is in accordance with what we have on the 2D gel electrophoresis. This means that enolase1 and α-enolase are coded by the same gene and the difference in their forms is due to post-translational modifications. Or this difference could also be as a result of almost identical gene duplication, but with little mutations/changes.

Our results show a clear difference in the protein expression patterns of these three proteins between cells with WT *p53*, null-*p53* and mutant *p53* suggesting a role of *p53* in the metabolism of tumors particularly in glycolysis. This, to large extent, is supported by several studies.

Triosephosphate isomerase I (TIM) (Spot no.8, Figure 28 results) and α enolase (Spot no.12, Figure 32 results) were clearly underexpressed in the WT compared to EV and both R273H and R249S mutants. The R249S mutation is known to be associated mainly with liver and lung cancers according to IARC. Yet, the sequence coverage of the protein identified from spot 8 (TIM) was 62%, which is considerably high and making this protein on the priority list to be validated. Similarly, α-enolase was overexpressed in all types, but underexpressed in WT however, the sequence coverage was (20%).

Also, enolase 1 (Spot no.11, Figure 31 results) was overexpressed in both mutants, but no expression could be detected in WT or in EV. The sequence coverage in MS was 38%. These results can be explained that mutant *p53* leads to increased expression of these important enzymes to facilitate glycolysis in tumor cells.

On the other hand, our results showed no expression of aldolase A (Spot no.5, Figure 27 results) in EV and R249S while it was expressed in WT and R273H (overexpressed in one of its gels). The sequence coverage of the protein identified in spot 5 with the aldolase A was 21%.

In contrast to normal cells, cancer cells have a high glycolytic rate and utilize anaerobic pathways to metabolize glucose and produce high levels of lactate even in the presence of oxygen (64;65). This metabolic shift to a higher rate of aerobic glycolysis is commonly referred to as the Warburg effect after the pioneer work of Warburg (1930). In part this is due to development of intratumoral regions of hypoxia, arising from disordered vascular development and flow (65). Because glycolysis produces energy (ATP) far less efficiently than aerobic respiration, tumor cells have a much higher rate of glucose uptake than normal cells (64). PET (positron emission tomography) has confirmed that the vast majority (>90%) of human primary and metastatic tumors demonstrate increased glucose uptake indicating abnormal metabolism. Furthermore, PET has been used to show a direct correlation between tumor aggressiveness and the rate of glucose consumption (66).

The physiological significance of the Warburg effect has been controversial since its discovery over 80 years ago, and now there is renewed and vigorous interest in understanding the relationship between cancer and altered energy metabolism (64). A commonly held view is that constitutive upregulation of glycolysis is likely to be an adaptation to hypoxia that develops as tumor cells grow progressively further away from their blood supply (67).

The shift from aerobic mitochondrial respiration to glycolysis in tumor cells could be the result of increased activity of glycolytic enzymes, decreased utilization of pyruvate by mitochondria, reduced capacity to transport cytosolic NADH into mitochondria through mitochondrial NADH/NAD^+ shuttle pathways, impaired tricarboxylic cycle, or defects in respiration at various points in the electron transport chain (64).

In a recent study, Matoba *et al.* (2006) showed that *p53* modulates the balance between the utilization of respiratory and glycolytic pathways (68). They showed that oxygen consumption (a measure of aerobic respiration) was lower in a preparation of liver mitochondria from *p53*-deficient mice compared with wild-type mice. They identified

synthesis of Cytochrome c Oxidase 2 (SCO2) as the downstream mediator of this effect in mice and human cancer cell lines. SCO2 is critical for regulating the cytochrome c oxidase (COX) complex, the major site of oxygen utilization in the eukaryotic cell. Disruption of the SCO2 gene in human cancer cells with wild-type *p53* recapitulated the metabolic switch toward glycolysis that is exhibited by *p53*-deficient cells. That SCO2 couples *p53* to mitochondrial respiration provides a possible explanation for the Warburg effect and offers new clues as to how *p53* might affect aging and metabolism (68).

P53 can also inhibit glycolysis through its transcriptional target, TIGAR, which lowers the levels of fructose 2,6-bisphosphate, a molecule that promotes glycolysis (69).

Ktuse *et al.* (2006) has also supported a role of *p53* in regulating aerobic respiration. They noted that loss of *p53* results in decreased oxygen consumption and aerobic respiration and promotes a switch to glycolysis, thereby reducing endurance during physical exercise (70).

In 2005 Jones *et al.* reported that inhibition of glycolysis by glucose withdrawal was shown to serve as a signal for the phosphorylation and activation of *p53*.

They showed that proliferating mammalian cells have a cell-cycle checkpoint that responds to glucose availability. The glucose-dependent checkpoint occurs at the G1/S boundary and is regulated by AMP-activated protein kinase (AMPK). AMPK activation induces phosphorylation of p53 on serine 15, and this phosphorylation is required to initiate AMPK-dependent cell-cycle arrest. AMPK-induced *p53* activation promotes cellular survival in response to glucose deprivation, and cells that have undergone a p53-dependent metabolic arrest can rapidly reenter the cell cycle upon glucose restoration (71).

A recent study on prostate cancer cells supports our findings that the expression of aldoalse A, TIM, and α-enolase are somehow controlled by *p53* and glycolysis as a result. Van den Bemd *et al.* (2006) performed proteomic analysis in a prostate cancer xenograft model in which immune-incompetent nude mouse were inoculated with human prostate cancer cells. Van den Bemd *et al.* identified six human enzymes involved in glycolysis (fructose-bisphosphate **aldolase A**, **triose-phosphate isomerase**, glyceraldehyde-3-phosphate dehydrogenase, **α-enolase**, and lactate dehydrogenases A and B) in the serum of the tumor-bearing mice (72). This study supports our findings that TIM and α-enolase

were obviously overexpressed in mutant and null *p53* cells compared to the WT *p53* cells. As a result, this supports the theory that *p53* controls the expression of these crucial enzymes.

Similar results in lung cancer were shown in another study by Nakanishi *et al.* (2006). They screened lung cancer for specific autoantibodies. Solubilized proteins from a cancer cell line (A549) were separated using 2D-Gel, followed by Western blotting (WB) analysis, in which the sera of individual patients were tested for primary antibodies. They identified eight proteins, **α-enolase**, inosine-5′-monophosphate dehydrogenase, aldehyde dehydrogenase, 3-phosphoglycerate dehydrogenase, 3-oxoacid CoA transferase, chaperonin, peroxiredoxin 6 and **triosephosphate isomerase**, which reacted with these antibodies in patients' sera using MALDI-TOF/TOF. All eight antibodies were not detected in the sera derived from lung tuberculosis and healthy controls (73).

In another interesting supportive study, Okano *et al.* (2006) investigated aberrant plasma proteins also in lung cancer by comparing the proteomic profiles of serum from lung cancer patients and from healthy volunteers. Mass spectrometric protein analysis identified among other proteins **triosephosphate isomerase** to be two fold higher in patients with lung cancer than in healthy volunteers (74).

Similarly, it was reported that increased amounts of triosephosphate isomerase in urine or bladder tissue may be indicative of squamous metaplasia, squamous cell carcinoma, or other bladder injuries (75).

Expression of **α-enolase** increased with tumor dedifferentiation and was significantly higher in poorly differentiated hepatocellular carcinoma HCC than in well-differentiated HCC. Expression of α-enolase also correlated positively with tumor size and venous invasion. This study suggested that α-enolase is one of the candidates for biomarkers for tumor progression that deserves further investigation in HCV-related HCC (76).These results support our finding that α-enolase can be overexpressed in cancer. Yet, our results go further in showing that α-enolase is linked to *p53* in cancer causing mutants such as R249S and R273H, but not WT 53.

Aldolase A has been reported earlier to be elevated in malignant tumors (63). Yet, it has been suggested in a very early study to be used as biomarker for renal cell carcinoma (RCC) by Takashi *et al.* (1992). They reported that serum aldolase A is a useful

biomarker for monitoring the clinical course of patients with RCC (77). Also Aldolase A mRNA was noticed to be approximately 10-fold higher in liver biopsies from patients with hepatocellular carcinoma vs patients with chronic hepatitis C or cirrhosis, and healthy individuals (78). Our results suggest that this elevation might be controlled by *p53*.

Spot no. 9: Carbonic Anhydrase I [Homo sapiens]:

The growing α-carbonic anhydrase (CA) gene family includes 11 enzymatically active members that catalyze the reversible hydration of carbon dioxide: $CO_2 + H_2O \rightleftharpoons HCO_3^- + H^+$ and participate in various biological processes, including respiration, bone resorption, renal acidification, gluconeogenesis, and formation of cerebrospinal fluid and gastric acid (79). The CA isozymes differ in their kinetic properties, their tissue distribution and subcellular localization, and their susceptibility to various inhibitors (79). Several CA isozymes (I and II) are expressed in the enterocytes of the normal intestine (80). However, two of them, CA IX and CA XII, have been linked to oncogenesis, and their overexpression has been observed in malignant tumor cells (79) (81) (82).

Our results, Figure 29, show that carbonic anhydrase I was overexpressed in WT, EV and one gel of R249S but it was not expressed at all in R273H, which is known to be frequently associated with colorectal cancers according to IARC. The sequence coverage of this protein was 33%. These results are in accordance with a possible role of *p53* in the decreased level of expression in colorectal cancers (presented below). However, for this protein being overexpressed in EV as in WT does not support the fact that this protein is controlled by *p53*.

Kivela *et al.* (2001) reported that while the normal mucosa of the large intestine showed high expression for CA I and II, the intensity of the immunostaining for both isozymes decreased in benign lesions and was very weak in malignant tumors. While CA I and II are prominent in normal colorectal mucosa, where they play a role in regulation of pH homeostasis and water and ion transport, loss of expression of these cytoplasmic isozymes consistently accompanies progression to malignant transformation (79).

Chiang *et al.* (2002) studied the possible relationship between the expression of cytosolic carbonic anhydrase (I and II) and non-small cell lung cancer (NSCLC). Their results showed that the CA activity and protein expression were significantly decreased in both squamous cell carcinoma (SCC) and adenocarcinoma (AD). From this study, it was suggested that the reduction of CA I and CA II in both SCC and AD patients may promote tumor cell motility and contribute to tumor growth and metastasis (83).

Also the majority of colorectal cancers do not express carbonic anhydrase isoenzyme I. The presence of any isoenzyme I-positive immunoreactive cancer cells may be associated with a more favorable outcome in colorectal cancer (84).

Zhang *et al.* (1997) examined the global gene expression profiles of normal and cancerous human colonic epithelium. They reported a concomitant decrease of CA I and CA II mRNA levels in the cancerous epithelium (85). However, another study by Cole *et al.* (2000) showed a decrease in CA I protein expression only (86).

Spot no. 10: Triosephosphate isomerase [Mus musculus]:

This spot, Figure 30, was not of interest since it was not Homo sapiens' protein. Besides, the covering sequence was low (9%) and does not give an extinctive presentation of the identified protein. However, this spot was very close to spot no 8 (Triosephosphate isomerase 1 (TIM) [Homo sapiens]), which means that it has a close MW and p*I*. So it could be an isoenzyme of the human enzyme and the identification of the mouse enzyme was artifact. Therefore this spot must be analyzed further later.

Concluding notes:

The association of specific proteins with cells that express different *p53* variants and understanding the regulation of their expression will aid in determination of their potential role as biomarkers and/or as targets for therapeutic development for at least some cancers. Nevertheless, our results in general need to be validated thoroughly and by first running more 2D gels and then performing other validating methods. These methods would include Western blot with appropriate antibodies as well as isolating mRNA and designing appropriate specific primers for the mRNA for the corresponding protein and running RT-PCR. These two methods (RT-PCR and WB) are also quantitative. Moreover

microarray, which is also quantitative can be used with total isolated mRNA to discover any differential expression of downstream genes, at the transcriptional level, whether it include the above discussed protein spots or not.

For the validation of the function of the discussed protein Spots (Tables 17 18), SiRNA against the identified genes can be made for experiments designed to validate the functional role of such proteins as related to cancer or a supporting role for p53. SiRNA is easier and less expensive than transgenic knock-out.

Table 18: Summary of the high priority differentially expressed proteins among *p53* different variants for validation.

Spot number	Identified Protein	Expression
1	Prolyl 4-hydroxylase beta-subunit	↑ WT, ↓ R273H. Not expressed: EV, R249S
8	Triosephosphate isomerase 1 (TIM)	↑ EV, R249S, R273H. ↓ WT
11	Enolase 1	↑ R249S, R273H. Not expressed: WT, EV
12	Alpha-enolase	↑ EV, R249S, R273H. ↓ WT
3	Vimentin	↑ WT, not expressed: EV, R249S, R273H

Reference List

1. Ljungman M. Dial 9-1-1 for p53: mechanisms of p53 activation by cellular stress. *Neoplasia.* 2000;2:208-25.

2. Xu H, El-Gewely MR. P53-responsive genes and the potential for cancer diagnostics and therapeutics development. *Biotechnol.Annu.Rev.* 2001;7:131-64.

3. Xu H, El-Gewely MR. Differentially expressed downstream genes in cells with normal or mutated p53. *Oncol.Res.* 2003;13:429-36.

4. Loging WT, Reisman D. Inhibition of the putative tumor suppressor gene TIMP-3 by tumor-derived p53 mutants and wild type p53. *Oncogene* 1999;18:7608-15.

5. Guimaraes DP, Hainaut P. TP53: a key gene in human cancer. *Biochimie* 2002;84:83-93.

6. Yu Q. Restoring p53-mediated apoptosis in cancer cells: new opportunities for cancer therapy. *Drug Resist.Updat.* 2006;9:19-25.

7. Lim YP, Lim TT, Chan YL, Song ACM, Yeo BH, Vojtesek B et al. The p53 knowledgebase: an integrated information resource for p53 research. http://p53.bii.a-star.edu.sg/. *Oncogene* 2006.

8. Lim YP, Lim TT, Chan YL, Song ACM, Yeo BH, Vojtesek B et al. The p53 knowledgebase: an integrated information resource for p53 research. *Oncogene* 2006.

9. el-Deiry WS. Regulation of p53 downstream genes. *Semin.Cancer Biol.* 1998;8:345-57.

10. Helton ES, Chen X. p53 modulation of the DNA damage response. *J Cell Biochem.* 2006.

11. Weinberg WC, Denning MF. P21Waf1 control of epithelial cell cycle and cell fate. *Crit Rev.Oral Biol.Med.* 2002;13:453-64.

12. el-Deiry WS, Tokino T, Velculescu VE, Levy DB, Parsons R, Trent JM et al. WAF1, a potential mediator of p53 tumor suppression. *Cell* 1993;75:817-25.

13. Xu H. Downstream gene expression of human tumor suppressor p53 and cancer-related mutants. 2002. Department of Molecular Biotechnology, Institute of Medical Biology, University of Tromsø.

14. Smits VA, Klompmaker R, Vallenius T, Rijksen G, Makela TP, Medema RH. p21 inhibits Thr161 phosphorylation of Cdc2 to enforce the G2 DNA damage checkpoint. *J Biol.Chem.* 2000; 275:30638-43.

15. Hermeking H, Benzinger A. 14-3-3 proteins in cell cycle regulation. *Semin.Cancer Biol.* 2006;16:183-92.

16. Rohaly G, Chemnitz J, Dehde S, Nunez AM, Heukeshoven J, Deppert W et al. A novel human p53 isoform is an essential element of the ATR-intra-S phase checkpoint. *Cell* 2005;122:21-32.

17. Jin Z, el-Deiry WS. Overview of cell death signaling pathways. *Cancer Biol.Ther.* 2005;4:139-63.

18. Owen-Schaub LB, Zhang W, Cusack JC, Angelo LS, Santee SM, Fujiwara T et al. Wild-type human p53 and a temperature-sensitive mutant induce Fas/APO-1 expression. *Mol Cell Biol.* 1995;15:3032-40.

19. Harms K, Nozell S, Chen X. The common and distinct target genes of the p53 family transcription factors. *Cell Mol Life Sci* 2004;61:822-42.

20. Rozan LM, el-Deiry WS. p53 downstream target genes and tumor suppression: a classical view in evolution. *Cell Death.Differ.* 2006.

21. Olivier M, Eeles R, Hollstein M, Khan MA, Harris CC, Hainaut P. The IARC TP53 database: new online mutation analysis and recommendations to users. http://www-p53.iarc.fr/index.html. *Hum.Mutat.* 2002;19:607-14.

22. Mashima T, Tsuruo T. Defects of the apoptotic pathway as therapeutic target against cancer. *Drug Resist.Updat.* 2005;8:339-43.

23. Yu Q. Restoring p53-mediated apoptosis in cancer cells: new opportunities for cancer therapy. *Drug Resist.Updat.* 2006;9:19-25.

24. Yu Q. Restoring p53-mediated apoptosis in cancer cells: new opportunities for cancer therapy. *Drug Resist.Updat.* 2006;9:19-25.

25. Klein C, Vassilev LT. Targeting the p53-MDM2 interaction to treat cancer. *British Journal of Cancer* 2004;91:1415-9.

26. Biotech News International. www.biotechdaily.com. 11. 9-10-2006.

27. Vogelstein B, Lane D, Levine AJ. Surfing the p53 network. *Nature* 2000;408:307-10.

28. arcon-Vargas D, Ronai Z. p53-Mdm2--the affair that never ends. *Carcinogenesis* 2002;23:541-7.

29. Invitrogen. Invitrogen manual for GeneSwitch™ System. A Mifepristone-Regulated Expression System for mammalian Cells. 2002. http://www.invitrogen.com/content/sfs/manuals/geneswitch_man.pdf.

30. El-Gewely MR, C Fenton E. Kjeldsen and H Xu. Mutagenesis: Site specific. Encyclopedia of Life Sciences, ELS. 2005.

31. Sanger F, Nicklen S, Coulson AR. DNA sequencing with chain-terminating inhibitors. *Proc.Natl.Acad.Sci U.S.A* 1977;74:5463-7.

32. Sigma-Aldrich Web site, http://www.sigmaaldrich.com. 2006.

33. Molecular Station Web site. http://www.molecularstation.com/.

34. Haberkorn U, Altmann A, Eisenhut M. Functional genomics and proteomics--the role of nuclear medicine. *Eur.J Nucl.Med.Mol Imaging* 2002;29:115-32.

35. Pandey A, Andersen JS, Mann M. Use of mass spectrometry to study signaling pathways. *Sci STKE.* 2000;2000:L1.

36. Berkelman T. and Stenstedt T. 2-D ELECTROPHORESIS USING IMMOBILIZED PH GRADIENTS PRINCIPLES & METHODS. 1998. Amersham Pharmacia Biotech.

37. Franke WW, Hergt M, Grund C. Rearrangement of the vimentin cytoskeleton during adipose conversion: formation of an intermediate filament cage around lipid globules. *Cell* 1987;49:131-41.

38. Li C, Xiao Z, Chen Z, Zhang X, Li J, Wu X et al. Proteome analysis of human lung squamous carcinoma. *Proteomics* 2006;6:547-58.

39. Hainaut P, Hernandez T, Robinson A, Rodriguez-Tome P, Flores T, Hollstein M et al. IARC Database of p53 gene mutations in human tumors and cell lines: updated compilation, revised formats and new visualisation tools. *Nucleic Acids Res.* 1998;26:205-13.

40. Olivier M, Eeles R, Hollstein M, Khan MA, Harris CC, Hainaut P. The IARC TP53 database: new online mutation analysis and recommendations to users. *Hum.Mutat.* 2002;19:607-14.

41. Prives C, Hall PA. The p53 pathway. *J Pathol.* 1999;187:112-26.

42. Myllyharju J. Prolyl 4-hydroxylases, the key enzymes of collagen biosynthesis. *Matrix Biol.* 2003;22:15-24.

43. John DC, Bulleid NJ. Intracellular dissociation and reassembly of prolyl 4-hydroxylase:the alpha-subunits associated with the immunoglobulin-heavy-chain

binding protein (BiP) allowing reassembly with the beta-subunit. *Biochem.J* 1996;317 (Pt 3):659-65.

44. Teodoro JG, Parker AE, Zhu X, Green MR. p53-mediated inhibition of angiogenesis through up-regulation of a collagen prolyl hydroxylase. *Science* 2006;313:968-71.

45. Vuori K, Pihlajaniemi T, Myllyla R, Kivirikko KI. Site-directed mutagenesis of human protein disulphide isomerase: effect on the assembly, activity and endoplasmic reticulum retention of human prolyl 4-hydroxylase in Spodoptera frugiperda insect cells. *EMBO J* 1992;11:4213-7.

46. Kivirikko KI, Helaakoski T, Tasanen K, Vuori K, Myllyla R, Parkkonen T et al. Molecular biology of prolyl 4-hydroxylase. *Ann.N.Y.Acad.Sci* 1990;580:132-42.

47. Freedman RB, Hirst TR, Tuite MF. Protein disulphide isomerase: building bridges in protein folding. *Trends Biochem.Sci* 1994;19:331-6.

48. Folkman J. Angiogenesis inhibitors generated by tumors. *Mol.Med.* 1995;1:120-2.

49. Holmgren L, Jackson G, Arbiser J. p53 induces angiogenesis-restricted dormancy in a mouse fibrosarcoma. *Oncogene* 1998;17:819-24.

50. O'Reilly MS, Boehm T, Shing Y, Fukai N, Vasios G, Lane WS et al. Endostatin: an endogenous inhibitor of angiogenesis and tumor growth. *Cell* 1997;88:277-85.

51. Marneros AG, Olsen BR. The role of collagen-derived proteolytic fragments in angiogenesis. *Matrix Biol.* 2001;20:337-45.

52. Tsukamoto A, Kaneko Y, Yoshida T, Ichinose M, Kimura S. Regulation of angiogenesis in human hepatomas: possible involvement of p53-inducible inhibitor of vascular endothelial cell proliferation. *Cancer Lett.* 1999;141:79-84.

53. Chang L, Goldman RD. Intermediate filaments mediate cytoskeletal crosstalk. *Nat.Rev.Mol.Cell Biol.* 2004;5:601-13.

54. Eriksson JE, He T, Trejo-Skalli AV, Harmala-Brasken AS, Hellman J, Chou YH et al. Specific in vivo phosphorylation sites determine the assembly dynamics of vimentin intermediate filaments. *Journal of Cell Science* 2004;117:919-32.

55. Tang DD, Bai Y, Gunst SJ. Silencing of p21-activated kinase attenuates vimentin phosphorylation on Ser-56 and reorientation of the vimentin network during stimulation of smooth muscle cells by 5-hydroxytryptamine. *Biochem.J* 2005;388:773-83.

56. Marganski WA, Gangopadhyay SS, Je HD, Gallant C, Morgan KG. Targeting of a novel Ca+2/calmodulin-dependent protein kinase II is essential for extracellular signal-regulated kinase-mediated signaling in differentiated smooth muscle cells. *Circ.Res.* 2005;97:541-9.

57. Eckes B, Dogic D, Colucci-Guyon E, Wang N, Maniotis A, Ingber D et al. Impaired mechanical stability, migration and contractile capacity in vimentin-deficient fibroblasts. *Journal of Cell Science* 1998;111:1897-907.

58. Hu L, Lau SH, Tzang CH, Wen JM, Wang W, Xie D et al. Association of Vimentin overexpression and hepatocellular carcinoma metastasis. *Oncogene* 2004;23:298-302.

59. Tang ZY. Hepatocellular carcinoma--cause, treatment and metastasis. *World J Gastroenterol.* 2001;7:445-54.

60. Thomas PA, Kirschmann DA, Cerhan JR, Folberg R, Seftor EA, Sellers TA et al. Association between keratin and vimentin expression, malignant phenotype, and survival in postmenopausal breast cancer patients. *Clin.Cancer Res.* 1999;5:2698-703.

61. Kudo Y, Ogawa I, Kitagawa M, Kitajima S, Samadarani Siriwardena BS, Aobara N et al. Establishment and characterization of a spindle cell squamous carcinoma cell line. *J Oral Pathol.Med.* 2006;35:479-83.

62. CAMPBELL M. K. and FARRELL S. O. BIOCHEMISTRY, Fourth Edition. 2003. THOMSON BOOKS/COLE, USA.

63. Taguchi K, Takagi Y. [Aldolase]. *Rinsho Byori* 2001;Suppl 116:117-24.

64. Assaily W, Benchimol S. Differential utilization of two ATP-generating pathways is regulated by p53. *Cancer Cell* 2006;10:4-6.

65. Smallbone K, Gatenby RA, Gillies RJ, Maini PK, Gavaghan DJ. Metabolic changes during carcinogenesis: Potential impact on invasiveness. *J Theor.Biol.* 2006.

66. Di CG, Hatazawa J, Katz DA, Rizzoli HV, De Michele DJ. Glucose utilization by intracranial meningiomas as an index of tumor aggressivity and probability of recurrence: a PET study. *Radiology* 1987;164:521-6.

67. Gatenby RA, Gillies RJ. Why do cancers have high aerobic glycolysis? *Nat.Rev.Cancer* 2004;4:891-9.

68. Matoba S, Kang JG, Patino WD, Wragg A, Boehm M, Gavrilova O et al. p53 regulates mitochondrial respiration. *Science* 2006;312:1650-3.

69. Bensaad K, Tsuruta A, Selak MA, Vidal MN, Nakano K, Bartrons R et al. TIGAR, a p53-inducible regulator of glycolysis and apoptosis. *Cell* 2006;126:107-20.

70. Kruse JP, Gu W. p53 aerobics: the major tumor suppressor fuels your workout. *Cell Metab* 2006;4:1-3.

71. Jones RG, Plas DR, Kubek S, Buzzai M, Mu J, Xu Y et al. AMP-activated protein kinase induces a p53-dependent metabolic checkpoint. *Mol Cell* 2005;18:283-93.

72. van den Bemd G-J, Krijgsveld J, Luider TM, van Rijswijk AL, Demmers JAA, Jenster G. Mass Spectrometric Identification of Human Prostate Cancer-derived Proteins in Serum of Xenograft-bearing Mice. *Molecular Cellular Proteomics* 2006;5:1830-9.

73. Nakanishi T, Takeuchi T, Ueda K, Murao H, Shimizu A. Detection of eight antibodies in cancer patients' sera against proteins derived from the

adenocarcinoma A549 cell line using proteomics-based analysis. *J Chromatogr.B Analyt.Technol.Biomed.Life Sci* 2006;838:15-20.

74. Okano T, Kondo T, Kakisaka T, Fujii K, Yamada M, Kato H et al. Plasma proteomics of lung cancer by a linkage of multi-dimensional liquid chromatography and two-dimensional difference gel electrophoresis. *Proteomics* 2006;6:3938-48.

75. Montgomerie JZ, Gracy RW, Holshuh HJ, Keyser AJ, Bennett CJ, Schick DG. The 28K protein in urinary bladder, squamous metaplasia and urine is triosephosphate isomerase. *Clin.Biochem.* 1997;30:613-8.

76. Takashima M, Kuramitsu Y, Yokoyama Y, Iizuka N, Fujimoto M, Nishisaka T et al. Overexpression of alpha enolase in hepatitis C virus-related hepatocellular carcinoma: association with tumor progression as determined by proteomic analysis. *Proteomics* 2005;5:1686-92.

77. Takashi M, Zhu Y, Nakano Y, Miyake K, Kato K. Elevated levels of serum aldolase A in patients with renal cell carcinoma. *Urol.Res.* 1992;20:307-11.

78. Castaldo G, Calcagno G, Sibillo R, Cuomo R, Nardone G, Castellano L et al. Quantitative analysis of aldolase A mRNA in liver discriminates between hepatocellular carcinoma and cirrhosis. *Clin.Chem.* 2000;46:901-6.

79. Antti JK, Juha S, Tuomo JK, Jyrki K, nna-Kaisa P, Silvia P et al. Differential Expression of Cytoplasmic Carbonic Anhydrases, CA I and II, and Membrane-

Associated Isozymes, CA IX and XII, in Normal Mucosa of Large Intestine and in Colorectal Tumors. *Digestive Diseases and Sciences* 2001;V46:2179-86.

80. Parkkila S, Parkkila AK, Juvonen T, Rajaniemi H. Distribution of the carbonic anhydrase isoenzymes I, II, and VI in the human alimentary tract. *Gut* 1994;35:646-50.

81. Tureci O, Sahin U, Vollmar E, Siemer S, Gottert E, Seitz G et al. Human carbonic anhydrase XII: cDNA cloning, expression, and chromosomal localization of a carbonic anhydrase gene that is overexpressed in some renal cell cancers. *Proc.Natl.Acad.Sci U.S.A* 1998;95:7608-13.

82. Zavada J, Zavadova Z, Pastorekova S, Ciampor F, Pastorek J, Zelnik V. Expression of MaTu-MN protein in human tumor cultures and in clinical specimens. *Int.J Cancer* 1993;54:268-74.

83. Chiang WL, Chu SC, Yang SS, Li MC, Lai JC, Yang SF et al. The aberrant expression of cytosolic carbonic anhydrase and its clinical significance in human non-small cell lung cancer. *Cancer Letters* 2002;188:199-205.

84. Mori M, Staniunas RJ, Barnard GF, Jessup JM, Steele GD, Jr., Chen LB. The significance of carbonic anhydrase expression in human colorectal cancer. *Gastroenterology* 1993;105:820-6.

85. Zhang L, Zhou W, Velculescu VE, Kern SE, Hruban RH, Hamilton SR et al. Gene expression profiles in normal and cancer cells. *Science* 1997;276:1268-72.

86. Cole AR, Ji H, Simpson RJ. Proteomic analysis of colonic crypts from normal, multiple intestinal neoplasia and p53-null mice: a comparison with colonic polyps. *Electrophoresis* 2000;21:1772-81.

Appendices

Appendix NO. 1 Human wild type p53 sequence:

DEFINITION: Homo sapiens tumor protein p53 (Li-Fraumeni syndrome) (TP53), mRNA.

SOURCE human

ORGANISM human

COMMENT Human wild type p53

```
   1 atggaggagc cgcagtcaga tcctagcgtc gagccccctc tgagtcagga aacattttca
  61 gacctatgga aactacttcc tgaaaacaac gttctgtccc ccttgccgtc ccaagcaatg
 121 gatgatttga tgctgtcccc ggacgatatt gaacaatggt tcactgaaga cccaggtcca
 181 gatgaagctc ccagaatgcc agaggctgct ccccccgtgg cccctgcacc agcagctcct
 241 acaccggcgg cccctgcacc agccccctcc tggcccctgt catcttctgt cccttcccag
 301 aaaacctacc agggcagcta cggtttccgt ctgggcttct tgcattctgg gacagccaag
 361 tctgtgactt gcacgtactc ccctgccctc aacaagatgt tttgccaact ggccaagacc
 421 tgccctgtgc agctgtgggt tgattccaca cccccgcccg gcacccgcgt ccgcgccatg
 481 gccatctaca agcagtcaca gcacatgacg gaggttgtga ggcgctgccc ccaccatgag
 541 cgctgctcag atagcgatgg tctggcccct cctcagcatc ttatccgagt ggaaggaaat
 601 ttgcgtgtgg agtatttgga tgacagaaac acttttcgac atagtgtggt ggtgccctat
 661 gagccgcctg aggttggctc tgactgtacc accatccact acaactacat gtgtaacagt
 721 tcctgcatgg gcggcatgaa ccggaggccc atcctcacca tcatcacact ggaagactcc
 781 agtggtaatc tactgggacg gaacagcttt gaggtgcgtg tttgtgcctg tcctgggaga
 841 gaccggcgca cagaggaaga gaatctccgc aagaaagggg agcctcacca cgagctgccc
 901 ccagggagca ctaagcgagc actgcccaac aacaccagct cctctcccca gccaaagaag
 961 aaaccactgg atggagaata tttcaccctt cagatccgtg ggcgtgagcg cttcgagatg
1021 ttccgagagc tgaatgaggc cttggaactc aaggatgccc aggctgggaa ggagccaggg
1081 gggagcaggg ctcactccag ccacctgaag tccaaaaagg gtcagtctac ctcccgccat
1141 aaaaaactca tgttcaagac agaagggcct gactcagact ga
```

Appendix NO.2 Inducible Recombinant p53wt in pGENE/V5-HIS:

CCGAGCTCTTACGCGGGTCGAAGCGGAGTACTGTCCTCCGAGTGGAGTACTGTCCTCCGAGCGGAGTACT
GTCCTCCGAGTCGAGGGTCGAAGCGGAGTACTGTCCTCCGAGTGGAGTACTGTCCTCCGAGCGGAGTACT
GTCCTCCGAGTCGACTCTAGAGGGTATATAATGGATCTCGAGATATCGGAGCTCGTTTAGTGAACCGTCA
GATCGCCTGGAGACGCCATCCACGCTGTTTTGACCTCCATAGAAGACACCGGGACCGATCCAGCCTCCGC
GGCCGGGAACGGTGCATTGGAACGCGCATTCCCCGTGTTAATTAACAGGTAAGTGTCTTCCTCCTGTTTC
CTTCCCCTGCTATTCTGCTCAACCTTCCTATCAGAAACTGCAGTATCTGTATTTTTGCTAGCAGTAATAC
TAACGGTTCTTTTTTTCTCTTCACAGGCCACCAAGCTTcatatggaggagccgcagtcagatcctagc
gtcgagccccctctgagtcaggaaacattttcagacctatggaaactacttcctgaaaacaacgttctgtc
Ccccttgccgtcccaagcaatggatgatttgatgctgtccccggacgatattgaacaatggttcactgaag
acccaggtccagatgaagctcccagaatgccagaggctgctccccccgtggcccctgcaccagcagctcct
acaccggcggcccctgcaccagccccctcctggcccctgtcatcttctgtcccttcccagaaaacctacca
gggcagctacggtttccgtctgggcttcttgcattctgggacagccaagtctgtgacttgcacgtactccc
ctgccctcaacaagatgttttgccaactggccaagacctgccctgtgcagctgtgggttgattccacaccc
ccgcccggcacccgcgtccgcgccatggccatctacaagcagtcacagcacatgacggaggttgtgaggcg
ctgcccccaccatgagcgctgctcagatagcgatggtctggcccctcctcagcatcttatccgagtggaag
gaaatttgcgtgtggagtatttggatgacagaaacacttttcgacatagtgtggtggtgccctatgagccg
cctgaggttggctctgactgtaccaccatccactacaactacatgtgtaacagttcctgcatgggcggcat
gaaccggaggcccatcctcaccatcatcacactggaagactccagtggtaatctactgggacggaacagct
ttgaggtgcgtgtttgtgcctgtcctgggagagaccggcgcacagaggaagagaatctccgcaagaaaggg
gagcctcaccacgagctgcccccagggagcactaagcgagcactgcccaacaacaccagctcctctcccca
gccaaagaagaaaccactggatggagaatatttcacccttcagatccgtgggcgtgagcgcttcgagatgt
tccgagagctgaatgaggccttggaactcaaggatgcccaggctgggaaggagccagggggagcagggct
cactccagccacctgaagtccaaaaagggtcagtctacctcccgccataaaaaactcatgttcaagacaga
agggcctgactcagactgGAATTCTGCAGATATCCAGCACAGTGGCGGCCGCTCGAGTCTAGAGGGCC
CGCGGTTCGAAGGTAAGCCTATCCCTAACCCTCTCCTCGGTCTCGATTCTACGCGTACCGGTCATCATCAC
CATCACCATTGAGTTTAAACCCGCTGATCAGCCTCGACTGTGCCTTCTAGTTGCCAGCCATCTGTTGTTTG
CCCCTCCCCCGTGCCTTCCTTGACCCTGGAAGGTGCCACTCCCACTGTCCTTTCCTAATAAAATGAGGAAA
TTGCATCGCATTGTCTGAGTAGGTGTCATTCTATTCTGGGGGGTGGGGTGGGGCAGGACAGCAAGGGGGAG
GATTGGGAAGACAATAGCAGGCATGCTGGGGATGCGGTGGGCTCTATGGCTTCTGAGGCGGAAAGAACCAG
CTGGGGCTCTAGGGGGTATCCCCACGCGCCCTGTAGCGGCGCATTAAGCGCGGCGGGTGTGGTGGTTACGC
GCAGCGTGACCGCTACACTTGCCAGCGCCCTAGCGCCCGCTCCTTTCGCTTTCTTCCCTTCCTTTCTCGCC
ACGTTCGCCGGCTTTCCCCGTCAAGCTCTAAATCGGGGGCTCCCTTTAGGGTTCCGATTTAGTGCTTTACG
GCACCTCGACCCCAAAAAACTTGATTAGGGTGATGGTTCACGTAGTGGGCCATCGCCCTGATAGACGGTTT
TTCGCCCTTTGACGTTGGAGTCCACGTTCTTTAATAGTGGACTCTTGTTCCAAACTGGAACAACACTCAAC
CCTATCTCGGTCTATTCTTTTGATTTATAAGGGATTTTGCCGATTTCGGCCTATTGGTTAAAAAATGAGCT
GATTTAACAAAAATTTAACGCGAATTAATTCTGTGGAATGTGTGTCAGTTAGGGTGTGGAAAGTCCCCAGG

CTCCCCAGCAGGCAGAAGTATGCAAAGCATGCATCTCAATTAGTCAGCAACCAGGTGTGGAAAGTCCCCAG
GCTCCCCAGCAGGCAGAAGTATGCAAAGCATGCATCTCAATTAGTCAGCAACCATAGTCCCGCCCCTAACT
CCGCCCATCCCGCCCCTAACTCCGCCCAGTTCCGCCCATTCTCCGCCCCATGGCTGACTAATTTTTTTTAT
TTATGCAGAGGCCGAGGCCGCCTCTGCCTCTGAGCTATTCCAGAAGTAGTGAGGAGGCTTTTTTGGAGGCC
TAGGCTTTTGCAAAAAGCTCCCGGGAGCTTGTATATCCATTTTCGGATCTGATCAGCACGTGTTGACAATT
AATCATCGGCATAGTATATCGGCATAGTATAATACGACAAGGTGAGGAACTAAACCATGGCCAAGTTGAC
CAGTGCCGTTCCGGTGCTCACCGCGCGCGACGTCGCCGGAGCGGTCGAGTTCTGGACCGACCGGCTCGGG
TTCTCCCGGGACTTCGTGGAGGACGACTTCGCCGGTGTGGTCCGGGACGACGTGACCCTGTTCATCAGCG
CGGTCCAGGACCAGGTGGTGCCGGACAACACCCTGGCCTGGGTGTGGGTGCGCGGCCTGGACGAGCTGTA
CGCCGAGTGGTCGGAGGTCGTGTCCACGAACTTCCGGGACGCCTCCGGGCCGGCCATGACCGAGATCGGC
GAGCAGCCGTGGGGGCGGGAGTTCGCCCTGCGCGACCCGGCCGGCAACTGCGTGCACTTCGTGGCCGAGG
AGCAGGACTGACACGTGCTACGAGATTTCGATTCCACCGCCGCCTTCTATGAAAGGTTGGGCTTCGGAAT
CGTTTTCCGGGACGCCGGCTGGATGATCCTCCAGCGCGGGGATCTCATGCTGGAGTTCTTCGCCCACCCC
AACTTGTTTATTGCAGCTTATAATGGTTACAAATAAAGCAATAGCATCACAAATTTCACAAATAAAGCAT
TTTTTTCACTGCATTCTAGTTGTGGTTTGTCCAAACTCATCAATGTATCTTATCATGTCTGTATACCGTC
GACATCTAGCTAGAGCTTGGCGTAATCATGGTCATAGCTGTTTCCTGTGTGAAATTGTTATCCGCTCACA
ATTCCACACAACATACGAGCCGGAAGCATAAAGTGTAAAGCCTGGGGTGCCTAATGAGTGAGCTAACTCA
CATTAATTGCGTTGCGCTCACTGCCCGCTTTCCAGTCGGGAAACCTGTCGTGCCAGCTGCATTAATGAAT
CGGCCAACGCGCGGGGAGAGGCGGTTTGCGTATTGGGCGCTCTTCCGCTTCCTCGCTCACTGACTCGCTG
CGCTCGGTCGTTCGGCTGCGGCGAGCGGTATCAGCTCACTCAAAGGCGGTAATACGGTTATCCACAGAAT
CAGGGGATAACGCAGGAAAGAACATGTGAGCAAAAGGCCAGCAAAAGGCCAGGAACCGTAAAAAGGCCGC
GTTGCTGGCGTTTTTCCATAGGCTCCGCCCCCCTGACGAGCATCACAAAAATCGACGCTCAAGTCAGAGG
TGGCGAAACCCGACAGGACTATAAAGATACCAGGCGTTTCCCCCTGGAAGCTCCCTCGTGCGCTCTCCTG
TTCCGACCCTGCCGCTTACCGGATACCTGTCCGCCTTTCTCCCTTCGGGAAGCGTGGCGCTTTCTCATAG
CTCACGCTGTAGGTATCTCAGTTCGGTGTAGGTCGTTCGCTCCAAGCTGGGCTGTGTGCACGAACCCCCC
GTTCAGCCCGACCGCTGCGCCTTATCCGGTAACTATCGTCTTGAGTCCAACCCGGTAAGACACGACTTAT
CGCCACTGGCAGCAGCCACTGGTAACAGGATTAGCAGAGCGAGGTATGTAGGCGGTGCTACAGAGTTCTT
GAAGTGGTGGCCTAACTACGGCTACACTAGAAGAACAGTATTTGGTATCTGCGCTCTGCTGAAGCCAGTT
ACCTTCGGAAAAAGAGTTGGTAGCTCTTGATCCGGCAAACAAACCACCGCTGGTAGCGGTTTTTTTGTTT
GCAAGCAGCAGATTACGCGCAGAAAAAAAGGATCTCAAGAAGATCCTTTGATCTTTTCTACGGGGTCTGA
CGCTCAGTGGAACGAAAACTCACGTTAAGGGATTTTGGTCATGAGATTATCAAAAAGGATCTTCACCTAG
ATCCTTTTAAATTAAAAATGAAGTTTTAAATCAATCTAAAGTATATATGAGTAAACTTGGTCTGACAGTT
ACCAATGCTTAATCAGTGAGGCACCTATCTCAGCGATCTGTCTATTTCGTTCATCCATAGTTGCCTGACT
CCCCGTCGCGTAGATAACTACGATACGGGAGGGCTTACCATCTGGCCCCAGTGCTGCAATGATACCGCGA
GACCCACGCTCACCGGCTCCAGATTTATCAGCAATAAACCAGCCAGCCGGAAGGGCCGAGCGCAGAAGTG
GTCCTGCAACTTTATCCGCCTCCATCCAGTCTATTAATTGTTGCCGGGAAGCTAGAGTAAGTAGTTCGCC
AGTTAATAGTTTGCGCAACGTTGTTGCCATTGCTACAGGCATCGTGGTGTCACGCTCGTCGTTTGGTATG
GCTTCATTCAGCTCCGGTTCCCAACGATCAAGGCGAGTTACATGATCCCCCATGTTGTGCAAAAAAGCGG

TTAGCTCCTTCGGTCCTCCGATCGTTGTCAGAAGTAAGTTGGCCGCAGTGTTATCACTCATGGTTATGGC
AGCACTGCATAATTCTCTTACTGTCATGCCATCCGTAAGATGCTTTTCTGTGACTGGTGAGTACTCAACC
AAGTCATTCTGAGAATAGTGTATGCGGCGACCGAGTTGCTCTTGCCCGGCGTCAATACGGGATAATACCG
CGCCACATAGCAGAACTTTAAAAGTGCTCATCATTGGAAAACGTTCTTCGGGGCGAAAACTCTCAAGGAT
CTTACCGCTGTTGAGATCCAGTTCGATGTAACCCACTCGTGCACCCAACTGATCTTCAGCATCTTTTACT
TTCACCAGCGTTTCTGGGTGAGCAAAAACAGGAAGGCAAAATGCCGCAAAAAAGGGAATAAGGGCGACAC
GGAAATGTTGAATACTCATACTCTTCCTTTTTCAATATTATTGAAGCATTTATCAGGGTTATTGTCTCAT
GAGCGGATACATATTTGAATGTATTTAGAAAAATAAACAAATAGGGGTTCCGCGCACATTTCCCCGAAAA
GTGCCACCTGACGTCGACGGATCGGGAGATCGTA

BLACK:	pGene/V5-His B vector sequence
BLUE:	p53 gene sequence
RED:	primer sequence
RED MARKED YELLOW:	Restriction enzyme site in the primers (HindIII and EcoRI)
GREEN:	ATG = start codon to the p53 gene
	TGG = a stop (TGA) codon has been changed to a Trp (W)(TGG) codon
Orange marked	His Tag 6xHis (CAT CAT CAC CAT CAC CAT)
Plum marked:	**Coding for the V5 Tag**

Studied mutants

BLUE MARKED GREEN:	agg = amino acid 249, R249S = AGG → AGC
BLUE MARKED PURPLE:	cgt = amino acid 273, R273H = CGT → CAT

Appendix NO.3 DNA Sequence analysis of R249S:

a. Results of Forward Primer

CCTATGGAAACTACTTCCTGAAAACAACGTTCTGTCCCCCTTGCCGTCCCAAGCAATGGATGATTTGATGC
TGTCCCCGGACGATATTGAACAATGGTTCACTGAAGACCCAGGTCCAGATGAAGCTCCCAGAATGCCAGAG
GCTGCTCCCCCCGTGGCCCCTGCACCAGCAGCTCCTACACCGGCGGCCCCTGCACCAGCCCCCTCCTGGCC
CCTGTCATCTTCTGTCCCTTCCCAGAAAACCTACCAGGGCAGCTACGGTTTCCGTCTGGGCTTCTTGCATT
CTGGGACAGCCAAGTCTGTGACTTGCACGTACTCCCCTGCCCTCAACAAGATGTTTTGCCAACTGGCCAAG
ACCTGCCCTGTGCAGCTGTGGGTTGATTCCACACCCCCGCCCGGCACCCGCGTCCGCGCCATGGCCATCTA
CAAGCAGTCACAGCACATGACGGAGGTTGTGAGGCGCTGCCCCCACCATGAGCGCTGCTCAGATAGCGATG
GTCTGGCCCCTCCTCAGCATCTTATCCGAGTGGAAGGAAATTTGCGTGTGGAGTATTTGGATGACAGAAAC
ACTTTTCGACATAGTGTGGTGGTGCCCTATGAGCCGCCTGAGGTTGGCTCTGACTGTACCACCATCCACTA
CAACTACATGTGTAACAGTTCCTGCATGGGCGGCATGAACCGGAGCCCCATCCTCACCATCATCACACTGG
AAGACTCCAGTGGTAATCTACTGGGACGGAACAGCTTTGAGGTGCGTGTTTGTGCCTGTCCTGGGAGAGAC
CGGCGCACAGAGGAAGAGAATCTCCGCAAGAAAGGGGAGCCTCACCACGAGCTGCCCCCAGGGAGCACTAA
GCGAGCACTGCCCAACAACACCAGCTCCTCTCCCCAGCCAAAGAAGAAACCACTGGNTGGAGAATATTTCA
CCNTTCAGATCCGNGGG

b. Results of Reverse Primer

ACCCTTTTTGGACTTCAGGTGGCTGGAGTGANNNNNGCTCCCCCCTGGCTCCTTCCCAGCCTGGGCATCCT
TGAGTTCCAAGGCCTCATTCAGCTCTCGGAACATCTCGAAGCGCTCACGCCCACGGATCTGAAGGGTGAAA
TATTCTCCATCCAGTGGTTTCTTCTTTGGCTGGGGAGAGGAGCTGGTGTTGTTGGGCAGTGCTCGCTTAGT
GCTCCCTGGGGGCAGCTCGTGGTGAGGCTCCCCTTTCTTGCGGAGATTCTCTTCCTCTGTGCGCCGGTCTC
TCCCAGGACAGGCACAAACACGCACCTCAAAGCTGTTCCGTCCCAGTAGATTACCACTGGAGTCTTCCAGT
GTGATGATGGTGAGGATGGGGCTCCGGTTCATGCCGCCCATGCAGGAACTGTTACACATGTAGTTGTAGTG
GATGGTGGTACAGTCAGAGCCAACCTCAGGCGGCTCATAGGGCACCACCACACTATGTCGAAAAGTGTTTC
TGTCATCCAAATACTCCACACGCAAATTTCCTTCCACTCGGATAAGATGCTGAGGAGGGGCCAGACCATCG
CTATCTGAGCAGCGCTCATGGTGGGGGCAGCGCCTCACAACCTCCGTCATGTGCTGTGACTGCTTGTANAT
GGCCATGGCGCGGACGCGGGTGCCGGGCGGGGGTGTGGAATCAACCCACAGCTGCACAGGGCAGGTCTTGG
CCAGTTGGCAAAACATCTTGTTGAGGGCAGGGGAGTACGTGCAAGTCACAGACTTGGCTGTCCCAGAATGC
AAGAAGCCCAGACGGAAACCGTAGCTGCCCTGGTAGGTTTTCTGGGAAGGGACAGAANATGACAGGGGCCA
GGAGGGGGCTGGTGCAGGGGCCGCCGGTGTAGGAGCTGCTGGTGCAGGGGCCACGGGGGGGAGCAGCCTCT
GGCATTCTGGGANCTTCATCT

Appendix NO.4 Analysis from Mass Spectrometry of the identified spots:

Spot 1 Analysis from Mass Spectrometry:

Match to: gi|190384 Score: 389

Prolyl 4-hydroxylase beta-subunit [Homo sapiens]

Nominal mass (Mr): 57480. Calculated p*I* value: 4.76. 508 amino acids (AA).

Taxonomy: Homo sapiens

Accession in NCBI:gi|48735337 from Homo sapiens

gi|20810352 from Homo sapiens

gi|14790033 from Homo sapiens

Sequence Coverage: 21%

Amino Acid sequence of prolyl 4-hydroxylase beta-subunit [Homo sapiens]:

Matched peptides shown in **Bold Red**

```
   1 MLRRALLCLA VAALVRADAP EEEDHVLVLR KSNFAEALAA HKYLLVEFYA
  51 PWCGHCKALA PEYAKAAGKL KAEGSEIRLA KVDATEESDL AQQYGVRGYP
 101 TIKFFRNGDT ASPKEYTAGR EADDIVNWLK KRTGPAATTL PDGAAAESLV
 151 ESSEVAVIGF FKDVESDSAK QFLQAAEAID DIPFGITSNS DVFSKYQLDK
 201 DGVVLFKKFD EGRNNFEGEV TKENLLDFIK HNQLPLVIEF TEQTAPKIFG
 251 GEIKTHILLF LPKSVSDYDG KLSNFKTAAE SFKGKILFIF IDSDHTDNQR
 301 ILEFFGLKKE ECPAVRLITL EEEMTKYKPE SEELTAERIT EFCHRFLEGK
 351 IKPHLMSQEL PEDWDKQPVK VLVGKNFEDV AFDEKKNVFV EFYAPWCGHC
 401 KQLAPIWDKL GETYKDHENI VIAKMDSTAN EVEAVKVHSF PTLKFFPASA
 451 DRTVIDYNGE RTLDGFKKFL ESGGQDGAGD DDDLEDLEEA EEPDMEEDDD
 501 QKAVKDEL
```

Coding sequence of prolyl 4-hydroxylase beta-subunit [Homo sapiens], Accession No. gi|190384:

```
   1 atgctgcgcc gcgctctgct gtgcctggcc gtggccgccc tggtgcgcgc cgacgccccc
  61 gaggaggagg accacgtcct ggtgctgcgg aaaagcaact tcgcggaggc gctggcggcc
 121 cacaagtacc tgctggtgga gttctatgcc ccttggtgtg gccactgcaa ggctctggcc
 181 cctgagtatg ccaaagccgc tgggaagctg aaggcagaag gttccgagat caggttggcc
 241 aaggtggacg ccacggagga gtctgacctg gcccagcagt acggcgtgcg cggctatccc
 301 accatcaagt tcttcaggaa tggagacacg gcttccccca aggaatatac agctggcaga
 361 gaggctgatg acatcgtgaa ctggctgaag aagcgcacgg gcccggctgc caccaccctg
 421 cctgacggcg cagctgcaga gtccttggtg gagtccagcg aggtggctgt catcggcttc
```

```
 481 ttcaaggacg tggagtcgga ctctgccaag cagtttttgc aggcagcaga ggccatcgat
 541 gacataccat ttgggatcac ttccaacagt gacgtgttct ccaaatacca gctcgacaaa
 601 gatggggttg tcctctttaa gaagtttgat gaaggccgga acaactttga aggggaggtc
 661 accaaggaga acctgctgga ctttatcaaa cacaaccagc tgccccttgt catcgagttc
 721 accgagcaga cagccccgaa gatttttgga ggtgaaatca agactcacat cctgctgttc
 781 ttgcccaaga gtgtgtctga ctatgacggc aaactgagca acttcaaaac agcagccgag
 841 agcttcaagg gcaagatcct gttcatcttc atcgacagcg accacaccga caaccagcgc
 901 atcctcgagt tctttggcct gaagaaggaa gagtgcccgg ccgtgcgcct catcaccctg
 961 gaggaggaga tgaccaagta caagcccgaa tcggaggagc tgacggcaga gaggatcaca
1021 gagttctgcc accgcttcct ggagggcaaa atcaagcccc acctgatgag ccaggagctg
1081 ccggaggact gggacaagca gcctgtcaag gtgcttgttg ggaagaactt tgaagacgtg
1141 gcttttgatg agaaaaaaaa cgtctttgtg gagttctatg ccccatggtg tggtcactgc
1201 aaacagttgg ctcccatttg ggataaactg ggagagacgt acaaggacca tgagaacatc
1261 gtcatcgcca agatggactc gactgccaac gaggtggagg ccgtcaaagt gcacagcttc
1321 cccacactca agttctttcc tgccagtgcc gacaggacgg tcattgatta caacggggaa
1381 cgcacgctgg atggttttaa gaaattcctg gagagcggtg gccaggatgg ggcaggggat
1441 gatgacgatc tcgaggacct ggaagaagca gaggagccag acatggagga agacgatgat
1501 cagaaagctg tgaaagatga actgtaa
```

Spot 3 Analysis from Mass Spectrometry:

Match to: **gi|37852** Score: **213**

Vimentin [Homo sapiens]

Nominal mass (Mr): 53710. Calculated p*I* value: 5.06. 466 AA.

Taxonomy: Homo sapiens

Sequence Coverage: **11%**

Amino Acid sequence of vimentin [Homo sapiens]:

Matched peptides shown in **Bold Red**

```
   1 MSTRSVSSSS YRRMFGGPGT ASRPSSSRSY VTTSTRTYSL GSALRPSTSR
  51 SLYASSPGGV YATRSSAVRL RSSVPGVRLL QDSVDFSLAD AINTEFKNTR
 101 TNEKVELQEL NDRFANYIDK VRFLEQQNKI LLAELEQLKG QGKSRLGDLY
 151 EEEMRELRRQ VDQLTNDKAR VEVERDNLAE DIMRLREKLQ EEMLQREEAE
 201 NTLQSFRQDV DNASLARLDL ERKVESLQEE IAFLKKLHEE EIQELQAQIQ
 251 EQHVQIDVDV SKPDLTAALR DVRQQYESVA AKNLQEAEEW YKSKFADLSE
 301 AANRNNDALR QAKQESTEYR RQVQSLTCEV DALKGTNESL ERQMREMEEN
 351 FAVEAANYQD TIGRLQDEIQ NMKEEMARHL REYQDLLNVK MALDIEIATY
 401 RKLLEGEESR ISLPLPNFSS LNLRETNLDS LPLVDTHSKR TFLIKTVETR
 451 DGQVINETSQ HHDDLE
```

Coding Sequence of vimentin [Homo sapiens]: Accession No. gi|37852:

```
   1 atgtccacca ggtccgtgtc ctcgtcctcc taccgcagga tgttcggcgg cccgggcacc
  61 gcgagccggc cgagctccag ccggagctac gtgactacgt ccacccgcac ctacagcctg
 121 ggcagcgcgc tgcgccccag caccagccgc agcctctacg cctcgtcccc gggcggcgtg
 181 tatgccacgc gctcctctgc cgtgcgcctg cggagcagcg tgcccggggt gcggctcctg
 241 caggactcgg tggacttctc gctggccgac gccatcaaca ccgagttcaa gaacacccgc
 301 accaacgaga aggtggagct gcaggagctg aatgaccgct tcgccaacta catcgacaag
 361 gtgcgcttcc tggagcagca gaataagatc ctgctggccg agctcgagca gctcaagggc
 421 caaggcaagt cgcgcctagg ggacctctac gaggaggaga tgcgggagct gcgccggcag
 481 gtggaccagc taaccaacga caaagcccgc gtcgaggtgg agcgcgacaa cctggccgag
 541 gacatcatgc gcctccggga gaaattgcag gaggagatgc ttcagagaga ggaagccgaa
 601 aacaccctgc aatctttcag acaggatgtt gacaatgcgt ctctggcacg tcttgacctt
 661 gaacgcaaag tggaatcttt gcaagaagag attgcctttt tgaagaaact ccacgaagag
 721 gaaatccagg agctgcaggc tcagattcag gaacagcatg tccaaatcga tgtggatgtt
 781 tccaagcctg acctcacggc tgccctgcgt gacgtacgtc agcaatatga aagtgtggct
 841 gccaagaacc tgcaggaggc agaagaatgg tacaaatcca agtttgctga cctctctgag
 901 gctgccaacc ggaacaatga cgccctgcgc caggcaaagc aggagtccac tgagtaccgg
 961 agacaggtgc agtccctcac ctgtgaagtg gatgccctta aaggaaccaa tgagtccctg
1021 gaacgccaga tgcgtgaaat ggaagagaac tttgccgttg aagctgctaa ctaccaagac
1081 actattggcc gcctgcagga tgagattcag aatatgaagg aggaaatggc tcgtcacctt
1141 cgtgaatacc aagacctgct caatgttaag atggcccttg acattgagat tgccacctac
1201 aggaagctgc tggaaggcga ggagagcagg atttctctgc ctcttccaaa cttttcctcc
1261 ctgaacctga gggaaactaa tctggattca ctccctctgg ttgataccca ctcaaaaagg
1321 acattcctga ttaagacggt tgaaactaga gatggacagg ttatcaacga aacttctcag
1381 catcacgatg accttgaata a
```

Spot 5 Analysis from Mass Spectrometry:

Match to: **gi|28595** Score: **73**

aldolase A protein [Homo sapiens]

Nominal mass (Mr): 11987; Calculated p*I* value: 8.76, 108 AA.

Taxonomy: Homo sapiens

Sequence Coverage: **21%**Amino Acid sequence of aldolase A protein [Homo sapiens]:

Matched peptides shown in **Bold Red**

```
  1 MPYQYPALTP EQKKELSDIA HRIVAPGKGI LAADESTGSI AKRLQSIGTE
 51 NTEENRRFYR QLLLTADDRV NPCIGGVILF HETLYQKADD GRPFPQVIKS
101 KGGVVGIK
```

Coding Sequence of aldolase A protein [Homo sapiens] Accession no. gi|28595:

```
  1 atgccctacc aatatccagc actgaccccg gagcagaaga aggagctgtc tgacatcgct
 61 caccgcatcg tggcacctgg caagggcatc ctggctgcag atgagtccac tgggagcatt
121 gccaagcggc tgcagtccat tggcaccgag aacaccgagg agaaccggcg cttctaccgc
181 cagctgctgc tgacagctga cgaccgcgtg aacccctgca ttgggggtgt catcctcttc
241 catgagacac tctaccagaa ggcggatgat gggcgtccct tcccccaagt tatcaaatcc
301 aagggcggtg ttgtgggcat caag
```

Spot 8 Analysis from Mass Spectrometry:

Protein View

Match to: **gi|17389815** Score: **672**

Triosephosphate isomerase 1 [Homo sapiens]

Nominal mass (Mr): 26910; Calculated p*I* value: 6.45, 249 AA.

Taxonomy: Homo sapiens

Sequence Coverage: **62%**

Amino Acid sequence of Triosephosphate isomerase 1 [Homo sapiens]:

Matched peptides shown in **Bold Red**

```
  1 MAPSRKFFVG GNWKMNGRKQ SLGELIGTLN AAKVPADTEV VCAPPTAYID
 51 FARQKLDPKI AVAAQNCYKV TNGAFTGEIS PGMIKDCGAT WVVLGHSERR
101 HVFGESDELI GQKVAHALAE GLGVIACIGE KLDEREAGIT EKVVFEQTKV
151 IADNAKDWSK VVLAYEPVWA IGTGKTATPQ QAQEVHEKLR GWLKSNVSDA
201 VAQSTRIIYG GSVTGATCKE LASQPDVDGF LVGGASLKPE FVDIINAKQ
```

Coding sequence of Triosephosphate isomerase 1 Accession No. gi|17389815:

```
  1 atggcgccct ccaggaagtt cttcgttggg ggaaactgga agatgaacgg gcggaagcag
 61 agtctggggg agctcatcgg cactctgaac gcggccaagg tgccggccga caccgaggtg
121 gtttgtgctc cccctactgc ctatatcgac ttcgcccggc agaagctaga tcccaagatt
181 gctgtggctg cgcagaactg ctacaaagtg actaatgggg cttttactgg ggagatcagc
241 cctggcatga tcaaagactg cggagccacg tgggtggtcc tggggcactc agagagaagg
301 catgtctttg gggagtcaga tgagctgatt gggcagaaag tggcccatgc tctggcagag
361 ggactcggag taatcgcctg cattggggag aagctagatg aaagggaagc tggcatcact
421 gagaaggttg ttttcgagca gacaaaggtc atcgcagata acgcgaagga ctggagcaag
481 gtcgtcctgg cctatgagcc tgtgtgggcc attggtactg gcaagactgc aacaccccaa
541 caggcccagg aagtacacga gaagctccga ggatggctga agtccaacgt ctctgatgcg
601 gtggctcaga gcacccgtat catttatgga ggctctgtga ctggggcaac ctgcaaggag
661 ctggccagcc agcctgatgt ggatggcttc cttgtgggtg gtgcttccct caagcccgaa
721 ttcgtggaca tcatcaatgc caaacaatga
```

Spot 9 Analysis from Mass Spectrometry:

Match to: **gi|179780** Score: **314**

Carbonic anhydrase II [Homo sapiens]

Nominal mass (Mr): 29285; Calculated p*I* value: 6.87, 260 AA.

Taxonomy: Homo sapiens

Accession in NCBI:

gi|179780 from Homo sapiens

gi|49456705 from Homo sapiens

gi|49168536 from Homo sapiens

Sequence Coverage: **33%**

Amino Acid sequence of carbonic anhydrase II [Homo sapiens]:

Matched peptides shown in **Bold Red**

```
  1 MSHHWGYGKH NGPEHWHKDF PIAKGERQSP VDIDTHTAKY DPSLKPLSVS
 51 YDQATSLRIL NNGHAFNVEF DDSQDKAVLK GGPLDGTYRL IQFHFHWGSL
101 DGQGSEHTVD KKKYAAELHL VHWNTKYGDF GKAVQQPDGL AVLGIFLKVG
151 SAKPGLQKVV DVLDSIKTKG KSADFTNFDP RGLLPESLDY WTYPGSLTTP
201 PLLECVTWIV LKEPISVSSE QVLKFRKLNF NGEGEPEELM VDNWRPAQPL
251 KNRQIKASFK
```

Coding Sequence of carbonic anhydrase II [Homo sapiens] Accession No. gi|179780:

```
  1 atgtcccatc actgggggta cggcaaacac aacggacctg agcactggca taaggacttc
 61 cccattgcca agggagagcg ccagtcccct gttgacatcg acactcatac agccaagtat
121 gacccttccc tgaagcccct gtctgtttcc tatgatcaag caacttccct gaggatcctc
181 aacaatggtc atgctttcaa cgtggagttt gatgactctc aggacaaagc agtgctcaag
241 ggaggacccc tggatggcac ttacagattg attcagtttc actttcactg gggttcactt
301 gatggacaag gttcagagca tactgtggat aaaaagaaat atgctgcaga acttcacttg
361 gttcactgga acaccaaata tggggatttt gggaaagctg tgcagcaacc tgatggactg
421 gccgttctag gtatttttt gaaggttggc agcgctaaac cgggccttca gaaagttgtt
481 gatgtgctgg attccattaa aacaaagggc aagagtgctg acttcactaa cttcgatcct
541 cgtggcctcc ttcctgaatc cttggattac tggacctacc caggctcact gaccacccct
601 cctcttctgg aatgtgtgac ctggattgtg ctcaaggaac ccatcagcgt cagcagcgag
661 caggtgttga aattccgtaa acttaacttc aatggggagg gtgaacccga agaactgatg
721 gtggacaact ggcgcccagc tcagccactg aagaacaggc aaatcaaagc ttccttcaaa
781 taa
```

Spot 10 Analysis from Mass Spectrometry:

Protein View

Match to: **gi|54855** Score: **65**

triosephosphate isomerase [Mus musculus]

Nominal mass (Mr): 27021; Calculated p*I* value: 6.90, 249 AA.

Taxonomy: Mus musculus

Sequence Coverage: **9%**

Amino Acid Sequence of triosephosphate isomerase [Mus musculus]:

Matched peptides shown in **Bold Red**

```
  1 MAPTRKFFVG GNWKMNGRKK CLGELICTLN AANVPAGTEV VCAPPTAYID
 51 FARQKLDPKI AVAAQNCYKV TNGPFTGEIS PGMIKDLGAT WVVLGHSERR
101 HVFGESDELI GQKVSHALAE GLGVIACIGE KLDEREAGIT EKVVFEQTKV
151 IADNVKDWSK VVLAYEPVWA IGTGKTATPQ QAQEVHEKLR GWLKSNVNDG
201 VAQSTRIIYG GSVTGATCKE LATPADVDGF LVGGASLKPE FVDIINAKQ
```

Coding Sequence of triosephosphate isomerase [Mus musculus] Accession no. gi|54855:

```
  1 atggcgccta ccaggaagtt cttcgttggg ggcaactgga agatgaacgg gaggaagaag
 61 tgcctgggag aactcatctg caccctgaac gcagccaacg tgccggcagg caccgaggtg
121 gtttgtgcac cgcccaccgc ttacatcgac tttgccagac agaagctgga tcccaaaatt
181 gctgtggccg cacagaactg ctacaaagtg accaatgggc ctttcactgg ggaaatcagc
241 cctggcatga tcaaagactt aggagccacc tgggtcgtgc tggggcactc agaaagaaga
301 catgtctttg gagaatcaga tgagctgatt ggccagaaag tgagccacgc cctagcagag
361 ggactcgggg tgatcgcctg catcggggag aagctagacg aaagggaagc cggcatcacc
421 gagaaggtcg tgttcgagca aaccaaggtc atcgcagata atgtgaaaga ctggagcaag
481 gtggtcctgg cctatgaacc tgtgtgggcc attgggactg gcaagacggc aacccctcag
541 caggcacagg aagtacacga gaagctccgg ggatggctga aatccaatgt caatgatggg
601 gtggctcaga gcacccggat catttatgga ggttctgtga ctggagcaac ctgcaaagag
661 ctggcaacgc cagctgacgt ggacggcttc cttgtgggtg gcgcatctct caagcctgaa
721 tttgtggaca tcatcaatgc caaacaatga
```

Spot 11 Analysis from Mass spectrometry:

Protein View

Match to: **gi|13325287** Score: **656**

Enolase 1 [Homo sapiens]

Nominal mass (Mr): 47481; Calculated p*I* value: 7.01, 434 AA.

Taxonomy: Homo sapiens

Accession in NCBI:

gi|18490320 from Homo sapiens

gi|13325287 from Homo sapiens

gi|15990505 from Homo sapiens

Sequence Coverage: **38%**

Amino Acids: 434 AA.

Amino Acid sequence of Enolase 1 [Homo sapiens]:

Matched peptides shown in **Bold Red**

```
  1 MSILKIHARE IFDSRGNPTV EVDLFTSKGL FRAAVPSGAS TGIYEALELR
 51 DNDKTRYMGK GVSKAVEHIN KTIAPALVSK KLNVTEQEKI DKLMIEMDGT
101 ENKSKFGANA ILGVSLAVCK AGAVEKGVPL YRHIADLAGN SEVILPVPAF
151 NVINGGSHAG NKLAMQEFMI LPVGAANFRE AMRIGAEVYH NLKNVIKEKY
201 GKDATNVGDE GGFAPNILEN KEGLELLKTA IGKAGYTDKV VIGMDVAASE
251 FFRSGKYDLD FKSPDDPSRY ISPDQLADLY KSFIKDYPVV SIEDPFDQDD
301 WGAWQKFTAS AGIQVVGDDL TVTNPKRIAK AVNEKSCNCL LLKVNQIGSV
351 TESLQACKLA QANGWGVMVS HRSGETEDTF IADLVVGLCT GQIKTGAPCR
401 SERLAKYNQL LRIEEELGSK AKFAGRNFRN PLAK
```

Coding sequence of Enolase 1 [Homo sapiens] Accession No. gi|13325287:

```
  1 atgtctattc tcaagatcca tgccagggag atctttgact ctcgcgggaa tcccactgtt
 61 gaggttgatc tcttcacctc aaaaggtctc ttcagagctg ctgtgcccag tggtgcttca
121 actggtatct atgaggccct agagctccgg gacaatgata agactcgcta tatggggaag
181 ggtgtctcaa aggctgttga gcacatcaat aaaactattg cgcctgccct ggttagcaag
241 aaactgaacg tcacagaaca agagaagatt gacaaactga tgatcgagat ggatggaaca
301 gaaaataaat ctaagtttgg tgcgaacgcc attctggggg tgtcccttgc cgtctgcaaa
361 gctggtgccg ttgagaaggg ggtccccctg taccgccaca tcgctgactt ggctggcaac
421 tctgaagtca tcctgccagt cccggcgttc aatgtcatca atggcggttc tcatgctggc
```

```
 481 aacaagctgg ccatgcagga gttcatgatc ctcccagtcg gtgcagcaaa cttcagggaa
 541 gccatgcgca ttggagcaga ggtttaccac aacctgaaga atgtcatcaa ggagaaatat
 601 gggaaagatg ccaccaatgt gggggatgaa ggcgggtttg ctcccaacat cctggagaat
 661 aaagaaggcc tggagctgct gaagactgct attgggaaag ctggctacac tgataaggtg
 721 gtcatcggca tggacgtagc ggcctccgag ttcttcaggt ctgggaagta tgacctggac
 781 ttcaagtctc ccgatgaccc cagcaggtac atctcgcctg accagctggc tgacctgtac
 841 aagtccttca tcaaggacta cccagtggtg tctatcgaag atccctttga ccaggatgac
 901 tggggagctt ggcagaagtt cacagccagt gcaggaatcc aggtagtggg ggatgatctc
 961 acagtgacca acccaaagag gatcgccaag gccgtgaacg agaagtcctg caactgcctc
1021 ctgctcaaag tcaaccagat tggctccgtg accgagtctc ttcaggcgtg caagctggcc
1081 caggccaatg gttggggcgt catggtgtct catcgttcgg gggagactga agataccttc
1141 atcgctgacc tggttgtggg gctgtgcact gggcagatca agactggtgc cccttgccga
1201 tctgagcgct tggccaagta caaccagctc ctcagaattg aagaggagct gggcagcaag
1261 gctaagtttg ccggcaggaa cttcagaaac cccttggcca agtaa
```

Spot 12 Analysis from Mass spectrometry:

Protein View

Match to: **gi|693933** Score: **427**

2-phosphopyruvate-hydratase alpha-enolase; carbonate dehydratase [Homo sapiens]

Nominal mass (Mr): 47421; Calculated p*I* value: 7.01. Amino Acids: 434 AA

Taxonomy: Homo sapiens

Sequence Coverage: **20%**

.Amino Acid sequence of 2-phosphopyruvate-hydratase alpha-enolase; carbonate dehydratase [Homo sapiens]:

Matched peptides shown in **Bold Red**

```
   1 MSILKIHARE IFDSRGNPTV EVDLFTSKGL FRAAVPSGAS TGIYEALELR
  51 DNDKTRYMGK GVSKAVEHIN KTIAPALVSK KLNVTEQEKI DKLMIEMDGT
 101 ENKSKFGANA ILGVSLAVCK AGAVEKGVPL YRHIADLAGN SEVILPVPAF
 151 NVINGGSHAG NKLAMQEFMI LPVGAANFRE AMRIGAEVYH NLKNVIKEKY
 201 GKDATNVGDE GGFAPNILEN KEGLELLKTA IGKAGYTDKV VIGMDVAASE
 251 FSRSGKYDLD FKSPDDPSRY ISPDQLADLY KSFIKDYPVV SIEDPFDQDD
 301 WGAWQKFTAS AGIQVVGDDL TVTNPKRIAK AVNEKSCNCL LLKVNQIGSV
 351 TESLQACKLA QANGWGVMVS HRSGETEDTF IADLVVGLCT GQIKTGAPCR
 401 SERLAKYNQL LRIEEELGSK AKFAGRNFRN PLAK
```

Coding sequence of 2-phosphopyruvate-hydratase alpha-enolase; carbonate dehydratase [Homo sapiens] Accession No. gi|693933:

```
   1 atgtctattc tcaagatcca tgccagggag atctttgact ctcgcgggaa tcccactgtt
  61 gaggttgatc tcttcacctc aaaaggtctc ttcagagctg ctgtgcccag tggtgcttca
 121 actggtatct atgaggccct agagctccgg gacaatgata agactcgcta tatggggaag
 181 ggtgtctcaa aggctgttga gcacatcaat aaaactattg cgcctgccct ggttagcaag
 241 aaactgaacg tcacagaaca agagaagatt gacaaactga tgatcgagat ggatggaaca
 301 gaaaataaat ctaagtttgg tgcgaacgcc attctggggg tgtcccttgc cgtctgcaaa
 361 gctggtgccg ttgagaaggg ggtccccctg taccgccaca tcgctgactt ggctggcaac
 421 tctgaagtca tcctgccagt cccggcgttc aatgtcatca atggcggttc tcatgctggc
 481 aacaagctgg ccatgcagga gttcatgatc ctcccagtcg gtgcagcaaa cttcagggaa
 541 gccatgcgca ttggagcaga ggtttaccac aacctgaaga atgtcatcaa ggagaaatat
 601 gggaaagatg ccaccaatgt gggggatgaa ggcgggtttg ctcccaacat cctggagaat
 661 aaagaaggcc tggagctgct gaagactgct attgggaaag ctggctacac tgataaggtg
 721 gtcatcggca tggacgtagc ggcctccgag ttctccaggt ctgggaagta tgacctggac
 781 ttcaagtctc ccgatgaccc cagcaggtac atctcgcctg accagctggc tgacctgtac
 841 aagtccttca tcaaggacta cccagtggtg tctatcgaag atccctttga ccaggatgac
 901 tggggagctt ggcagaagtt cacagccagt gcaggaatcc aggtagtggg ggatgatctc
 961 acagtgacca acccaaagag gatcgccaag gccgtgaacg agaagtcctg caactgcctc
1021 ctgctcaaag tcaaccagat tggctccgtg accgagtctc ttcaggcgtg caagctggcc
1081 caggccaatg gttggggcgt catggtgtct catcgttcgg gggagactga agataccttc
1141 atcgctgacc tggttgtggg gctgtgcact gggcagatca agactggtgc cccttgccga
1201 tctgagcgct tggccaagta caaccagctc ctcagaattg aagaggagct gggcagcaag
1261 gctaagtttg ccggcaggaa cttcagaaac cccttggcca agtaa
```